8-1-2015

Geotechnical Surrogates for Sediment Shear Behavior in Southern Nevada

Rinu Ann Samuel
University of Nevada, Las Vegas, rinusamuel@gmail.com

GEOTECHNICAL SURROGATES FOR SEDIMENT SHEAR BEHAVIOR IN SOUTHERN NEVADA

By

Rinu Ann Samuel

Bachelor of Science in Geological Engineering

University of Alaska Fairbanks

2010

A thesis submitted in partial fulfillment

of the requirements for the

Master of Science in Engineering – Civil and Environmental Engineering

Department of Civil and Environmental Engineering and Construction

Howard R. Hughes College of Engineering

The Graduate College

University of Nevada, Las Vegas

August 2015

UNLV | GRADUATE COLLEGE

Thesis Approval

The Graduate College
The University of Nevada, Las Vegas

May 6, 2015

This thesis prepared by

Rinu Samuel

entitled

Geotechnical Surrogates for Sediment Shear Behavior in Southern Nevada

is approved in partial fulfillment of the requirements for the degree of

Master of Science in Engineering- Civil and Environmental Engineering
Department of Civil and Environmental Engineering and Construction

Barbara Luke, Ph.D.
Examination Committee Chair

Kathryn Hausbeck Korgan, Ph.D.
Graduate College Interim Dean

William Savage, Ph.D.
Examination Committee Member

Haroon Stephen, Ph.D.
Examination Committee Member

Wanda Taylor, Ph.D.
Graduate College Faculty Representative

ABSTRACT

GEOTECHNICAL SURROGATES FOR SEDIMENT SHEAR BEHAVIOR IN SOUTHERN NEVADA

by

Rinu Ann Samuel

Dr. Barbara Luke, Examination Committee Chair

Professor, Department of Civil and Environmental Engineering and Construction

University of Nevada, Las Vegas

The Nevada Department of Transportation design standards for deep foundations, particularly drilled shafts, in the Las Vegas Valley (LVV) may be overly conservative due to the challenges in characterizing strong but difficult-to-sample sediment strata, such as dense gravel, heavily cemented sediments, and mixed materials, which occur commonly in the LVV. Consequently, there is a need for investigating methods to assess the shear behavior of sediments that occur in the LVV *in situ* in working ranges of stress/strain, with the end goal of improving abilities to predict the capacity of drilled shafts in the LVV. To this end, global correlations of readily measured *in situ* tests – specifically, Standard Penetration Testing (SPT), shear wave velocity (VS) testing, and pressuremeter testing (PMT), with laboratory-measured shear parameters of sediments

are reviewed to evaluate their applicability in the LVV. Direct measurements of shear wave velocity are conducted using downhole testing at a site in the LVV known to have cementation and dense gravels. Local LVV datasets of aforementioned *in situ* tests and laboratory tests used to determine shear strength parameters are obtained from local consultants and government entities and are analyzed to detect possible relationships between *in situ* tests and shear parameters (such as friction angle, cohesion, undrained shear strength) beneficial for deep foundation design . Despite the high sediment heterogeneity across the LVV, variations in testing procedures, and lack of laboratory data, results show that readily measured *in situ* test data can be valuable for deep foundation design in the LVV when complemented with each other and laboratory data. In the datasets analyzed, blow counts are highly variable. Some local data show weak trends of increasing friction angle and cohesion with increasing blow count. Comparisons of blow counts with VS did not yield any useful correlations. Neither seismic velocities nor N_{60} is more informative than the other, but when complemented with each other they provide valuable insight regarding stiffness and relative density of sediments and their variability with respect to depth. Most correlations from other sites considered in this study are not representative of the shear behavior of the local sediments that were studied. Local VS profiles correspond better with local reference profiles than with others studied.

ACKNOWLEDGEMENTS

I thank my advisor, Dr. Barbara Luke, for the opportunity to work with her, and the invaluable time, guidance, and supervision that she provided me on this research. I also wish to thank my committee members - Dr. William Savage, Dr. Haroon Stephen, and Dr. Wanda Taylor for their advice, assistance, and support.

This research was funded by the Nevada Department of Transportation (NDOT) under agreement number P019-13-803. Additional graduate-student support was provided by the "Cataloging Legacy Seismic Data" project under U.S. DOE's National Security Technologies prime contract number DE-AC52-06NA25946 (subcontract number 104777, task order number 39).

I am grateful to Jonathan Bahr and Werner Helmer of Clark County (Nevada) Department of Development Services - Building Division, Jonathan Lehman-Svoboda of Kleinfelder Inc., and Walter Vanderpool of Terracon Consulting Engineers and Scientists, for providing invaluable data necessary for the research.

Special thanks to Jesse Basinski for her technical assistance with ArcGIS operations necessary for the research.

I thank Andy Lawrence of NDOT for his valuable discussion and insight regarding downhole velocity testing conducted in this research. I also thank Dr. Eric Thompson at San Diego State University for his assistance with helping me understand his code written using the programming language R, which accounts for refractions across layer boundaries to interpret downhole seismic data.

I am thankful for my colleagues at the Applied Geophysics Center – Suchan Lamichhane, Yasaman Badrzadeh, Dev Raj Sharma, and Chris Cothrun. They provided

valuable reviews of my work, assisted with field operations and have been a great source of encouragement, support, and intellectual development.

Words cannot express my gratitude towards my family for their love and support throughout this research. I greatly appreciate my wonderful husband, Sonu Varghese, for being unconditionally encouraging, supportive, patient, and understanding, even while I was away from him for long periods of time working on this research. Thank you to my mother and father, Omana and Madhu Samuel, for their constant guidance and optimism, and for helping me see the bright side of things even in the most difficult of situations. And above all, I am thankful to Almighty God for being my rock, provider and protector.

TABLE OF CONTENTS

LIST OF TABLES

LIST OF FIGURES

LIST OF ACRONYMS

AGC – Applied Geophysics Center

CCDDS-BD – Clark County Department of Development Services - Building Division

DS – Direct shear

ER – energy transfer ratio (for hammer system in SPT)

ESGI – Electronic Submittal of Geotechnical Information (Clark County, Nevada)

IDW – Inverse Distance Weighting

LVV – Las Vegas Valley

MASW – Multi-channel Analysis of Surface Waves

MC – Modified California

NDOT – Nevada Department of Transportation

QA/QC – Quality Assurance/Quality Control

ReMi – Refraction Microtremor

SDS – Single-point Direct shear

SPT – Standard Penetration Test

UNLV – University of Nevada, Las Vegas

USCS – Unified Soil Classification System

UU – unconsolidated undrained

VP – compression wave velocity

VS – shear wave velocity

CHAPTER 1

INTRODUCTION

1.1. Background

Las Vegas is located in Clark County in the Las Vegas Valley (LVV) of southern Nevada. The LVV is situated above a deep, sediment-filled basin in the Basin and Range geomorphic province of the western United States. The general area is characterized by sub-parallel north-south-oriented block-faulted mountain ranges, created by east-west extensional tectonics, separated by sediment-filled basins (Wyman et al., 1993). The region has an arid to semi-arid climate that, along with depositional activity in the unsaturated zones, results in challenging soil conditions, such as hydro-collapsible soils, chemical heave, swelling clays, and carbonate cemented soils (Werle and Luke, 2007).

The Nevada Department of Transportation (NDOT) design standards for deep foundations, particularly drilled shafts, in the LVV may be overly conservative due to the challenges in characterizing strong but difficult-to-sample sediment strata, such as dense gravel, heavily cemented sediments, and mixed materials, all of which occur commonly in the LVV. The material formed by the calcareous cementation of sediments (of any grain size) is locally known as ‘caliche’ (Werle and Luke, 2007); it tends to occur in localized lenses with thickness of up to 2 m or more and at depths ranging from the ground surface to 350 m or more (Murvosh et al., 2013a). Heavily cemented caliche behaves like rock with compressive strengths ranging from a few tens of kPa to tens of MPa (Werle and Luke, 2007). It is a valuable element for load transfer when sufficiently

thick and laterally continuous. Cemented sediments that occur in the LVV are therefore beneficial for drilled shaft design, as is confirmed by Stone (2009).

The American Association of State Highway and Transportation Officials (AASHTO) has not established guidelines to quantify the strength and deformation characteristics of carbonate cemented sediments; the author postulates that it is because of their relative rarity nationwide, the cost of expensive coring required in case of highly cemented sediments, and the potential for disintegration during sample collection in partially cemented sediments. Design of drilled shafts in cemented sediments and dense gravels is complicated by significant variability in the thickness, lateral extent and compressive strength of these units (Werle and Luke, 2007). Laboratory strength data for cemented sediments and dense gravels are sparsely available in the LVV and, when available, may not be representative across the area under consideration due to material heterogeneity.

1.2. Purpose, objectives and approach

The purpose of this research is to investigate expedient methods to assess the shear behavior of sediments that occur in the LVV in working ranges of stress/strain. Local datasets from *in situ* tests and laboratory tests are obtained from direct measurements, local consultants, and government entities, with the intent of studying their relationships with stress-strain characteristics of sediments relevant to deep foundation design, specific to the LVV. Comparisons are made to global correlations by others for the same properties, to test their relevance in the LVV. The outcomes of this research will aid

NDOT with their end goal of improving the ability to predict the capacity of drilled shafts in the LVV using site characteristics that are readily measured *in situ*.

Most geotechnical site investigations involve Standard Penetration Tests (SPTs), which yield blow counts (ASTM D1586-11); additionally, surface-based testing to determine 30-m depth-averaged shear-wave velocity (VS) has been conducted for much of the LVV to determine seismic hazard class (Louie et al., 2011). Therefore blow count and VS data are widely available across the LVV. Blow counts may not always be representative of the *in situ* soil conditions, as, for example, gravels may plug the samplers and clays can be remolded by samplers (U.S. Department of the Interior, 2001; Holtz et al., 2011). Similarly, blow count data are not instructive in cemented sediments once the sampler meets "refusal" (per ASTM D1586; discussed later). The use of VS is investigated to supplement blow count data. Because stiff sediment layers are unlikely to undergo large strain in service, the characterization of sediment stress-strain behavior at low strain levels is beneficial to obtain serviceability criteria for design. The small-strain shear modulus, G_{max}, is closely related to VS ($G_{max} = \rho \cdot VS^2$, where ρ is density); therefore, VS measurements give valuable *in situ* information.

Results of tests used to determine shear strength parameters in the laboratory are compared with *in situ* test results to investigate relationships between the two. To this end, the author conducted downhole velocity testing at a major highway interchange in the LVV in collaboration with NDOT. The measured velocity profiles are compared with blow counts from SPT to investigate trends, and VS profiles are compared with existing

local and global reference profiles of similar sediments. The University of Nevada, Las Vegas (UNLV) Applied Geophysics Center (AGC) and NDOT (Andrew Lawrence, NDOT, personal communication, October 5, 2014) will analyze seismic test results with respect to co-located test shaft outcomes, to investigate trends that might benefit deep-foundation design in the LVV.

Local data are compared with correlations published by others for various sediment types from different sites around the world. Ideally, the locally-based correlations will contribute to reducing overconservatism in design of drilled shaft foundations in Las Vegas and other regions where cemented soils are prevalent

1.3. Organization of thesis

This thesis is organized into six chapters: (1) Introduction, (2) Published correlations of *in situ* test data with shear characteristics of sediments, (3) Downhole velocity testing at US95/CC215 Interchange, (4) Local datasets, (5) Discussion, and (6) Conclusions and recommendations. Chapter 2 provides a review of correlations prepared by others of shear parameters with *in situ* tests - SPT, VS, and pressuremeter testing - regardless of location. Chapter 3 presents the seismic subsurface investigation conducted by the author at a major highway interchange in the LVV where drilled-shaft foundations will be installed; the VS dataset is analyzed in conjunction with some other data available for the site. Chapter 4 presents the comparison of local *in situ* datasets collected by others with each other and with laboratory data; this chapter is further divided into two parts: a) major project datasets, and b) Clark County valley-wide dataset. Chapter 5 discusses the

findings of the study, and compares the *in situ* and laboratory test data from the LVV (Chapters 3 and 4) with published global correlations (Chapter 2). Chapter 6 presents the conclusions and recommendations of this thesis.

CHAPTER 2

PUBLISHED CORRELATIONS OF *IN SITU* TEST DATA WITH SHEAR CHARACTERISTICS OF SEDIMENTS

This chapter consists of a brief introduction of the shear strength of sediments and compilations of relationships in published literature of shear strength parameters with some *in situ* tests that are conducted in the LVV, namely SPT, VS, and pressuremeter. CPT is not the test of choice in Las Vegas due to the widespread presence of cementation and dense sediments. Therefore, although correlations of shear strength parameters with CPT have been published, they are not addressed here. While this literature review is extensive, it is not comprehensive.

2.1. Overview of shear strength in sediments

The strength of the soil is the maximum stress it can endure before it undergoes failure (Das, 2010). Shear strength is a measure of the resistance of soils to shearing stresses, and depends mostly on inter-particular interaction (Das, 2010). It can be represented by the famous Mohr-Coulomb failure criterion equation as:

$$S = c + \sigma \tan \phi \qquad (2.1)$$

where S is shear strength, c is cohesion, σ is normal stress, and ϕ is angle of internal friction (hereafter referred to as friction angle). Equation 2.1 describes shear strength in two parts, a cohesive component and a frictional component; c and ϕ are referred to here as the shear strength parameters of soil. Often for cohesive soils in undrained loading, ϕ

is assumed to be zero, while for cohesionless soils in drained loading, c is assumed to be zero.

The total normal stress at a point in a saturated soil is the sum of the effective stress (σ') and pore water pressure (u), expressed as $\sigma = \sigma' + u$. According to Das (2010), σ' is the sum of the vertical force components developed at the points of contact of the soil particles per unit cross-sectional area of the soil mass. While the shear strength expression in Equation 2.1 is based on total stress, Equation 2.2 expresses shear strength using effective stress parameters:

$$S = c' + \sigma' \tan \phi' \tag{2.2}$$

where c' is effective cohesion and ϕ' is effective friction angle. It is important to note that the shear strength of soils is a function of effective stress, regardless of whether failure occurs under drained or undrained conditions (Duncan et al., 2014).

Sediment shear strength parameters are most commonly determined in the laboratory using either the direct shear test or the triaxial shear test (Das, 2010). Laboratory tests provide precise shear strength measurements, ideally on undisturbed specimens. Useful laboratory measurements of shear strength can be difficult to obtain due to unavailability of undisturbed samples, economic and time constraints, and difficulty in replicating critical field conditions such as pore pressure, degree of saturation and *in situ* loading conditions. In such cases, laboratory tests might be conducted under less than ideal conditions (e.g., on disturbed specimens), or shear strength parameters may be estimated using correlations with *in situ* tests that are relatively simple to conduct and better

represent the *in situ* conditions. It can be more beneficial to conduct a large number of relatively inexpensive field tests at multiple locations around a site having high soil heterogeneity than a couple of highly precise laboratory tests on samples that might not be representative of the site conditions. According to Murthy (2003), "the present trend is to rely more on field tests as these tests have been found to be more reliable than even the more sophisticated laboratory methods" (p. 256).

2.2. SPT (Standard Penetration Test)

SPT is a popular *in situ* test to determine geotechnical properties of sediments, due to its simplicity. SPT is conducted in a borehole by driving a split-spoon sampler 0.76 m (30 in.) into the soil by repeatedly dropping a 623-N (140-lbf) hammer. The number of blows applied in each 0.15-m (0.5-ft) increment is counted until the sampler is advanced 0.45 m (1.5 ft). The sum of the number of blows required to drive the sampler over the depth interval of 0.15 to 0.45 m (6 to 18 in.) is known as the 'N-value' or blow count, also known as the standard penetration resistance (ASTM D1586-11). N-values give an idea of relative density and consistency in coarse-grained and fine-grained soils respectively (Rogers, 2006).

Although called the Standard Penetration Test, it is not completely standardized. For example, SPT can be conducted using different types of hammers, such as the cat-head, donut and automatic hammer, which transfer different amounts of energy to the sampler and thus lead to variance in N-values recorded. The amount of energy delivered to the drill rods by the hammer is a major factor affecting the measured N-value and can vary

from about 30% to 85% of the free-fall hammer energy (Schmertmann and Palacios, 1979). This lack of standardization has led to correction factors applied to N-values to better standardize them.

Conventionally, N denotes the uncorrected raw N-value, while N_{60} denotes N adjusted for 60% hammer efficiency.

$$N_{60} = (ER / 60\%) N \quad (2.3)$$

where ER is hammer efficiency expressed as percent of theoretical free fall energy delivered by the hammer system used (AASHTO, 2012).

Regarding overburden correction, according to the standard for determining the normalized penetration resistance of sands for evaluation of liquefaction potential (ASTM D6066-11), the overburden correction is applied only to cohesionless soils. Because most of the soils obtained for this study from the LVV are cohesive, overburden correction is not applied to N in this research.

The author's literature search found several direct and indirect correlations of SPT, using N and N_{60}, with shear strength parameters. Correlations with N were more prevalent than correlations with N_{60}. N and N_{60} used for correlations vary greatly in energy corrections, sampler sizes, and other parameters. In some of the earlier cases reported here where no corrections to N are mentioned, the values reported are assumed to be uncorrected. Most of the correlations were generated empirically. Note that the scatter in the data from which each correlation was drawn is not addressed in this thesis.

2.2.1. Cohesionless soils

SPT correlations with shear strength for cohesionless soils have been formulated using the frictional component of the Mohr-Coulomb failure criterion equation, ϕ'. Table 2.1 shows a compilation of early work presented by Kulhawy and Mayne (1990) to directly correlate N with effective friction angles measured in triaxial compression tests. Kulhawy and Mayne (1990) state that the correlation developed by Peck and others in 1974 "appears to be more common, perhaps because it is more conservative" (p. 4-14). Other direct correlations of N and N_{60} with ϕ' for cohesionless soils expressed as equations are tabulated in Table 2.2. Most of the correlations in Table 2.2 are exponential relationships of either N or N_{60} with ϕ', while one is a second order polynomial and another, by Hettiarachchi and Brown, is a rational trigonometric equation.

Direct correlations of N or N_{60} values with ϕ' from Table 2.2 are plotted in Figure 2.1; note that the correlation by Hettiarachchi and Brown (2009) is not plotted in Figure 2.1 because the value of one parameter or instructions on how to obtain it are not provided in the reference. For Schmertmann's study of cohesionless soils in 1975 (as cited in Kulhawy and Mayne, 1990) the ratio of effective overburden pressure (σ'_o) to atmospheric pressure (p_a = 100 kPa) was assumed to be 1; according to Terzaghi et al. (1996), the most common values of σ'_o obtained from field performance data range between 50 and 150 kPa, therefore 100 kPa is a reasonable value for reference σ'_o. For Hatanaka and Uchida's study in 1996 (as cited in Hettiarachchi and Brown, 2009) a value of 0.889 was used for the correction factor, C_N. Several published SPT correlation plots

display N and N_{60} plotted to 100, therefore they are plotted to a maximum value of 100 in most plots in this study. The typical values of ϕ' for cohesionless soils range between 25 and 50 degrees (Das, 2010). Ohsaki's study of sandy soils in 1959 (as cited in Baxter et al., 2005) consistently calculates a much higher value of ϕ' than other correlations. The maximum value of ϕ' at N=100 is calculated to be about 70 degrees using Ohsaki's correlation, which is 40% higher than the upper limit given by Das (2010). The difference between the lowest and highest ϕ' values calculated from the different correlations range between 12 and 18 degrees for the lowest and highest blow count values respectively.

2.2.2. Cohesive soils

One of the earliest and a frequently used correlation of undrained shear strength (S_u), normalized by atmospheric pressure, with N for cohesive soils was developed by Terzaghi and Peck in 1967 (Kulhawy & Mayne, 1990), and is shown in Table 2.5. According to Kulhawy and Mayne (1990), a representative equation for that dataset is:

$$S_u / p_a \approx 0.06 \times N \quad (2.4)$$

which is essentially the correlation by Terzaghi and Peck (as cited in Nassaji and Kalantari, 2011) tabulated in Table 2.6 when pa has a value of 100 kPa.

Of the many correlations that exist between N and S_u, one by Hara et al. (1974) uses the same SPT procedure and drilling equipment for all data pairs, thus providing a more consistent correlation than many others. The authors tested 25 cohesive soil sites in Japan, 15 of which were alluvial deposits, 9 were diluvial deposits and 1 was a tertiary

deposit. The soils tested had overconsolidation ratios of 1.0 to 3.0, void ratios of 0.5 to 3.0, and degree of saturation of 90% to 100% (Hara et al., 1974). The authors' correlation is provided in Table 2.6 along with several other correlations of SPT with S_u for cohesive soils. Most correlations of S_u in Table 2.6 are directly proportional to N or N_{60}, while some are exponential relationships.

The correlations of N or N_{60} with S_u from Table 2.6 are plotted in Figure 2.2. A universal correlation between S_u and N or N_{60} is not indicated, due to the wide range of results. The variability in S_u from different correlations is observed to increase considerably with increasing N or N_{60}. S_u for all correlations is under 200 kPa for N or N_{60} under 15, while at the N or N_{60} value of 100, S_u ranges from about 120 kPa to 1250 kPa for different correlations. Typical values of S_u range from 0 to 200 kPa for very soft to very stiff clays, while S_u for very hard clays is more than 200 kPa (Das, 2010). For N or N_{60} over 50, most correlations yield S_u values that are much higher than the typical range of values observed in clays; therefore it is possible that the typical S_u values estimated by Das (2010) represent soils having N or N_{60} values under 50. The correlation developed by Terzaghi and Peck in 1967 (as cited in Nassaji and Kalantari, 2011) lies mid-range compared to other correlations and estimates S_u to be under 300 kPa for N below 50. The Hara et al. (1974) correlation estimates a much higher range of S_u (500 kPa or less) for N below 50.

2.3. VS (Shear wave velocity)

VS test measurements can be made by intrusive or non-intrusive *in situ* wave propagation test methods such as suspension logging, cross-hole, downhole, seismic refraction, seismic reflection, and surface wave methods (e.g., Kramer, 1996; Park et al., 1999). The author found only a few correlations of VS with shear strength parameters. Several correlations of VS with N or N_{60} exist; these can be used to analyze how N or N_{60} relate to stiffness of soil and might tie VS indirectly to shear strength.

2.3.1. Correlations with S_u

Although shear strength is measured at large strains (shear strain (γ) ~ 1-30%) and shear waves are a small strain phenomenon ($\gamma < \sim$ 10-3 %) and therefore a direct correlation may not seem justified, according to Cha and Cho (2007), stress conditions and void ratio highly impact both entities. Kulkarni et al. (2010) give an empirical correlation between VS and S_u from unconsolidated undrained triaxial tests for soft clays with a R^2 value of 0.82. (R^2, also known as the coefficient of determination or regression coefficient, provides the "proportion of variance that two variables in a bivariate distribution have in common" (Spatz (2011), p. 102). R^2 ranges between 0.0 and 1.0 and has no units. The higher the R^2 value, the better the model fits the data; therefore, the R^2 value demonstrates how well one variable can be predicted by another. In a study by Dickenson (as cited in Wair et al., 2012), a relationship between VS and S_u is given for four cohesive soils in the San Francisco Bay area of California (Bay Mud, Yerba Buena Mud, and Alameda Formation (marine and oxidized)). Table 2.7 shows these correlations of

VS with S_u for those cohesive soils, along with two others. All correlations are simple exponentials with VS as base.

Correlations of VS with S_u from Table 2.7 are plotted in Figure 2.3. Typical VS for very soft to gravelly soils range from about 75 m/s to 700 m/s respectively (Subramanian, 2008), while VS for limestone ranges from 2000 m/s to 3300 m/s (Mavko, 2005). Measured field VS values for caliche in the LVV range between 1000 m/s and 2000 m/s (Murvosh et al., 2013a). Axis limits in Figure 2.3 for VS are set to 2000 m/s to account for VS of caliche. The correlations were developed for soft clays, so the author does not expect them to be valid for stiff materials like caliche. Most of the correlations show J-shaped growth curves confirming the exponential relationship between VS and S_u, while the Schultheiss (1985) correlation has such a low growth rate that it appears linear for the given axis limits. For a VS of 300 m/s, the S_u ranges from about 50 kPa to 2300 kPa, demonstrating high variability in S_u from different correlations. Note that saturated clays typically have VS ranging between 200 and 800 m/s (Mavko, 2005) while S_u typically ranges from 0 to 200 kPa for very soft to stiff clays and over 200 kPa for hard clays (Das 2010; as stated earlier). S_u obtained from all correlations except Schultheiss (1985) are 10 times more than typical S_u range of soils stated earlier for a clay at VS of ~300 m/s and therefore should not be extrapolated. Schultheiss (1985) calculates the lowest S_u values among the correlations provided.

2.3.2. Correlations with blow counts

Many of the early correlations of VS with SPT are based on N, while some of the more recent ones are based on N_{60}. As mentioned before, N and N_{60} vary greatly in energy corrections, sampler sizes, and other parameters. Similarly, VS used for correlations is attained by various methods, which is another source of uncertainty. Some published, empirical correlations of VS with N or N_{60} for 'all' (irrespective of soil classification), sandy, and clayey soils are listed in Tables 2.8, 2.9 and 2.10 respectively. All correlations are simple exponentials with N or N_{60} as base. One correlation in Table 2.9 (sandy soils), that of Brandenberg et al. (2010), applies an overburden correction to N_{60}. According to the authors, the effective vertical stress (σ'_v) is an important factor in the relationship between VS and N_{60} because VS and N_{60} normalize differently with overburden. As explained earlier, overburden correction is not applied to blow counts in this research because most of the soils obtained for this study from the LVV are cohesive.

Correlations of VS with N and N_{60} for 'all', sandy and clayey soils are plotted in Figures 2.4, 2.5, and 2.6, respectively. All correlations from Tables 2.8, 2.9, and 2.10 are plotted together in Figure 2.7 as well. All correlations show a J-shaped growth curve indicating an exponential increase in VS with increasing N or N_{60}. Note that the correlation by Brandenberg et al. (2010) has a steeper growth curve that predicts the lowest VS when compared to most other correlations for sandy soils (Fig. 2.5). The maximum value of VS at a N or N_{60} of 100 is around 600 m/s. High variability is observed in correlations for 'all' soils, the largest of the three datasets, while lowest variability is observed in correlations for clayey soils, the smallest of the three datasets.

2.4. Pressuremeter test

The pressuremeter is essentially a cylindrical probe with a chamber that expands radially when pressurized. The pressuremeter test (PMT) is conducted on the wall of a borehole. The pressuremeter is lowered into a borehole and uniform pressure is applied to the borehole walls by an inflatable flexible membrane. The deformation of the borehole walls and soil stress-strain characteristics are derived from the change in the volume of the expanding membrane with respect to applied pressure.

The PMT is a large-strain test used to estimate shear strength parameters, deformation characteristics, and *in situ* horizontal stress of the soil (Mair and Wood, 1987). The pressuremeter curve, which plots the applied pressure with respect to the change in volume of the expansive chamber, is used for calculations of all PMT parameters. Limit pressure (p_L) and net limit pressure (p_L*) are outcomes of PMT used for correlations with shear strength parameters. p_L is defined as the pressure reached when the soil cavity has been inflated to two times its initial size, and p_L* is a function of p_L ($p_L^* = p_L - \sigma_{OH}$, where σ_{OH} is the horizontal total stress at rest) (Briaud, 1992). Table 2.11 shows correlations of S_u with PMT parameters. The author observed that PMT relationships to determine shear strength parameters are presented mostly for clayey soils. According to Clayton et al. (1995), analytical techniques to interpret PMT results in cohesionless soils are still developing and are limited compared to their use in cohesive soils.

Summary This literature review provides a compendium of published correlations of data from selected *in situ* tests (relevant for the LVV) with shear strength parameters: effective friction angle for primarily cohesionless soils and undrained shear strength for primarily cohesive soils. Correlations of SPT with both parameters are extensive. Correlations of shear strength parameters with VS and PMT are fewer in number, and are available mostly for cohesive soils. Several correlations exist between two *in situ* tests, VS and SPT. The correlations presented in this chapter were developed from soils around the world. No correlations were found for dense clays or gravels or soils with cementation, which are common to the LVV. Consequently, there is a need for exploring the relationship of shear strength parameters with data from *in situ* tests specifically for the LVV, which will be addressed in the upcoming chapters.

Table 2.1 – Relationship of N versus effective friction angles measured in triaxial compression tests (ϕ'_{tc}) for cohesionless soils (As referenced by Kulhawy & Mayne (1990))

N	Relative Density	Approximate ϕ'_{tc} (deg.)	
		Peck et al. (1974)	Meyerhof (1956)
0 - 4	Very loose	< 28	< 30
4 - 10	Loose	28 - 30	30 - 35
10 - 30	Medium	30 - 36	35 - 40
30 - 50	Dense	36 - 41	40 - 45
> 50	Very dense	> 41	> 45

Table 2.2 – Correlations of N and N_{60} with effective friction angle (ϕ') for cohesionless soils

Authors	Soil Type	ϕ' (deg.)
Dunham (1954)[1]	Uniform sands	$(12*N)^{0.5} + 20$
Ohsaki (1959)[1]	Sandy	$(20*N)^{0.5} + 25$
Muromachi et al. (1974)[1]	Granular	$3.5*(N)^{0.5} + 20$
Schmertmann (1975)[2]	Sand	$\tan^{-1}[N/(12.2+20.3\ (\sigma'_{v0}/p_a))]^{0.34}$
Wolff (1989)[3]	Cohesionless	$27.1 + 0.3N_{60} - 0.00054*N_{60}^2$
Japan Road Association (1990)[1]	Sandy	$(15*N)^{0.5} + 15$
Hatanaka & Uchida (1996)[3]	Sand	$(20*N_{60} * C_N)^{0.5} + 20$
Hettiarachchi & Brown (2009)	Sand	$\beta'\tan^{-1}[(0.2N_{60})/(K*(\sigma'/p_a)) - 0.68B]$

σ'_{v0}/p_a – effective overburden pressure normalized by atmospheric pressure [2]
C_N – correction factor [3]
β' – constant of proportionality [3]
K – coefficient of lateral earth pressure [3]
σ' – effective overburden pressure [3]
p_a – atmospheric pressure [3]
B – parameter depending on the relative density of sand, varies between 0 and 1 [3]
[1] As referenced by Baxter et al. (2005)
[2] As referenced by Kulhawy & Mayne (1990)
[3] As referenced by Hettiarachchi & Brown (2009)

Table 2.3 – Relationship of approximate undrained shear strength normalized by atmospheric pressure (S_u/p_a) versus N for cohesive soils from Terzaghi and Peck (1967) (As referenced by Kulhawy & Mayne (1990))

N	Consistency	Approximate S_u/p_a
0 - 2	Very soft	< 1/8
2 - 4	Soft	1/8 – 1/4
4 - 8	Medium	¼ - ½
8 - 15	Stiff	½ - 1
15 - 30	Very stiff	1 - 2
> 30	Hard	> 2

Table 2.4 – Correlations of N and N_{60} with undrained shear strength (S_u) for cohesive soils

Author(s)	Soil Type	S_u (kPa)
Terzaghi & Peck (1967)[1]	Clay	6.25N
Sanglerat (1972)[1]	Clay	12.5 * N
Sanglerat (1972)[1]	Silty clay	10 * N
Hara et al. (1974)	Clay	$29 * (N)^{0.72}$
Stroud (1974)[3]	London clay	$4.4 * (N_{60})^{0.72}$
Schmertmann (1975)[5]	High plasticity clay	12.5N
Schmertmann (1975)[5]	Medium plasticity clay	7.5N
Schmertmann (1975)[5]	Low plasticity clay	3.75N
Sowers (1979)[1]	High plasticity soil	12.5 * N
Sowers (1979)[1]	Medium plasticity clay	7.5 * N
Sowers (1979)[1]	Low plasticity soil	3.75 *N
Wroth et al. (1979)[4]	Clay	$(0.243 * (N)^{0.761})p_a$
Nixon (1982)[1]	Clay	12 * N
Ajayi & Balogun (1988)[1]	Fine-grained soil	1.39N + 74.2
Kulhawy & Mayne (1990)[5]	Fine-grained soil	$29N^{0.72}$
DeCourt (1990)[1]	Clay	$15 * N_{60}$
Sivrikaya & Togrol (2006)	Clay	$6.90 * N_{60}$
Hettiarachchi &Brown (2009)[1]	Fine-grained soils	$4.1 * N_{60}$
Nassaji & Kalantari (2011)	Fine-grained soils	$(2.1 * N_{60}) + 17.6$

p_a – atmospheric pressure (kPa) [4]

[1] As referenced by Nassaji & Kalantari (2011)

[2] As referenced by Kulhawy & Mayne (1990)

[3] As referenced by Terzaghi, Peck, Mesri (1996)

[4] As referenced by Djoenaidi (1985)

[5] As referenced by Kalantary (2009)

Table 2.5 – Correlations of VS (m/s) with undrained shear strength (S_u) for cohesive soils

Authors	Soil Type	S_u (kPa)
Schultheiss (1985)[1]	Normally consolidated clays	$(8.95*10^{-2}) * V_s^{1.12}$
Dickenson (1994)[2]	San Francisco Bay area cohesive soils	$(1.34*10^{-3}) * V_s^{2.11}$
Yun et al. (2006)[3]	Gulf of Mexico high plasticity inorganic clays	$(2.65*10^{-4}) * V_s^{2.8}$
Kulkarni et al. (2010)	Soft clays	$(5*10^{-4}) * V_s^{2.5}$

[1] As referenced by Blake and Gilbert (1997)
[2] As referenced by Wair et al. (2012)
[3] As referenced by Kulkarni et al. (2010)

Table 2.6 – Correlations of N and N_{60} with VS – 'all' soils

Authors	Location	VS (m/s)
Kanai (1966)[2]	Japan	$19 N^{0.6}$
Ohba & Toriumi (1970)[1]	Japan	$84 N^{0.31}$
Imai & Yoshimura (1970)[1]	Japan	$76 N^{0.33}$
Fujiwara (1972)[1]	Japan	$92.1 N^{0.337}$
Ohsaki & Iwasaki (1973)[1]	Japan	$82 N^{0.39}$
Imai & Yoshimura (1975)[2]	Japan	$92 N^{0.329}$
Imai (1977)[1]	Japan	$91 N^{0.337}$
Ohta & Goto (1978)[1]	Japan	$85.35 N^{0.348}$
Seed & Idriss (1981)[1]	not provided	$61 N^{0.5}$
Imai & Tonouchi (1982)[1]	Japan	$97 N^{0.314}$
Jinan (1987)[1]	Shanghai	$116.1 (N + 0.3185)^{0.202}$
Sisman (1995)[1]	not provided	$32.8 N^{0.51}$
Iyisan (1996)[1]	not provided	$51.5 N^{0.516}$
Kiku et al. (2001)[1]	Turkey	$68.3 N^{0.292}$
Hasancebi & Ulusay (2007)	Turkey	$90 N^{0.309}$ ($r = 0.73$)
Hasancebi & Ulusay (2007)	Turkey	$104.79 N_{60}^{0.26}$
Maheshwari et al. (2010)	India	$95.64 N^{0.301}$ ($R^2 = 0.84$)
Maheshwari et al. (2010)	India	$90.75 N_{60}^{0.304}$($R^2 = 0.83$)
Tsiambaos & Sabatakakis (2011)	Greece	$105.7 N_{60}^{0.327}$

[1] As referenced by Hasancebi & Ulusay (2007)
[2] As referenced by Maheshwari et al. (2010)

Table 2.7 – Correlations of N and N_{60} with VS – sandy soils

Authors	Location	VS (m/s)
Shibata (1970)[2]	not provided	$32\ N^{0.5}$
Ohta et al. (1972)[2]	Japan	$87\ N^{0.36}$
Imai (1977)[1]	Japan	$80.6\ N^{0.331}$
Ohta & Goto (1978)[2]	Japan	$88\ N^{0.34}$
Japan Road Association (1980)[2]	Japan	$80\ N^{0.33}$
Sykora & Stokoe (1983)[1]	United States	$100.5\ N^{0.29}$
Lee (1990)[1]	Taiwan	$57.4\ N^{0.49}$
Pitilakis et al. (1999)[1]	Greece	$145\ (N_{60})^{0.178}$
Hasancebi & Ulusay (2007)	Turkey	$90.8\ N^{0.319}$ (r = 0.65)
Hasancebi & Ulusay (2007)	Turkey	$131\ N_{60}^{0.205}$
Maheshwari et al. (2010)	India	$100.53\ N^{0.265}$ (R^2 = 0.84)
Maheshwari et al. (2010)	India	$96.29\ N_{60}^{0.266}$ (R^2 = 0.83)
Brandenberg et al. (2010)	California	$87.8 * N_{60}^{0.253} * (P_a/\sigma'_v)^{-0.124}$
Tsiambaos & Sabatakakis (2011)	Greece	$79.7\ N_{60}^{0.365}$

P_a – atmospheric pressure (kPa) [3]
σ'_v – vertical effective stress (kPa) [3]
[1] As referenced by Hasancebi & Ulusay (2007)
[2] As referenced by Maheshwari et al. (2010)
[3] As referenced by Brandenberg et al. (2010)

Table 2.8 – Correlations of N and N_{60} with VS – clayey soils

Author(s)	Location	VS (m/s)
Imai (1977)[1]	Japan	$V_s = 80.2\ N^{0.292}$
Japan Road Association (1980)[2]	Japan	$V_s = 100\ N^{0.33}$
Lee (1990)[1]	Taiwan	$V_s = 114.43\ N^{0.31}$
Pitilakis et al. (1999)[1]	Greece	$V_s = 132\ (N_{60})^{0.271}$
Hasancebi & Ulusay (2007)	Turkey	$V_s = 97.9\ N^{0.269}$ (r = 0.75)
Hasancebi & Ulusay (2007)	Turkey	$V_s = 107.63\ N_{60}^{0.237}$
Maheshwari et al. (2010)	India	$V_s = 89.31\ N^{0.358}$ (R^2 = 0.93)
Maheshwari et al. (2010)	India	$V_s = 83.27\ N_{60}^{0.365}$ (R^2 = 0.92)
Tsiambaos & Sabatakakis (2011)	Greece	$V_s = 112.2\ N_{60}^{0.324}$

[1] As referenced by Hasancebi & Ulusay (2007)
[2] As referenced by Maheshwari et al. (2010)

Table 2.9 – Mechanisms to derive undrained shear strength (S_u) from pressuremeter testing parameters for cohesive soils

Method	**S_u (kPa)**
Limit pressure[1]	$(p_L - \sigma_{OH})/\beta$
Limit pressure variation[1]	$0.21\ (p_L - \sigma_{OH})^{0.75}\ p_a^{0.25}$
Yield pressure[1]	$p_y - \sigma_{OH}$
Gibson Anderson[1]	$(\sigma_{rr} - p_y)/\ \ln[(G/S_u)(\Delta V/V)]$
Baguelin et al. (1978)[1]	$0.67\ (p_L - \sigma_{OH})^{0.75}$
Menard (1957)[2]	$(p_L - p_0)/5.5$
Amar Jezequel (1972)[2]	$((p_L - p_0)/10) + 25$

p_L – limit pressure [1]
σ_{OH} – *in situ* horizontal stress [1]
β – correction factor [1]
p_a – atmospheric pressure [1]
p_y – yield pressure [1]
σ_{rr} – corrected pressuremeter pressure [1]
G/S_u – rigidity index (I_r), where G is shear modulus [1]
$\Delta V/V$ – volumetric strain [1]
p_0 – *in situ* total horizontal stress [2]
[1] As referenced by Briaud (1992)
[2] As referenced by Bahar et al. (2013)

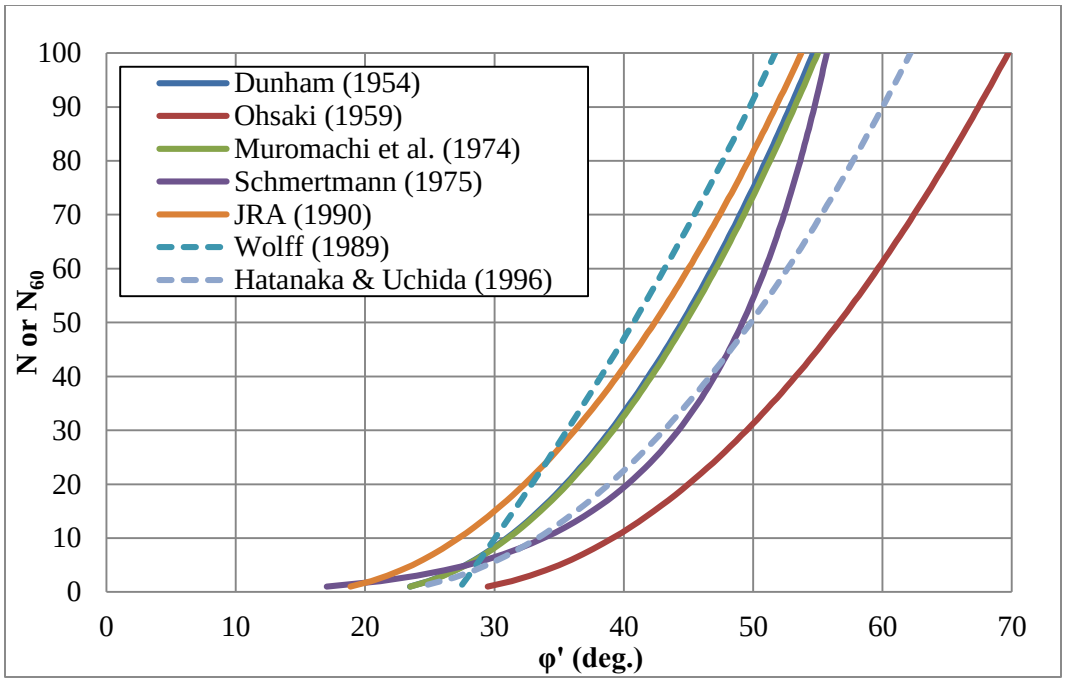

Figure 2.1: Equations from Table 2.2 – N or N_{60} versus effective friction angle (φ′) for cohesionless soils; dashed lines represent correlations using N_{60} as opposed to those using N (solid lines).

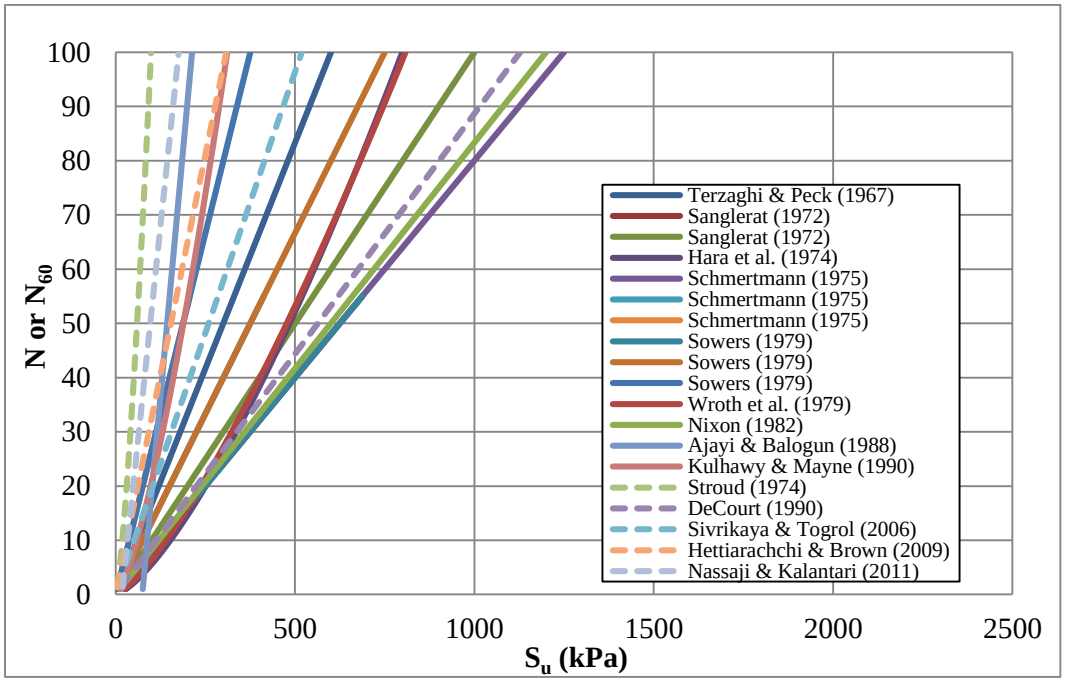

Figure 2.2: Equations from Table 2.4 – N or N_{60} versus undrained shear strength (S_u) for cohesive soils; dashed lines represent correlations using N_{60} as opposed to those using N (solid lines).

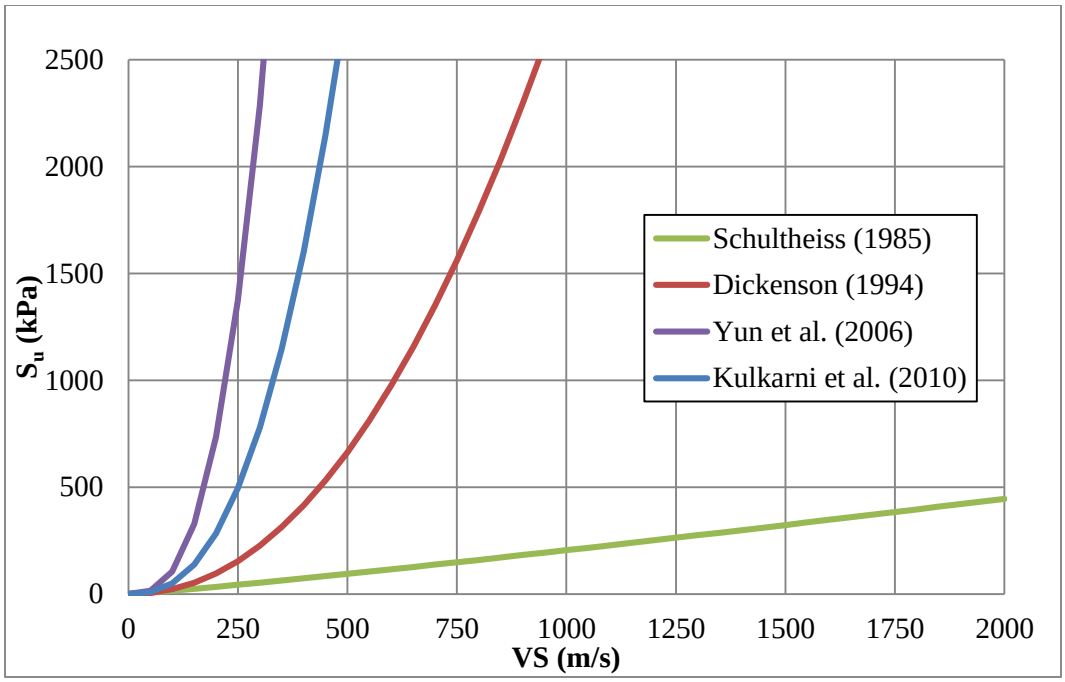

Figure 2.3: Equations from Table 2.5 – VS versus undrained shear strength (S_u) for cohesive soils

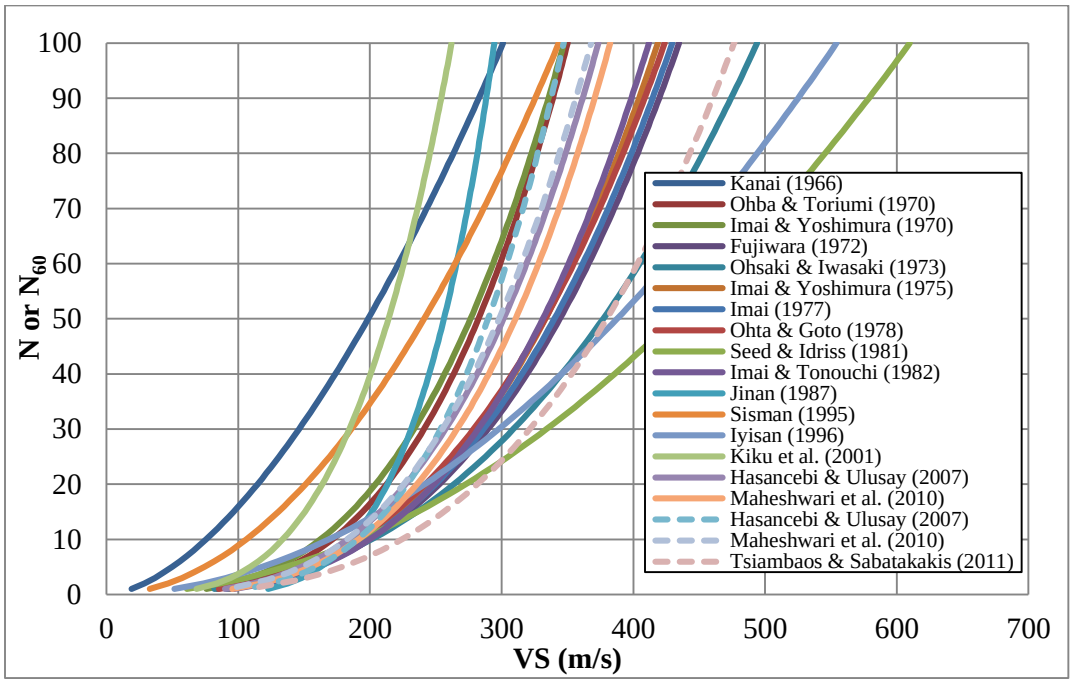

Figure 2.4: Equations from Table 2.6 – VS versus N or N_{60} for 'all' soils; dashed lines represent correlations using N_{60} as opposed to those using N (solid lines).

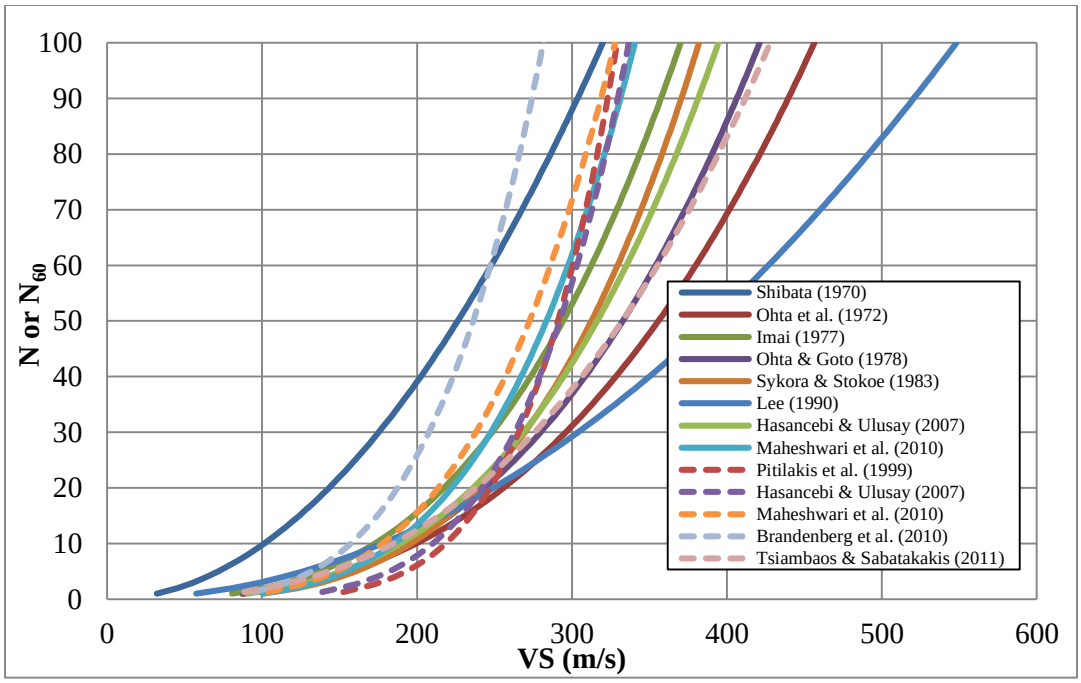

Figure 2.5: Equations from Table 2.7 – VS versus N or N_{60} for sandy soils; dashed lines represent correlations using N_{60} as opposed to those using N (solid lines).

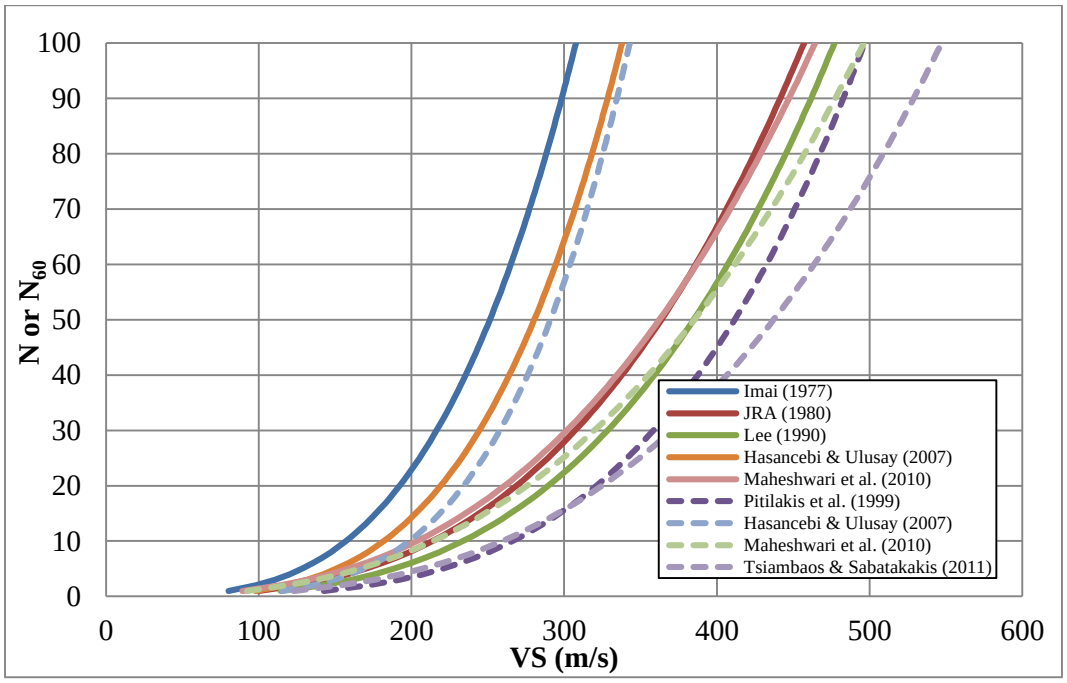

Figure 2.6: Equations from Table 2.8 – VS versus N or N_{60} for clayey soils; dashed lines represent correlations using N_{60} as opposed to those using N (solid lines).

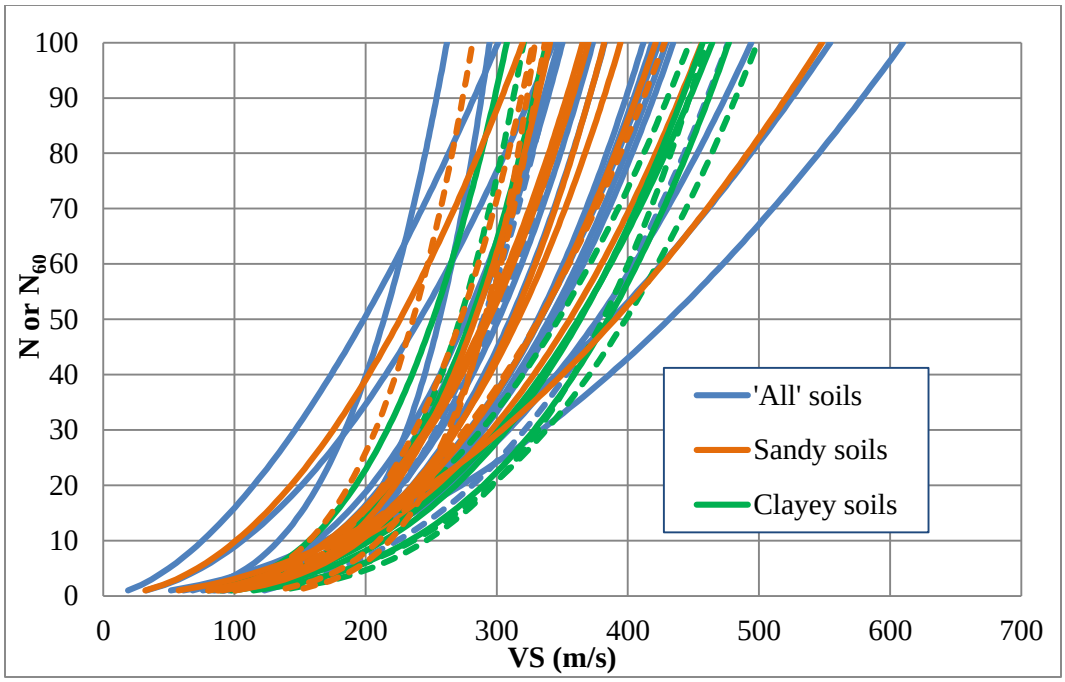

Figure 2.7: Equations from Tables 2.6, 2.7, and 2.8 – VS versus N or N_{60} for 'all', sandy, and clayey soils plotted together; dashed lines represent correlations using N_{60} as opposed to those using N (solid lines).

CHAPTER 3

DOWNHOLE VELOCITY TESTING AT US 95/CC 215 INTERCHANGE

Parts of this chapter were published for the International Foundations Congress and Equipment Expo 2015 as a technical paper (Samuel et al., 2015). Co-authors are Yasaman Badrzadeh, Barbara Luke, Andrew Lawrence, Raj Siddharthan, and Abbas Bafghi. The author of this thesis is the first author for the manuscript of the technical paper and led the team in downhole seismic testing and data acquisition. The author was responsible for the analysis and processing of the downhole data as described in this chapter in order to obtain velocity profiles. The author wrote the first draft of the technical paper and addressed all editorial comments from co-authors and reviewers.

This chapter discusses the seismic field testing conducted at the United States 95 (US95) / Clark County Beltway 215 (CC215) Interchange, a proposed System-to-System freeway interchange located in northwest Las Vegas, Clark County, Nevada (Figure 3.1). Drilled shafts were selected as the primary foundation type for the flyover ramps of the project due to the congested nature of the area and the heavy loadings to be supported. Test shafts were constructed for Osterberg cell® load testing, to get a better understanding of the capacity of the proposed drilled shafts. Note that much of the author's work predated the construction of the tests shafts. As part of this study, the author conducted downhole velocity testing with the purpose of comparing co-located velocity profiles with sediment classification and blow counts from SPT, in order to investigate trends that benefit deep-

foundation design. Note that the analysis of laboratory strength data and comparison of VS and N to test shaft performance is beyond the scope of this thesis.

3.1. Site description

The project site is in the northwest part of the LVV. It is located in a transition zone between gently sloping alluvial fans and more flat-lying valley-fill deposits. It is underlain primarily by coarse-grained deposits derived from coalescing alluvial fans (Kleinfelder, Inc., 2011). According to a 3-D lithological model developed by the UNLV Applied Geophysics Center (AGC) (Luke et al. 2009), depth to Miocene-aged indurated sediments at the site is about 200 m, while depth to Paleozoic bedrock is 1 km or more.

3.2. Borehole data

Investigatory boreholes were drilled to ~39-m depth by NDOT at each of two sites of planned test shafts located about 400 m apart (Figure 3.1). The boreholes were sampled continuously in the upper 18 m and for 0.91 m every 1.52 m for the remaining depth. The soil sampling was accomplished using a combination of standard penetration sampler, modified California sampler, and Shelby tube (thin-walled sampler). Soil-sampler blow counts (both standard and modified California samplers) were collected at each interval, and all the recovered samples were characterized using visual/manual procedures (ASTM D2488-09a), which were confirmed by means of laboratory testing (ASTM D2487-11). Laboratory testing for moisture content, compressibility and strength was conducted on selected samples. Borehole logs, obtained from NDOT, are shown in Appendix A.

3.2.1. Sediment classification and moisture

Fig 3.2 shows simplified sediment logs for the two holes. Sediments are broadly classified into their predominant sediment types: clay, silt, sand and gravel. For example, clayey sand with gravel is classified as sand, and sandy fat (high-plasticity) clay is classified as clay. Sediments logged as having any amount of cementation, ranging from weak to strong, are denoted as cemented sediments, regardless of predominant sediment class. Note that almost every material description in the borehole logs included clay.

The boring at the location of Test Shaft 1 (Fig. 3.1) is referred hereon as Hole 1. From the surface to 17 m, Hole 1 is characterized by dry to moist, stiff to very hard, variable, clayey soils ranging from sandy clays to clayey gravels and having fines ranging from low to high plasticity. Thin layers of silty gravel and sandy silt were also logged. The sediments transition from dry to moist at 9.6 m, in a lean clay with sand. A carbonate cemented horizon extends from 17.4 m to 18.9 m; the degree of cementation noted in the logs ranges from moderate to strong. The natural water table is found immediately below the cemented horizon at 18.9 m. This depth was established from field observation of boreholes after they had been left open for a few weeks and confirmed through moisture content tests in the lab (Andrew Lawrence, NDOT, personal communication, November 6, 2014). Below this depth are saturated, stiff to very hard, clayey soils, with low to moderate plasticity and some silt.

The westernmost of the two borings, at the location of Test Shaft 2 (Fig. 3.1) is referred hereon as Hole 2. In the upper 19 m, sediments are mostly predominantly coarse-grained

with a few layers of predominantly fine-grained sediments. Below 19 m are predominantly clay sediments, with a couple of cemented layers present. Hole 2 is characterized by dry to saturated, stiff to very hard, variable, clayey soils, ranging from clayey gravels to gravelly clays, with intermediate layers of lean clay, clayey sand, and silty gravel. Cemented layers with thickness of ~1.4 and ~1.3 m lie at about 27 and 32 m depths respectively; the degree of cementation ranges from weak to strong. Below the cemented layers are stiff to very hard, clayey and silty sediments. The sediments transition from dry to moist at 15.5 m. The transition from dry-to-moist occurred in a thick layer of clayey gravel with sand, about 4 m above the observed groundwater table, which was encountered at 19.1 m, close to the depth to groundwater for Hole 1. The cementation in both holes was insufficiently continuous to yield intact (unbroken) core specimens.

3.2.2. Blow counts

Blow counts were reported in the borehole logs. While driving the SPT sampler, the number of blows applied is counted as stated earlier, until one of the following limiting blow counts occurs (ASTM D1586-11):

- A total of 50 blows have been applied during any one of the three 0.15-m (0.5-ft) increments
- A total of 100 blows have been applied.
- There is no observed advance of the sampler during the application of 10 successive blows of the hammer.

These limiting blow count criteria are considered as ‘penetration refusal’. Tests that met refusal were reported in the borehole logs by the number of blows for the distance advanced in feet, such as 50 blows for 0.4 feet. Here, the author converts penetration refusal values to ‘equivalent total’ N as if the sampler were to be advanced to completion, at the same rate. For instance, if the blow count is reported as 50 blows for 0.4 feet, the ‘equivalent total’ N over the full 1 foot is 125.

N are obtained from SPT samplers (ID = 1.3 inch, OD = 2 inch) and Modified California (MC) split spoon samplers (ID = 2.4 inch, OD = 3 inch), also known as ring samplers. Non-standard N from MC samplers are converted to SPT-equivalent N using a conversion factor of 0.62 developed by NDOT using an in-house database (Andrew Lawrence, NDOT, personal communication, November 6, 2014). The boreholes were drilled with NDOT Drill Unit 1627 which has an ER of 74% (Andrew Lawrence, NDOT, personal communication, November 6, 2014). As explained earlier, the ratio of ER to the standard 60% hammer efficiency yields an energy correction of 1.23, which is applied to N to obtain N_{60}.

3.3. Seismic testing

Downhole body wave (compression and shear) measurements were conducted per ASTM D7400-08 in both holes, which had been cased with 2.5-inch diameter PVC. The casing was installed to 38.5 m and 29.2 m depths in Holes 1 and 2 respectively. Depth of casing for Hole 2 was short because the hole caved in; the caving of soils might be explained by the presence of gravelly clays and weakly cemented materials just below the depth of

casing. Casing was grouted in place with a bentonite-cement mixture. For installation, the casing had been filled with water, which was bailed before seismic testing. The top of the casing was 1.05 m and 0.93 m above the ground surface in Holes 1 and 2 respectively.

The downhole measurement depths were not in integer values with respect to the ground surface because the depth reference was the top of casing; therefore measurements were actually at 0.95, 1.95, 2.95 etc. and at 1.07, 2.07, 3.07 etc. meter depths with respect to the ground surface in Holes 1 and 2 respectively. Downhole measurements in Hole 1 were recorded as conducted to 41.95 m, which is (inexplicably) beyond the reported depth of the casing. Measurements in Hole 2 were conducted to 27.07 m, just above the reported bottom of casing. Measurements were made at 1-m depth intervals in both holes, except beyond 37.95 m in Hole 1, where the last two measurements were made at 2-m depth intervals. A sledgehammer fitted with an inertial trigger switch was struck vertically on an aluminum plate placed on the ground ~1.5 m from the borehole to generate compression waves. Shear wave energy was generated by striking with the same hammer the end of a large wooden beam placed ~1.5 m from the borehole, held in contact with the ground by the weight of a truck; layout was as presented by Crice (2011). Both ends of the wooden beam were struck to produce shear waves with opposite polarities. A Geostuff downhole tool containing triaxial, 40-Hz geophones and a Geometrics Geode seismograph were used to collect data; the downhole geophones were oriented with respect to the magnetic north. Other geophones placed on the surface near the strike plate and shear beam were used to verify accurate triggering. In order to align the system for shear, the shear beam was placed in the magnetic East-West direction and

the surface geophone axis was oriented in the direction of energy input from the hammer. Orientation was done by eye using a hand-held magnetic compass. Individual records and stacks of three or more records were collected at each depth. The sampling rate was 20.833 μs and record length was 0.5 s with a signal delay of -0.01 s for both compression and shear measurements.

MASW-type surface wave testing was conducted independently, led by Yasaman Badrzadeh of UNLV AGC in the vicinity of Hole 2. MASW is a surface wave seismic technique that can use an impulsive signal, such as a sledgehammer or weight drop, to generate surface waves; usually, the fundamental mode Rayleigh wavefield generated by the impulsive source is used to obtain VS (e.g., Stephenson et al., 2005). The MASW testing conducted at this site was reported in more detail by Samuel et al. (2015). Here, the VS profile generated from Badrzadeh′s MASW testing is compared with the downhole VS measurements.

In addition, NDOT conducted complementary seismic testing at the site that is to be compared with results from this study at a later date.

3.3.1. Processing and analysis

Downhole data were converted from SEG-2 to .txt format using TomTime software. Geogiga Front End 7.1 was used to visually select downhole data records with good signal-to-noise ratio for each depth measurement, because multiple records were collected at each depth. Individual records provided good signal-to-noise ratio in most

cases; some stacked records for depths beyond 16 m, mostly for compression data, were used for Hole 1. The selected compression and shear time histories were plotted with respect to depth using MATLAB and arrival times were picked visually, with great care, through an iterative process. Time histories were scaled individually to aid in picking of arrival times. Compression wave arrivals were picked first; these were used to constrain picks for shear arrivals.

The direct method described by Kim et al. (2004; Fig. 3.3) was applied to develop velocity profiles from the arrival picks. In this method, for every depth tested (D), provided the trigger is accurate (checked with surface geophone), the picked arrival time is assumed to be the straight-ray-path travel time (t). The equivalent travel time for a vertical path (t_c) is

$$t_C = D \ \frac{t}{R} \tag{3.1}$$

where R is the straight-line distance between source and downhole geophone (Kim et al., 2004). The t_c values are plotted with respect to D (e.g., Fig. 3.3). The data are interpreted by visually identifying different slopes and manually fitting line segments, each representing a layer whose velocity is equal to the slope of the fitted line segment.

First arrival picks for both compression and shear are chosen by careful visual inspection of the seismic waves recorded. It is difficult to pick first arrivals with necessary precision. The process used is as follows. The time histories are plotted jointly in order of increasing depth. The time at which the first peak in the wave (compression or shear) begins (i.e., onset of the pulse) is selected as the first arrival pick. Picks are selected from

the top to bottom to maintain a consistent distance-time relationship. (Arrival times are required to increase with increasing depth.) The author calculated the fastest and slowest possible arrival times for each depth based on Kim et al. (2014); this range of predicted first arrival times assists in deciding whether the first arrival picks chosen are reasonable. In some cases where the first arrival picks are not within the predicted range, they were still considered reasonable if the chosen first arrival pick is in agreement with the slope of adjacent picks and/or is at the onset of the first wave. Shear picks are more challenging than compression picks, therefore shear wave records of opposing source polarities are superimposed on each other to better identify the onset of the first shear wave. In addition, all shear first arrival picks were required to occur after the compression first arrival picks. Difficulty in picking of first arrivals generally increased with increasing depth, likely due to signal attenuation. Distortion of wave trains, likely caused by signal refraction and scattering due to 3-D variability, particularly in the presence of high impedance contrasts (e.g., cemented media juxtaposed against relatively soft uncemented clay) also made picking first arrivals challenging. Time histories with finalized first arrival picks for compression and shear for both holes are shown in Figures 3.4 through 3.7. The last two time histories in Hole 1 at ~ 40 and ~ 42 m have the poorest quality. Assessment of reasonableness of VP was based on the author's confidence in arrival picks and agreement with published VP values for similar sediments. The author finds 38 of the 40 first arrival picks for compression time histories in Hole 1, 36 of the 40 first arrival picks for shear in Hole 1, 25 of the 27 first arrival picks for compression in Hole 2, and 23 of the 27 first arrival picks for shear in Hole 2 to satisfy the selection criteria.

VS profiles were developed in a similar way. Poisson's ratio was calculated for trial VS values using finalized VP. VS was finalized on the basis of the author's confidence in shear picks and on whether it provides Poisson's ratio that fits with published values for similar sediments. Typical values from the literature of VP, VS and Poisson's ratio that were used in these assessments are given in Tables 3.1, 3.2, and 3.3 respectively.

Figures 3.8 through 3.11 show the interpretations of first arrival times resulting in compression and shear wave velocity profiles for Holes 1 and 2. As explained earlier, line segments are fitted on the first arrival time data to represent different velocity layers based on the slope of each line segment. The interfaces of the velocity layers are determined visually based on the change in slope of the data. The slope determined for each layer provides velocity averaged over the thickness of the layer, which is several meters thick. Note that the velocity layer interfaces were forced to match between compression and shear waves. Hole 1 has three layers. VP is calculated to be 755 m/s, 1151 m/s, and 2275 m/s with interfaces at 14 m and 27 m. VS is 491 m/s, 299 m/s, and 513 m/s with interfaces at 14 m and 27 m as well. In order to understand the goodness of fit of the manually fitted line segments on the data, R^2 of each line segment with respect to the data points is calculated manually. For Hole 1, the R^2 of the line segments corresponding to VP1, VP2, and VP3 of Figure 3.8 are 0.98, 0.99, and 0.78 respectively. Similarly, the R^2 of the line segments corresponding to VS1, VS2, and VS3 of Hole 2 (Figure 3.9) are 0.98, 0.98, and 0.98 respectively. As shown in Figures 3.10 and 3.11, Hole 2 has a two-layer velocity profile for VP with an interface at 14 m, while it has a four layer velocity profile for VS with interfaces at 14 m, 19 m, and 24 m. VP is

calculated to be 813 m/s above its transitional depth and 1664 m/s below it. VS is 531 m/s, 894 m/s, 206 m/s and 347 m/s for layers 1, 2, 3, and 4 respectively. For Hole 2, the R^2 of the line segments corresponding to VP1 and VP2 of Figure 3.10 are 0.97 and 0.94 respectively. Similarly, the R^2 of the line segments corresponding to VS1, VS2, VS3, and VS4 of Figure 3.11 are 0.99, 0.99, 0.98, and 0.99 respectively.

There are several sources of uncertainty involved in the process of conducting downhole velocity testing and its interpretation to determine velocities of subsurface sediments. Deviation of boreholes during construction, improper calibration of the downhole device, imprecise positioning of the source and receiver, and errors in orientation of geophones could cause errors in measurement. Another source of error is the straight-line ray path assumed in the direct method by Kim et al. (2004) which does not take into consideration the refraction of waves, which is likely in layered systems having strong stiffness contrasts, as with sporadic cementation.

The author attempted to analyze the downhole seismic data and interpret layered (stair-stepped) velocity models to account for refractions across layer boundaries using a code written in R, an open source language, by Eric M. Thompson at San Diego State University (Thompson, 2007). Thompson (2007) presents an algorithm that automatically finds layer-interfaces, which is expected to increase the efficiency of the picking and interpretation processes. After many iterations, the author was unable to obtain a result that yielded acceptable Poisson's ratio values, and therefore decided to proceed with the more straightforward and more general direct method of Kim et al. (2004).

3.4. Discussion

The VP, VS and Poisson's ratio for Hole 1 are shown in Figure 3.12. Simplified sediment logs with predominant sediment types and N_{60} from both standard and Modified California samplers are shown as well. N_{60} values over 100 are assigned numerical values of 100 for plotting purposes so that they won't overly skew the plots. The actual blow count values are reported in Appendix A. VP increases with increasing depth. VS remains fairly constant at ~500 m/s, although it decreases by ~40% in layer 2, from 14 m to 27 m. The layer 1 (L1) to layer 2 (L2) velocity transition boundary is in thinly layered sediments, while L2 to layer 3 (L3) transition is in a thick, predominantly clay unit. The L1-L2 boundary corresponds with the dry-to-moist transition depth (Fig. 3.2). N_{60} values in L1 range mostly between 15 and 50. Beyond the L1-L2 boundary, N_{60} ranges mostly between 50 and 100, with some over 100. The higher N_{60} corresponds with the presence of cemented sediments between 17 m and 19 m and stiffer clays below 19 m. The reduction in VS in L2 does not agree with the presence of cementation as well as higher N_{60} reported in the borehole logs in this region, and therefore reduces the author's confidence in the intermediate low-velocity layer. L2 also has the lowest N_{60} that was encountered in Hole 1, which supports the evidence for the lower VS value for L2. Note that the author expressed high confidence in the arrival picks and goodness of fit of the manually fitted line segments for L2 in Hole 1 before comparing it with other available data. For L3, N and VS values both imply stiffer material, as described in the logs.

Corresponding results for Hole 2 are shown in Figure 3.13. A four-layered profile with the same VP of 1700 m/s for layers 2, 3, and 4 is identified. The velocity transition depths are at 14 m, 19 m and 24 m, as stated earlier. The L1-L2 transition corresponds approximately to the depth at which moist soil was encountered (15.5 m). Similar to Hole 1, VP increases with increasing depth. VS increases with increasing depth for L2, but in L3 it decreases by ~77% with respect to L2. The increase in VS in L2 coincides with the 'very dense' notation in borehole logs and corresponds to a thick layer of clayey gravel with sand. The reduction of VS in L3 is consistent with the presence of silty, lean clay, below the L2 clayey gravel. This distinction in sediments does not appear in the simplified sediment log; therefore classifying sediments by predominant sediment type may not be effective for identifying cause of velocity transitions, as it is not solely the predominant sediment that governs soil characteristics. VS increases slightly in layer 4 (L4) with respect to L3, corresponding to the presence of gravelly clays and cemented sediments. (Recall that Appendix A contains detailed sediment lithology in the borehole logs.) The velocity transitions at L1-L2, L2-L3 and L3-L4 correspond to approximate sediment boundaries. In Hole 2, N_{60} values range close to 100 or over 100 in the upper 6 meters of L1. These high N_{60} values correspond to the presence of gravel. From 6 m to the L1-L2 transition, N_{60} are mostly under 50. Below the L1-L2 transition, N_{60} is mostly above 50 with some over 100. The higher N_{60} values below the L1-L2 transition correspond to the presence of gravels, stiff clays and cemented sediments. In both holes, seismic velocities correspond to N_{60} only occasionally. Neither seismic velocities nor N_{60} is more informative than the other, but when complemented with each other provide

valuable insight regarding stiffness and relative density of sediments and their variability with respect to depth.

A side-by-side analysis of the velocity and Poisson′s ratio profiles from Holes 1 and 2 is shown in Figure 3.14. The two holes have comparable VS and VP in the upper 14 m. The VP is a strong indicator of soil moisture, it increases to a value close to that for water (~1500 m/s) at the depth where moist soil is encountered (presumably due to capillary rise) in Hole 2. VP in Hole 1 increases to ~1150 m/s at ~14 m, about 4 m below its logged dry-to-moist transition depth, but above the recorded groundwater table. VP in Hole 2 increases to about ~1600 m/s at 14 m as well. Because both holes show an increase in VP close to the VP of water around 14 m, velocity data indicates that a significant change in moisture content occurs at that depth at the site. From depths of about 14 m to 27 m (end of testing for Hole 2), the VP for Hole 2 is ~45% higher than VP for Hole 1, however just below ~27 m the VP for Hole 1 jumps to almost 2300 m/s. In Hole 1, the VP for L2 is about equal to the average of the velocities of L1 and L3. The VS is a better indicator of sediment stiffness than VP. VS of ~500 m/s in the top ~14 meters for both holes is consistent with the presence of the mostly dry, very dense gravel and sand, and sandy clay that were logged. (Refer to typical values for these sediment types in Table 3.2.) Low VS ranging from ~200 m/s to ~350 m/s observed between 19 m and 27 m in both holes is consistent with the presence of stiff clays that were logged. (Refer to typical values for this sediment type in Table 3.2.)

Poisson's ratio for both holes ranges from 0.13 to 0.48, with a distinct increase at about 14 m, where moisture was encountered and VP jumps closer to the expected VP of water (~1500 m/s). For both holes, Poisson's ratio of 0.13 was calculated in the upper layer (0 to 14 m). This value is consistent with the Poisson's ratio of unsaturated clay (Table 3.3), which is logged in the upper 14 m of the boreholes. In Hole 2, Poisson's ratio of 0.3 is calculated for layer 2; this value falls within the typical range of Poisson's ratio for gravelly sand (Table 3.3). Poisson's ratio of over 0.45, which is consistent with saturated clay (Table 3.3) is calculated below depths of 14 m and 19 m in Holes 1 and 2 respectively.

A comparison of VS profiles from the downhole testing of Holes 1 and 2 with VS from MASW testing conducted near Hole 2 (Samuel et al., 2015), as well as two sets of sediment-specific "reference" VS profiles is shown in Figure 3.15.

One reference VS profile set is specific to the Las Vegas Valley (Murvosh et al., 2013b). It was defined by Murvosh et al. (2013b) in the course of building a 3-D VS model for the LVV. The model is based on more than 200 VS profiles and 1,400 geologic well logs. Characteristic VS profiles were developed for five sediment units in the LVV - clay, sand, gravel, mixed and cemented sediments. These characteristic VS profiles were produced by correlating pairs of VS measurement sites and sediment lithology from wells located within 500 m or less of one another (Murvosh et al., 2013b). Characteristic VS profiles of clay, sand and gravel by Murvosh et al. (2013b) are compared in this study.

The other reference VS profile set comes from farther afield. Lin et al. (2014) provide parameters to generate sediment-specific VS profiles for dense sand, dense gravel and 'Imperial Valley soft sands, silts and clays', which are referred to as sand, gravel and clay, respectively in this study. According to the authors, the 'Imperial Valley soft sands, silts and clays' as the name suggests are from Imperial Valley, California; the parameters for dense sands and dense gravels were obtained from the work of Menq (2003). According to Menq (2003), data for dense sands and gravels come from laboratory testing of 59 reconstituted specimens from the United States; for 49 of the specimens, material was sourced from the Pence Ranch site in Idaho, from sediments that liquefied during the Borah Peak earthquake. VS for this set was calculated using Equation 3.2:

$$VS = A_s \, (\sigma'_o / P_a)^{n_s} \tag{3.2}$$

where A_s and n_s are constants specific to sediment type, provided by Lin et al. (2014). Densities needed to compute effective stresses were derived from VP as shown in Equation 3.3, following recommendations by Boore (2007):

$$\rho = 1.74 \, VP^{0.25} \tag{3.3}$$

where ρ is in g/cm^3 and VP is in km/s. VP from Hole 1 was used to derive densities. For the upper layer where VP = 755 m/s, ρ = 1622 kg/m^3, for the intermediate layer where VP = 1151 m/s, ρ = 1802 kg/m^3, and for the lower layer where VP = 2275 m/s, ρ = 2137 kg/m^3. These densities of 1622 kg/m^3, 1802 kg/m^3, and 2137 kg/m^3 are typically seen in clayey, sandy, and gravelly soils respectively (Subramanian, 2008). The densities calculated for the upper and lower layers are in agreement with the predominant presence of clays in Hole 1, while the density calculated for the intermediate layer is lower than what is expected of gravelly soils present in this layer in Hole 1.

The reference VS for local sediments is consistently and significantly higher than for the more generic reference set (Figure 3.15). This difference could be due to the dense configuration of local sediments and the preponderance of carbonate cementation. For the same depth of the reference profiles, VS increases with increasing grain size of predominant sediment type: clays have lower VS than sands, which have lower VS than gravels. The downhole VS profiles for the study site tracked with the VS from the local MASW measurement (performed close to Hole 1; ref. Figure 3.1) and local reference profiles in the upper ~15 m. The VS of L2 in Hole 1 from this study was slower than the MASW VS and local profiles, falling between the generic reference curves (from Lin et al., 2014) for dense sand and dense gravel. The VS of L2 in Hole 2 is much higher than both reference profiles and the MASW profile, and becomes much lower than them in layer 3, after which it falls close to the generic reference curve for sand in the vicinity of the cemented layer. The VS in L3 of Hole 1 is best represented by the local reference profile for clay. Local VS measurements agree more closely with local reference profiles than the more generic reference profiles. In the upper 27 m, VS from MASW represents approximately the average velocity of the two layers in Hole 1. Beyond 27 m, VS from MASW is ~ 35% higher than VS from downhole velocity testing in Hole 1.

Differences between the VS profiles from downhole and MASW measurements are expected because test locations differ (Fig. 3.1) and because of the measurement geometry. An array-based test on the ground surface such as MASW will average subsurface properties over ever-increasing volumes as depth increases. Therefore, we

would expect to see less layer-to-layer variability in the MASW profile than in the downhole profiles, and the MASW profile should represent an average of the velocities measured in a co-located downhole test. As expected, the MASW profile shows much less variability than the downhole profiles.

VS from downhole testing is plotted with corresponding N_{60} values in Figure 3.16; data are distinguished by predominant sediment type. Note that N_{60} values over 100 are not distinguished in plots hereon in this thesis; most N_{60} values over 100 are extrapolated by the author from a refusal number. Comparisons are hindered because of the nature of the two datasets; the N_{60} applies to a unique point, while the VS obtained from the direct method is representative of a layer that is several meters thick, as explained earlier. As explained earlier, all N_{60} values over 100 are assigned numerical values of 100. Recall that clay is present in most sediments, even those that are predominantly coarse grained. Gravels have the widest range of VS, from ~300 m/s to 900 m/s. As expected, the highest and lowest VS are in gravels and clays respectively. Clay is the most predominant sediment type. N_{60} is highly variable with respect to VS within sediment type. Two of the three cemented sediment specimens have N_{60} values over 100. 100-plus N_{60} is found in all sediment types, except silt which has a small sample size (two). A very weak trend (R^2 = 0.07) of VS increasing linearly with increasing N_{60} is observed in gravels. On the contrary, another weak trend (R^2 = 0.1) of VS decreasing linearly with increasing N_{60} is observed in clays. R^2 values obtained from linear fits of the data were higher than R^2 values obtained from exponential fits, therefore linear fits were chosen instead of exponential fits. Values of VS at N_{60} =100 were included while plotting best fit lines for

clay and gravel, while values of VS with N_{60} over 100 were not. Trends were not computed for sands or silts because of their small sample sizes.

Following the testing presented here, two Osterberg cell® load tests were conducted by NDOT as planned. According to Andrew Lawrence (NDOT, personal communication, October 15, 2014), the test shafts indicated relatively low strengths in the upper, dry, sediment layers; however, the results were quite variable. Weakly to strongly cemented sediments exhibited high strengths as anticipated. The saturated clay layers below the groundwater table showed higher than expected strengths, at times two to three times those of the upper dry sediments. The results between the two test shafts were similar, indicating that the results are representative of the soils in the area of the interchange. The low strengths in the upper, dry sediment layers agree with the low VS (~500 m/s) obtained from this study, however VS from deeper depths do not correspond to the high strengths of the cemented sediments or saturated clay layers indicated from the load tests. Most N_{60} values in the upper layers are lower than 50 corresponding to low strengths, while most N_{60} at deeper depths are over 50 and close to 100 corresponding to higher strength; hence N_{60} values are mostly in agreement with Osterberg cell® test results.

Summary *In situ* seismic measurements were conducted in advance of drilled-shaft Osterberg cell® load tests, at a site in the LVV known to have strong carbonate cementation and dense sediments. These are materials whose strengths and stiffnesses are difficult to characterize by more traditional and straightforward means. Downhole VP and VS profiling complemented logging of the sediment lithology of boreholes and

penetration testing of soil samples. VS is a better indicator of sediment stiffness than VP, while VP results reflect the depth to moist soil. The local VS measurements are more consistent with expectations from local reference profiles than more generic reference profiles; the reference VS for local sediments is consistently and significantly higher than for the more generic reference set. This outcome implies that a design that is based on global standards for such sediment types would be over- conservative. Neither blow counts nor VS is a straight surrogate for shear behavior of sediments. No strong trend is observed between blow counts and downhole VS for this small dataset, likely due at least in part to different volumes of material represented with the two tests. In spite of the lack of correlation between blow counts and VS, they provide information relevant to deep foundation design along with sediment lithology.

Table 3.1 – Typical values of VP for soils (As referenced by Mavko (2005))

Description	VP (m/s)
Scree, vegetal soil	300 - 700
Dry sand	400 - 1200
Wet sand	1500 - 2000
Saturated clay	1100 - 2500
Marl	2000 - 3000
Limestone	3500 - 6000

Table 3.2 – Typical values of VS for soils

Description	VS (m/s)
Soft soil[1]	100 - 200
Scree, vegetal soil[2]	100 - 300
Stiff clays and sandy soil[1]	200 - 375
Gravelly soil[1]	375 - 700
Dry sand[2]	100 - 500
Wet sand[2]	400 - 600
Saturated clay[2]	200 - 800
Marl[2]	750 - 1500
Limestone[2]	2000 - 3300

[1] As referenced by Subramanian (2008)
[2] As referenced by Mavko (2005)

Table 3.3 – Typical values of Poisson's ratio for soils

Description	Poisson's ratio
Clay (saturated)[1,2]	0.4 - 0.5
Clay (unsaturated)[1,2]	0.1 - 0.3
Sandy clay[1,2]	0.2 - 0.3
Silt[1,2]	0.3 - 0.35
Sand, gravelly sand[2]	0.3 - 0.4
Dense sand[1]	0.2 - 0.4
Rock[1,2]	0.1 - 0.4

[1] As referenced by Subramanian (2008)
[2] As referenced by Bowles (1996)

Figure 3.1: Vicinity of the borings and drilled load-test shafts at the US95/CC215 interchange; Hole 1 is denoted by 'Test Shaft 1, Boring 1-2" and Hole 2 is denoted by 'Test Shaft 2, Boring 3/3A".

Figure 3.2: Simplified sediment logs showing predominant sediment types in a) Hole 1, and b) Hole 2. Depths are shown in meters.

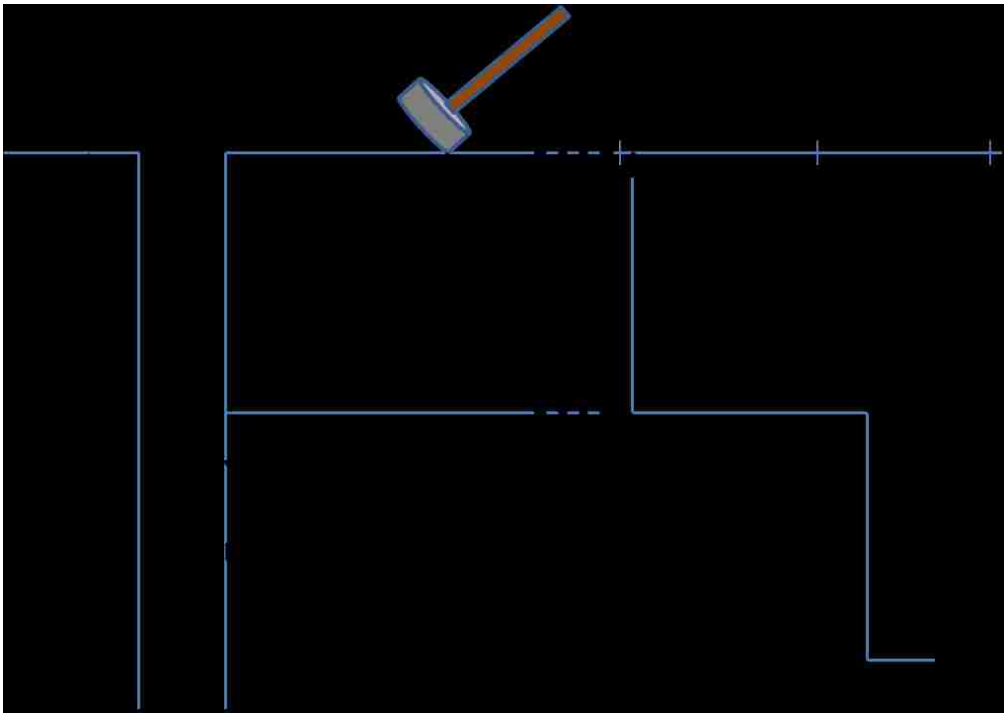

Figure 3.3: Illustration of the direct method for interpreting downhole velocities (after Kim et al., 2004).

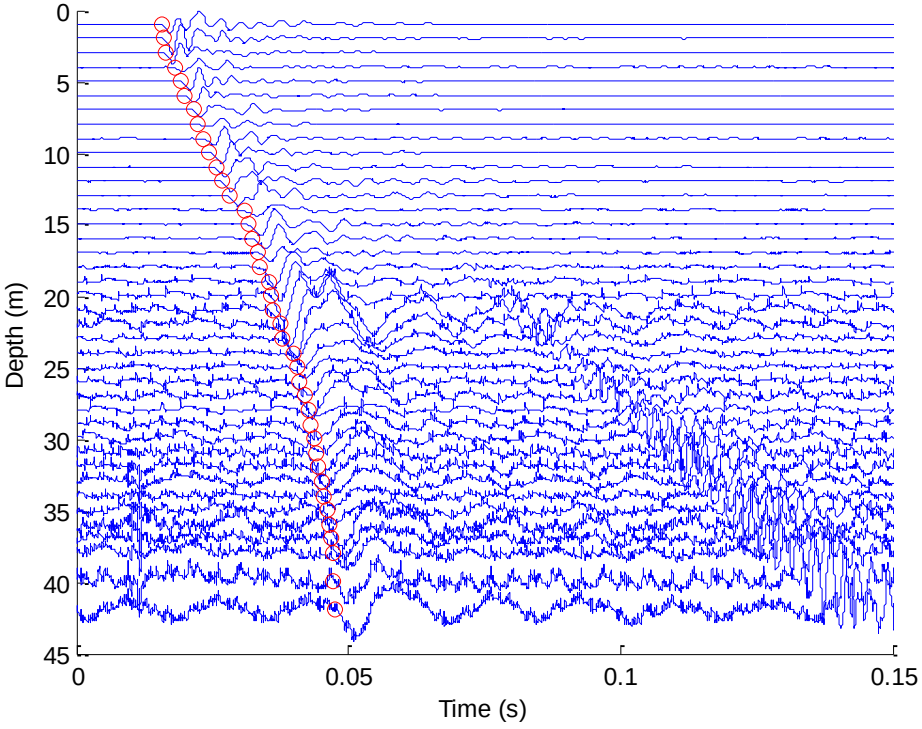

Figure 3.4: P-wave time histories with first arrival picks (red circles) for Hole 1.

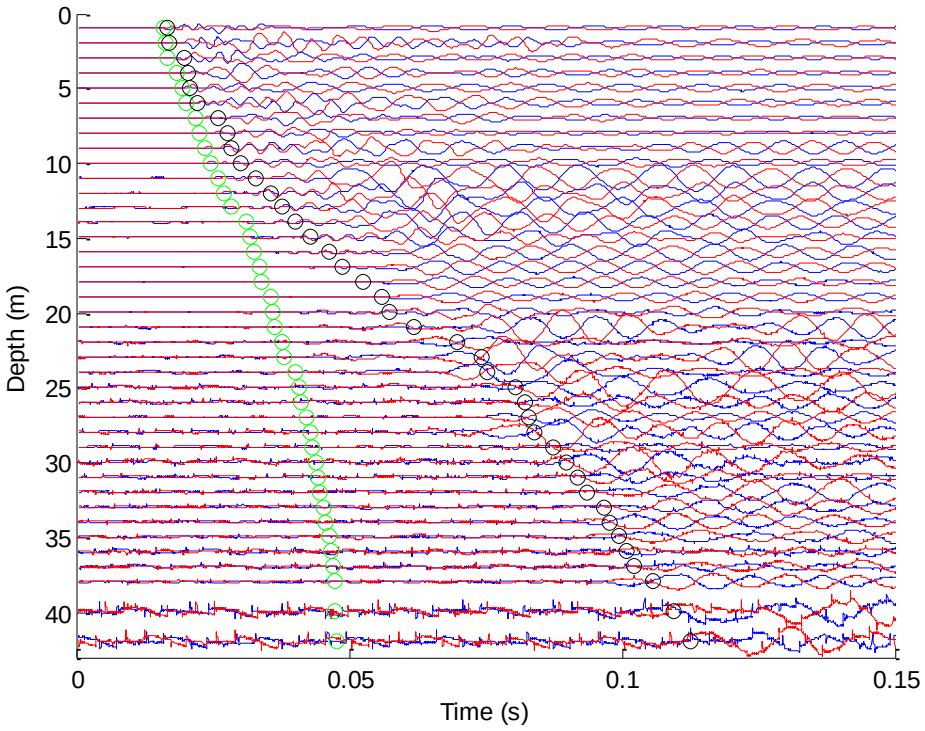

Figure 3.5: S-wave time histories with first arrival picks (black circles) for Hole 1; P-wave first arrival picks also shown as green circles.

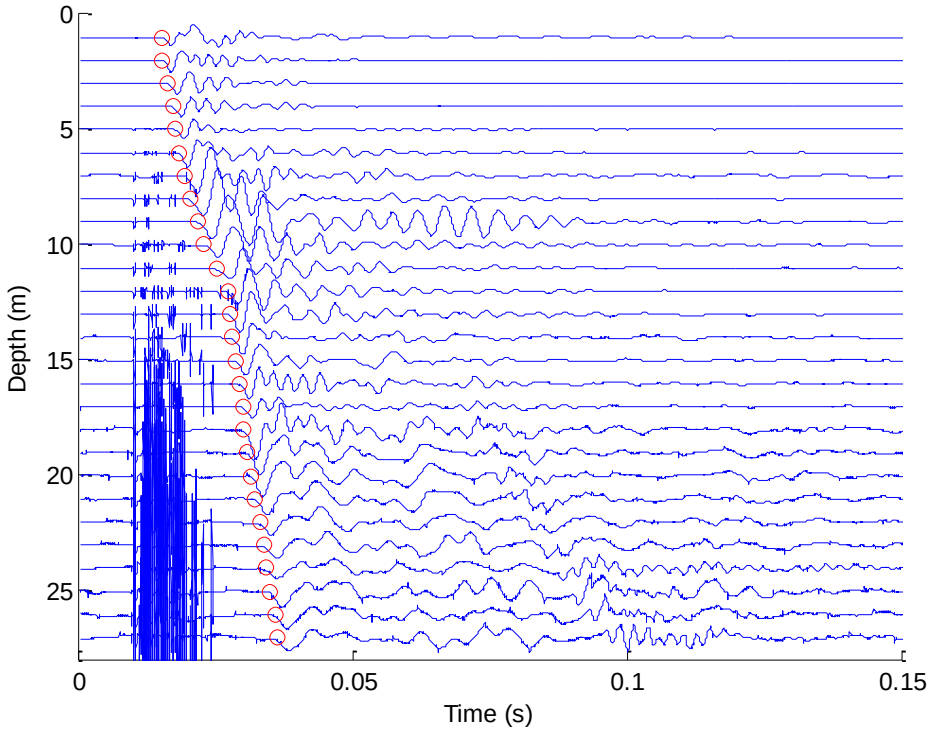

Figure 3.6: P-wave time histories with first arrival picks (red circles) for Hole 2.

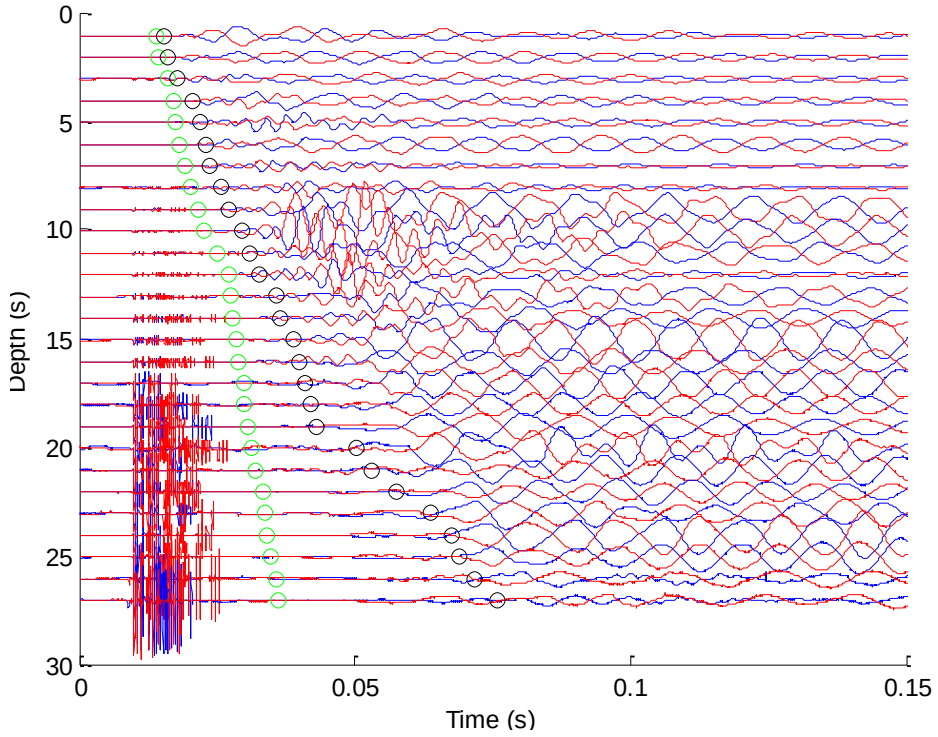

Figure 3.7: S-wave time histories with first arrival picks (black circles) for Hole 2; P-wave first arrival picks also shown as green circles.

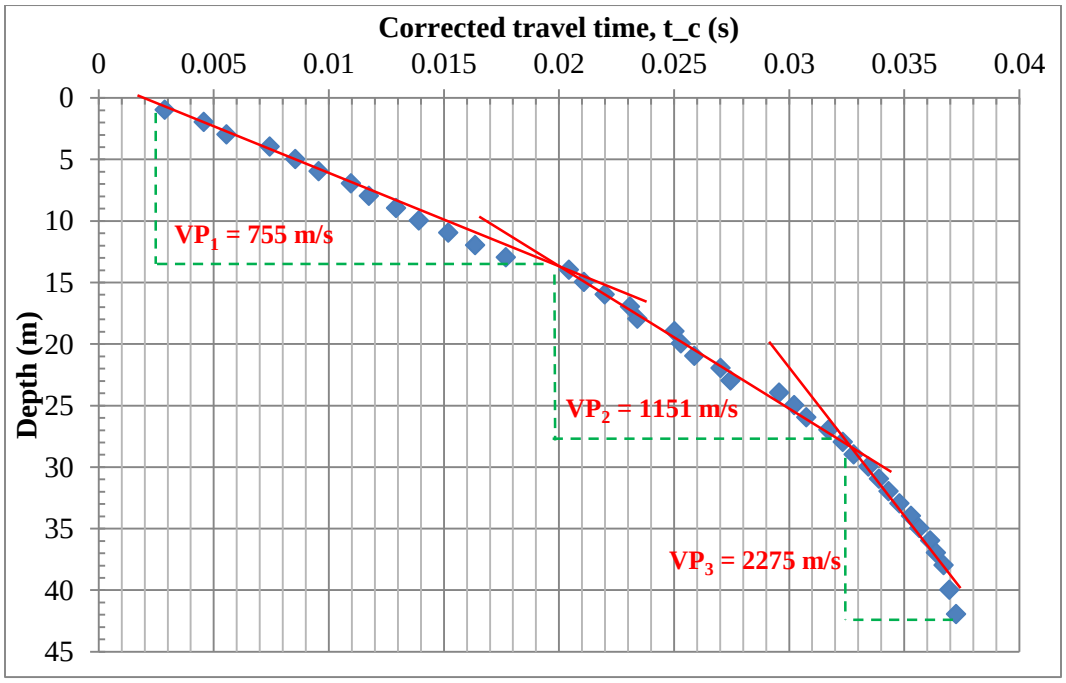

Figure 3.8: Downhole test, interpretation of P-wave first arrival picks for Hole 1.

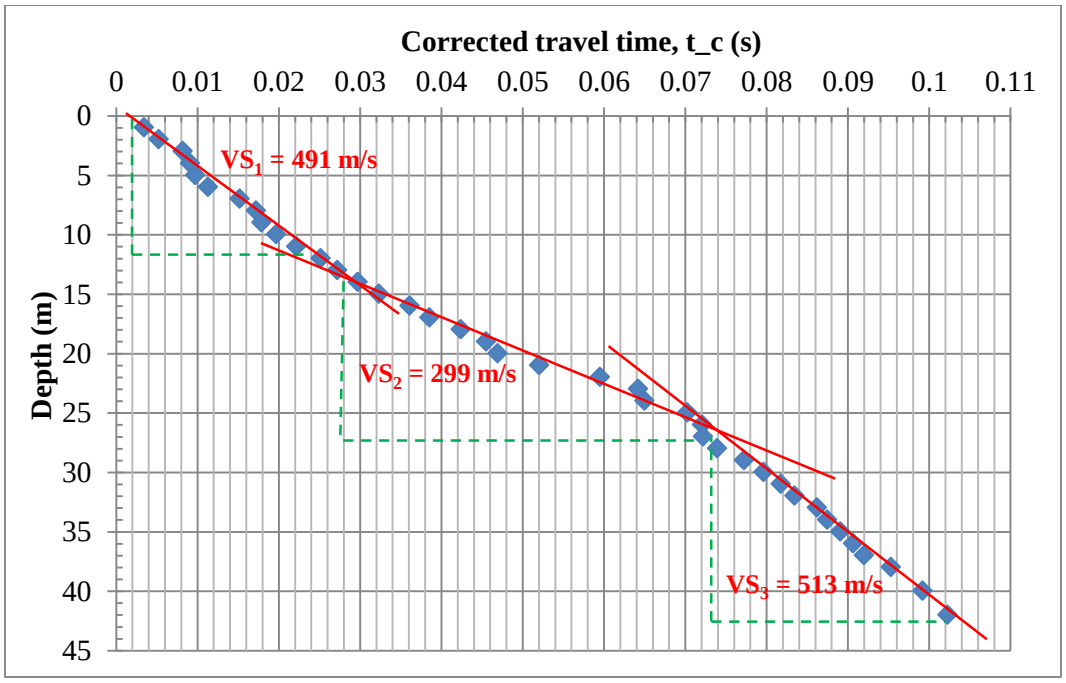

Figure 3.9: Downhole test, interpretation of S-wave first arrival picks for Hole 1.

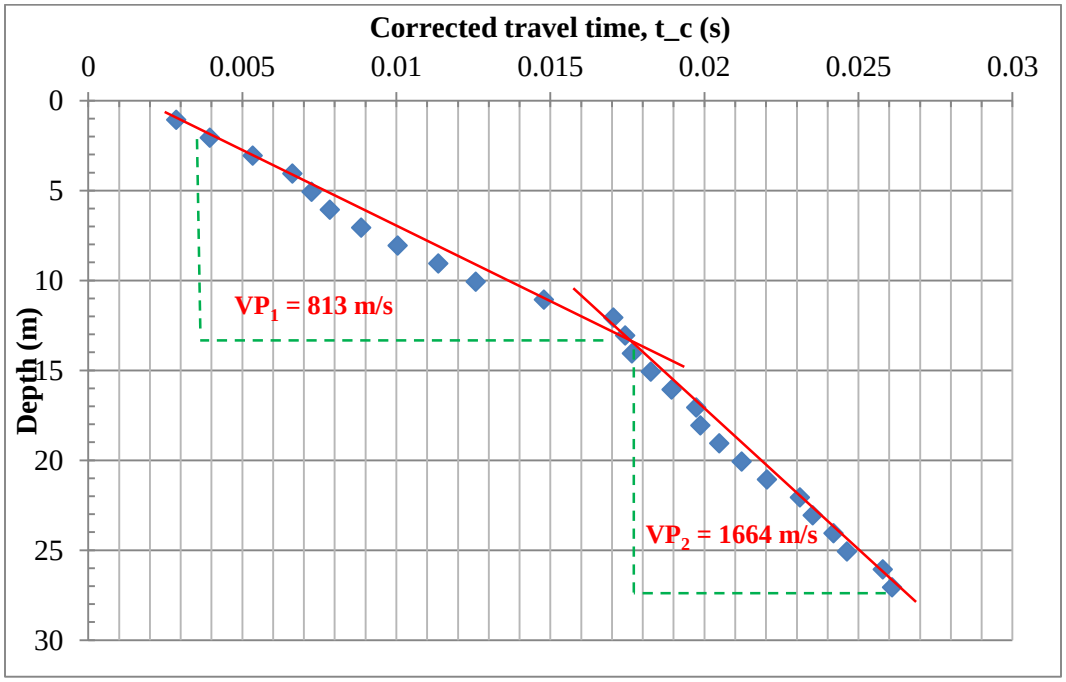

Figure 3.10: Downhole test, interpretation of P-wave first arrival picks for Hole 2.

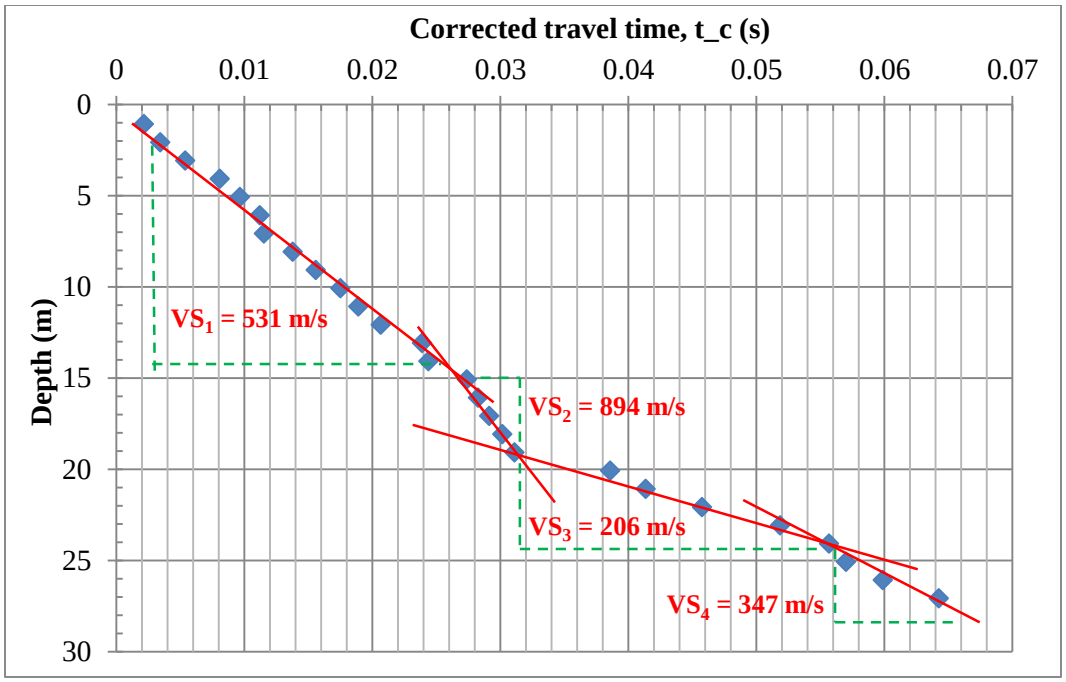

Figure 3.11: Downhole test, interpretation of S-wave first arrival picks for Hole 2.

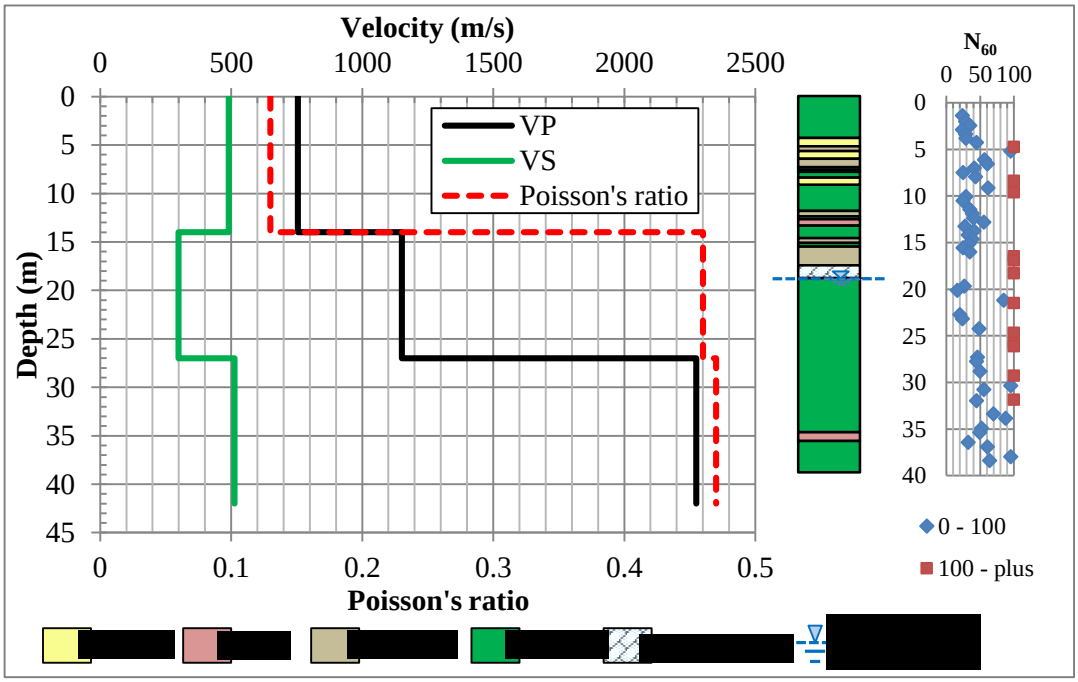

Figure 3.12: VP, VS and Poisson's ratio for Hole 1, along with simplified sediment log and N_{60} with respect to depth.

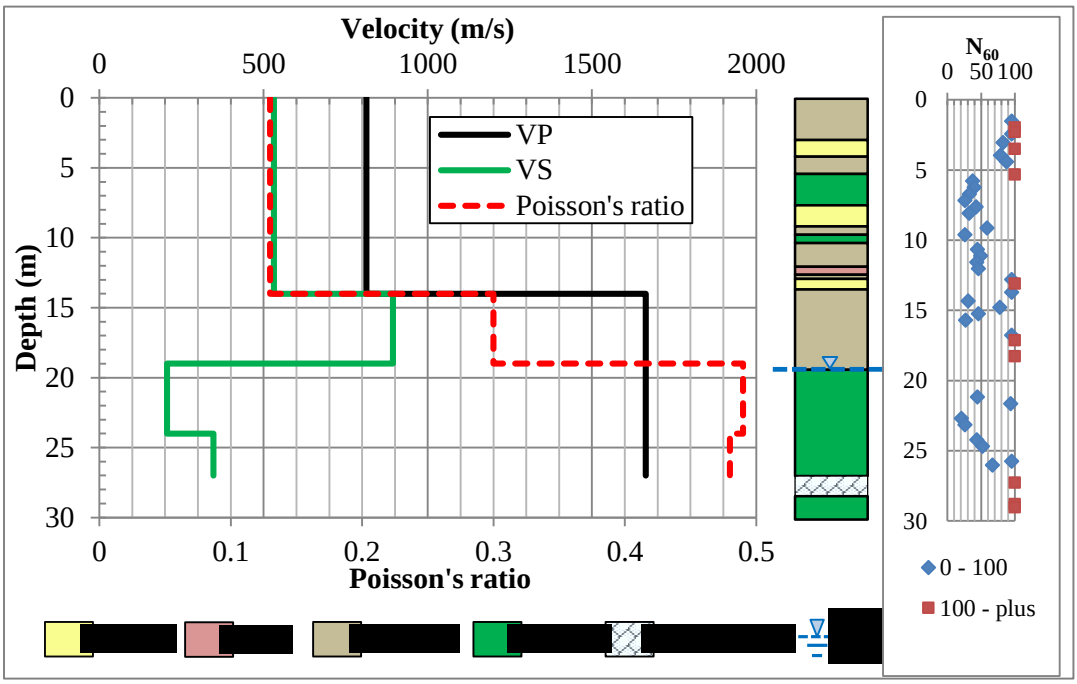

Figure 3.13: VP, VS and Poisson's ratio for Hole 2, along with simplified sediment log and N_{60} with respect to depth.

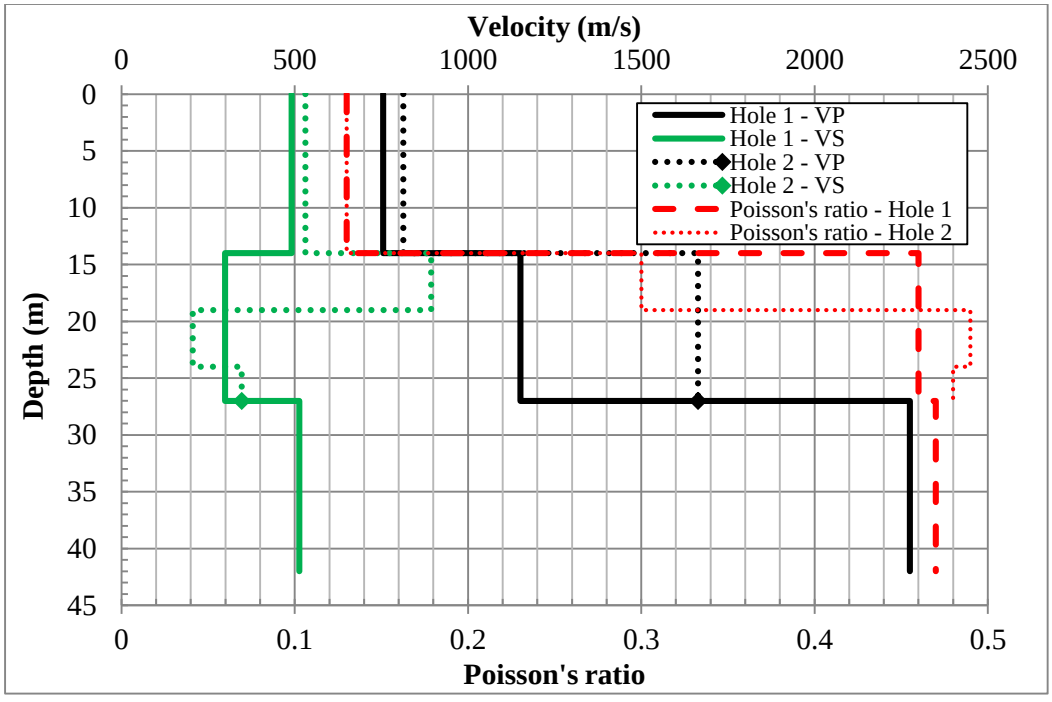

Figure 3.14: Comparison of velocity profiles and Poisson's Ratio from Holes 1 and 2. Note that Poisson's ratios for Holes 1 and 2 are identical in the upper 14 m.

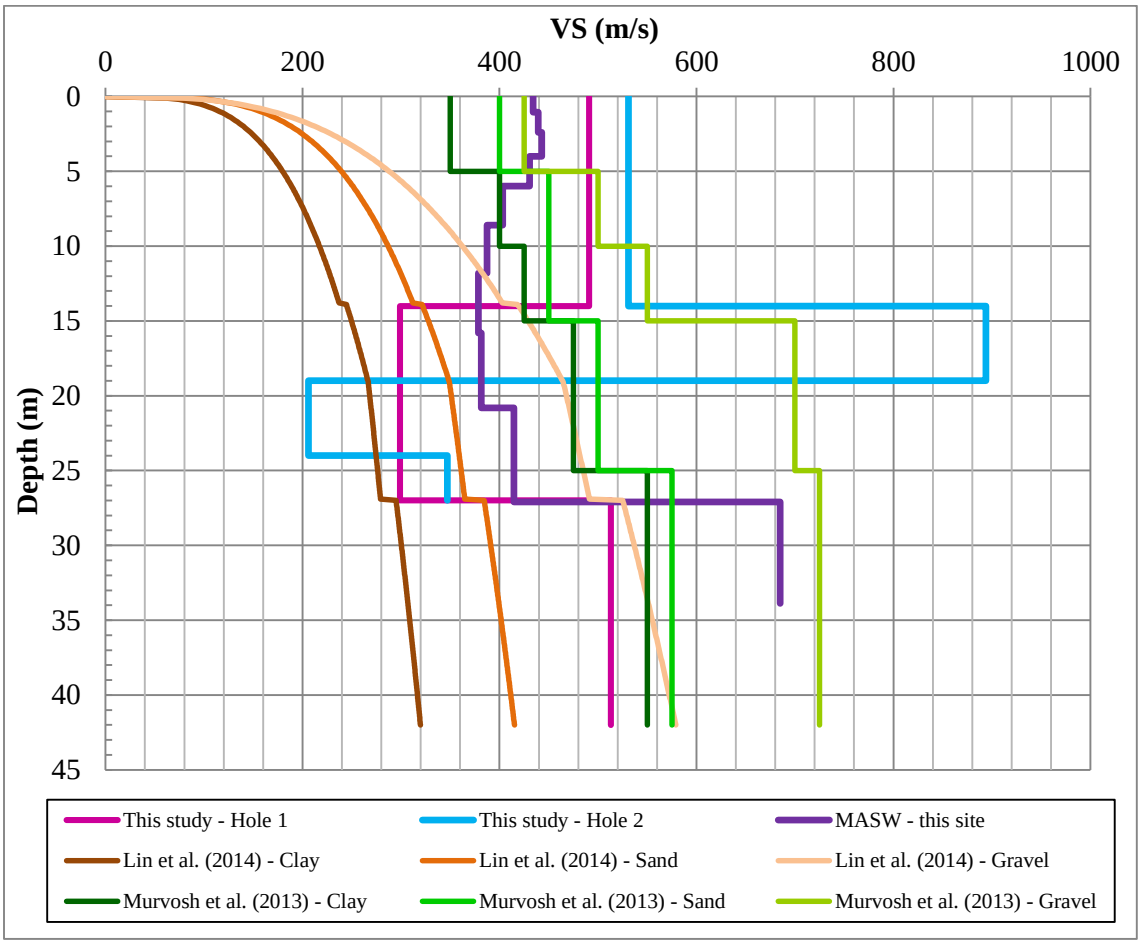

Figure 3.15: VS from Holes 1 and 2 with soil-specific representative VS profiles. Reference profiles from Lin et al. (2014) are for Imperial Valley soft sands, silts and clays ("Clay"); dense sands ("Sand"); and dense gravels ("Gravel").

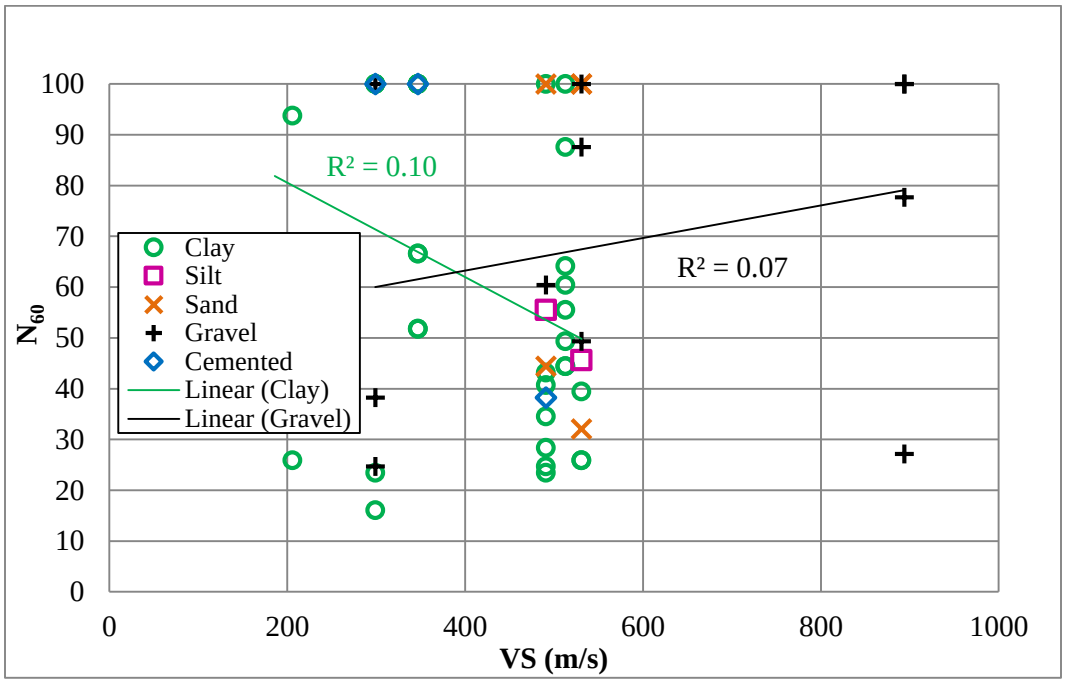

Figure 3.16: VS from downhole velocity testing compared with N_{60}, distinguished by predominant sediment type. Linear fits to clay and gravel data are shown.

CHAPTER 4

LOCAL DATASETS

This chapter addresses a broader dataset than the US95/CC215 Interchange dataset (Ch.3) in order to explore general trends for the LVV. Multiple sets of *in situ* and laboratory strength test data obtained from around the LVV are analyzed to study their relationships with shear behavior of sediments in the LVV. Datasets were obtained by request. Five datasets are from major projects, obtained directly from local geotechnical engineering consultants. Another set of data, from multiple smaller projects around the LVV, was obtained from Clark County (Nevada) Department of Development Services - Building Division (CCDDS-BD).

4.1. Major project datasets

In situ and laboratory test data from some major projects in the LVV were obtained from local geotechnical consultants Kleinfelder Inc. and Terracon Consulting Engineers and Scientists. Sediment lithology varies from site to site. Each project has its own set of tests and they are presented in a distinct manner. Data provided did not include full geotechnical reports, therefore many pertinent details of tests conducted are not known to the author. For privacy, project names and locations are not specified in every case; instead, the project is identified by a nearby street intersection or landmark.

4.1.1. Methodology

Content from the major project geotechnical datasets that was analyzed included sediment classifications and results of relevant *in situ* and laboratory tests, taking into consideration their methods of execution. Refer to Table 4.1 for the tests from the major project datasets used in this study.

4.1.1.1. Sediment classification

For this study, sediments are broadly classified by predominant sediment type: clay, silt, sand or gravel; as explained earlier. As observed with the highway interchange project (Ch. 3), most sediments studied that are predominantly granular (sands and gravels) are not clean and have clayey components that lend cohesion. In a few cases, sediments were described with uncertainty, such as "silty sand or sandy silt"; these tended to occur at transitions. Such sediments are denoted as ′transitional′ in this study. Sediments logged as having cementation, ranging from partial cementation to highly cemented, are classified for this study simply as cemented, regardless of the sediment class. Even sediments logged as having "trace calcareous nodules" were classified as cemented if they exhibited N or N_{60} of 50 or more.

4.1.1.2. Blow counts

Blow counts for refusal states reported as the number of blows for a limited penetration length, such as 50 blows for 4 inches, were converted to 'equivalent total' N as explained earlier. Most of the equivalent total N are well above 100 and are plotted at N=100 as described for the interchange project (Ch.3). Sediments associated with 100-plus N are

usually described as heavily cemented, although a few are logged as having trace cementation or cementation is not mentioned. Note that some N-values below 100 are extrapolated from refusal numbers. Initially the author distinguished one dataset based on N extrapolated from refusal numbers and regular N-values; no useful observations were obtained from this distinction, therefore datasets in this research do not distinguish N extrapolated from refusal numbers from regular N-values.

Most N presented in the major project datasets are from SPT samplers, although MC split spoon samplers, also known as ring samplers, were also used for SPT and sampling. The N from MC samplers were used only in cases where N from SPT samplers was unavailable. According to Rogers (2006), non-standard N can be converted to SPT-equivalent N using the LaCroix and Horn correction. According to Rogers (2006), this method provides a more conservative estimate of the SPT-equivalent N than the Burmister energy correction, and is most valid when sampling is performed within 38 - 76 cm (15 – 30 in.) of stiffer horizons such as cemented sands or gravels. Therefore the LaCroix and Horn correction should be applicable in the LVV, where cemented sediments and other hard materials are ubiquitous. For the MC samplers in the major project datasets, the LaCroix and Horn correction yields a factor of 0.44 (as cited in Rogers, 2006), by which non-standard N recorded is multiplied to obtain SPT-equivalent N. Thus, in the major project datasets, all N reported using the MC samplers are converted to SPT-equivalent N using the conversion factor 0.44. All specimens tested for comparisons in the major projects dataset are listed in Appendix B, along with but not limited to concise sediment descriptions and raw N. Although not differentiated in the

plots, non-standard N from MC samplers and their SPT-equivalent N are also listed in Appendix B. N from MC samplers account for about 26% of all N reported in Appendix B.

When possible, energy correction is applied to obtain N_{60} values. Tropicana & I-15 and 3rd St. & Gass Ave. are the only projects for which hammer efficiency was provided. SPT measurements for these projects were conducted using a Diedrich D120 drill rig with an average ER of 77.4% (Jennifer LaPutt, Terracon, personal communication, September 17, 2013). This ER yields an energy correction of 1.29.

4.1.1.3. VS (Shear wave velocity)

VS measurements are available for most local datasets. The testing methods that generated VS data in this study are: Refraction Microtremor (ReMi), downhole, and suspension logging.

ReMi is a testing method that measures Rayleigh-type surface waves along a linear array on the ground surface using ambient-noise sources (e.g., Niehoff, 2010). ReMi differs from the particular MASW surface wave testing method used in the interchange project (Ch. 3) in regards to the source signal type, among other things. The hindrance in comparisons of VS with point-based SPT measurements mentioned earlier applies to the ReMi measurements; further, when the seismic source is ambient noise, as with ReMi, the volumes averaged are even greater, exacerbating the difference with respect to point-based measurements. For the major project datasets, when VS results from ReMi testing

are compared with borehole-based test results, the following process is used to select relevant boreholes: (1) the length of the ReMi array is approximated from the map provided by the geotechnical consultant; (2) half the length is taken to describe the radius of a circle with its center at the midpoint of the ReMi line; (3) all boreholes within the circle are selected.

In the suspension logging test, a probe that houses a mechanical source and two receivers is inserted into a borehole (Kramer, 1996). For projects in this chapter reporting suspension logging data, the source is located about 2.14 m from the nearest receiver, and data are collected at 0.5 m intervals. Suspension logging tests thus provide VS while averaging properties of a much smaller volume of soil, compared to surface wave methods. Therefore, velocities from suspension logging may be more comparable to blow counts that also target small volumes of soil.

4.1.1.4. Pressuremeter

A few major project datasets included pressuremeter results. PMT is not conducted at the same depths as SPT. For this study, N for comparison with pressuremeter data were obtained from depths not more than 0.7 m above or below the PMT location and in sediments having the same description.

While most projects with PMT data provide p_L values as the outcome, the Neon project provides both p_L and S_u derived from the logarithmic and mathematical modelling methods. S_u from both methods is presented to see how they compare to each other.

According to In Situ Engineering (2012), in the logarithmic method, a plot of pressure versus the logarithm of radial displacement divided by pressuremeter radius will be a straight line, "provided the shear strength remains constant with strain" (p. 13). S_u provided from the logarithmic plot of the Neon project is determined from the slope of the line and will hereon be referred to as 'S_u by log method'. The p_L provided is obtained from the log method as well. It is determined by projecting the estimated pressure versus log strain line until the strain reaches 41%, at which point the pressuremeter has doubled in size. According to In Situ Engineering (2012), p_L is approximately 5 times the S_u by log method plus the *in situ* lateral pressure.

In the mathematical modelling method, two models were evaluated - The Hughes' sand model, used to obtain friction angle for sand, and the Gibson clay model, used to obtain S_u for clays. In both models, shear strength parameters are determined from unload-reload loops (Clarke and Gambin, 1998). Results from the Hughes' sand model were available for only a few specimens, most of which were cohesive soils; therefore, the Hughes' sand model outcomes were not used for comparisons. According to In Situ Engineering (2012), the Gibson clay model assumes the material to be purely cohesive and to fail at a constant shear strength and volume. S_u determined from the unloading cycle of the Gibson clay model often produces low values because of the disturbance of soil by movement of the pressuremeter prior to unloading (In Situ Engineering, 2012). Therefore S_u provided from the loading cycle of the Gibson clay model plots of the Neon

project, hereon referred to as the 'Gibson loading S_u' is used for comparisons in this study.

4.1.1.5. Laboratory tests

Laboratory tests used for shear strength comparisons in this study include direct shear, single point direct shear, unconfined compression, and unconsolidated undrained (UU) triaxial. Other laboratory test results provided include gradation by sieve analysis, Atterberg limits, expansivity, consolidation, corrosivity, moisture content and density.

Direct shear (DS) test (ASTM 3080-11) results presented c and ϕ values describing Mohr-Coulomb failure envelopes for specimens under consolidated-drained conditions obtained using standard and MC samplers. Note that specimens obtained using standard samplers were reconstituted for DS testing (Tanner Hartranft, Terracon, personal communication with Barbara Luke, April 10, 2015). Single-point direct shear (SDS) tests are essentially direct shear tests conducted at a single confining pressure, unlike the three or more confining pressures specified in ASTM 3080-11. SDS data were provided as plots of normal pressure applied with respect to shear pressure at which the specimen failed. To obtain a rough idea of the failure envelopes for each SDS test using data provided, zero cohesion is assumed to estimate ϕ. The zero cohesion assumption is unrealistic for the LVV due to the preponderance of cohesive sediments, even when a material is predominantly coarse grained. Nonetheless, it provides an upper-limit (unconservative) estimate of ϕ. Resulting Mohr-Coulomb failure envelopes are plotted according to N.

According to the ASTM standard for unconfined compressive strength of soil (ASTM D2166-13), the unconfined compressive strength (q_u) is defined as the compressive stress at which an unconfined cylindrical specimen of soil fails in a simple compression test. The S_u for an unconfined compression test specimen is approximated to be half of the q_u (e.g., Das, 2010). In this study, q_u reported from unconfined compression tests was used to calculate S_u.

4.1.2. McCarran

The McCarran International Airport is located in south-central Las Vegas. As part of the construction and geotechnical study for the recent Terminal 3 addition to the airport facilities, *in situ* and laboratory tests were conducted to assess the geotechnical properties of the underlying sediments. Data from borehole logs, ReMi, PMT, SDS, and unconfined compression tests were analyzed for this site. Clay is the dominant sediment type in this dataset (Appendix B). The borehole logs show that most sediments have some form of trace cementation. SDS test results were used to calculate ϕ_{max} values which range between 25 and 60 degrees (Table 4.2). VS values were obtained from the ReMi method. The longest length of ReMi lines recorded is 156 m. The distances between the center of the ReMi line and the nearest borehole range from 0 to 70 m. S_u and p_L* were obtained from unconfined compression and PMT tests respectively.

Test results are shown in Figures 4.1 through 4.3. Figure 4.1 shows ϕ_{max}, S_u, and p_L* with respect to N and VS, distinguished by predominant sediment type. Figure 4.2 shows

upper-bound Mohr-Coulomb failure envelopes from SDS tests, distinguished by sediment type and N range. Figure 4.3 summarizes VS as a function of N for the entire dataset, distinguished by predominant sediment type. Regarding predominant sediment types, as mentioned previously, this dataset has mostly clay. Sand and cemented materials are represented at approximately one quarter the frequency. Predominance of silt and gravel are uncommon (fewer than four data points for either), therefore, no general conclusions are drawn about these sediment types from this dataset.

N (Blow counts)

N are mostly low, ranging between 0 and 20, with only two over 100. High variability of N is observed in cemented sediments. Most sediments with 100-plus N are predominantly cemented. A few clays and sands (whose logs do not indicate cementation) also have N over 100. (Refer to Appendix B for the entire dataset used for comparisons.)

Strength parameters (ϕ_{max}, S_u) and surrogate for strength (p_L) with respect to N

ϕ_{max} As expected, overall ϕ_{max} (Fig. 4.1 a, b) is higher than typical values of ϕ: ϕ_{max} values cluster in the range of 30 to 50 degrees, while typical ϕ for sands (cohesionless) ranges between 27 and 45 degrees (Das, 2010; as stated earlier). As expected, sands have higher ϕ_{max} than clays (Fig. 4.1 a, b). N appears to be almost independent of ϕ_{max}.

S_u According to Fig. 4.1 c, d, sediments that are predominantly clays have higher S_u values than sediments that are predominantly sands, ranging up to about 70 kPa while

those for sands range only up to 30kPa; typically S_u ranges from 0 to 200 kPa or more in clays (Das, 2010; as stated earlier). S_u shows high variability with respect to N (Fig. 4.1c)

p_L The p_L* data are available mostly for clays that have low N (under 10) (Fig. 4.1 e). p_L* values range between 500 and 1700 kPa; typically p_L ranges from 50 to 2500 kPa in clays and 1200 to 5000 kPa in sands and gravels (Newcomb and Birgisson, 1999). The highest and lowest values of N correspond with highest and next-to-lowest values of p_L* respectively (Fig. 4.1 e). A single cemented specimen shows the highest p_L* yet blow count is only 10, lower than would be expected for a cemented sediment. This situation can be explained by the localized nature of cementation; recall that the SPT is made 0.7 m above or below the PMT. As such, a reliable correlation between PMT and N is unlikely.

VS (Shear wave velocity)

The slowest sediments are predominantly clay, while the fastest sediments are predominantly clay, sand and cemented (Fig. 4.3). Most clays have VS in the range of ~300 m/s to ~600 m/s. Cemented sediments have VS as low as ~ 300 m/s and as high as ~1300 m/s, far lower than VS of limestone which ranges between 2000 to 3300 m/s (Mavko, 2005). This difference is unsurprising for several reasons. First, because of the variation in the degree of cementation in sediments classified as cemented. For example, one of the specimens with low VS classified as "cemented" is logged as a 'clayey sand with partially cemented zones'; the low degree of cementation may not be enough to boost the VS. And second, as discussed previously, the ReMi test yields volumetric

averages of larger volumes of soil than are encompassed by a cemented layer. It is also probable that Mavko (2005) is referring to a lab measurement that would reflect values from an intact rock, whereas in the field cemented sediments are likely to have major discontinuities that will affect velocity.

N with respect to VS

A weak trend ($R^2 = 0.08$) of increasing N with increasing VS is observed in sands for N under 100 (Fig. 4.3). Even weaker trends in cemented sediments ($R^2 = 0.07$) and clay ($R^2 = 0.03$) also show increasing N with increasing VS. The linear approximation is quite similar for clay and sand.

Strength parameters (ϕ_{max}, S_u) and surrogate for strength (p_L) with respect to VS

The subset of strength parameter data that have VS nearby (within 70 m of an array center point) is smaller than the overall dataset for the McCarran site by more than half.

ϕ_{max} Only eight data pairs of ϕ_{max} and VS are available (Fig. 4.1b). Of those, four are cemented specimens, three are sand and one is clay. VS values are clustered in the range 300-600 m/s and ϕ_{max} ranges from ~30 to 50 degrees. This sparse dataset shows weak trends for increasing ϕ_{max} with increasing VS, for both cemented and sand categories.

S_u The data pairs of S_u and VS are richest in the clay category (12 clay, 2 sand, 1 gravel; Fig. 4.1d). Unfortunately, the VS values for the clays are clustered in a narrow range (300-400 m/s), while S_u varies over more than an order of magnitude.

p_L* With only one exception, the p_L* data apply to sediments associated with the same VS (Fig. 4.1f). As discussed, this situation is a shortcoming of having only passive-source surface-wave data for VS. The p_L* values are highly variable, ranging by a factor of more than three. The cemented sediment has the highest p_L* while the highest VS is attributed to a clay.

As explained earlier, VS data available for this site are averages for large volumes, unlike each shear strength parameter, which is obtained from a discrete location, laterally and vertically. This situation results in VS with insufficient resolution for useful comparison; for example, one ReMi-derived VS profile for this project shows constant VS over the depth range from 0 to 18 m. Further, this profile represents spatial averaging laterally as well as vertically. So all strength data applicable to the upper 18 m in a borehole closest to the array in question will be paired with the same VS, thereby seriously diluting the ability to distinguish trends. Therefore, the ReMi method, which provides VS with low resolution as a function of depth, will not be used further for comparisons with shear strength parameters in this thesis, although they will be used to explore relationships with blow counts.

4.1.3. Tropicana & I-15

In situ and laboratory tests were obtained for a project near Tropicana Ave. and Interstate-15 (I-15), hereafter referred to as the Tropicana & I-15 dataset. Data from borehole logs, ReMi, downhole velocity, and DS tests were analyzed for this site. Clay is

the dominant sediment type in this dataset as well, closely followed by sand (Appendix B). The borehole logs show that most sediments have cementation in varying degrees. DS test results provided ϕ and c. Of the local datasets obtained for this research, this one has the most DS test data. VS values were obtained from the ReMi and downhole testing methods. The longest ReMi array recorded is about 213 m. The distances between the center of the ReMi array and the nearest borehole used for comparisons range between 10 and 90 m.

Test results are shown in Figures 4.4 through 4.7. Figure 4.4 shows ϕ and c with respect to N_{60}, distinguished by predominant sediment type. Figure 4.5 shows Mohr-Coulomb failure envelopes from DS tests, distinguished by sediment type and N_{60} range. Figure 4.6 plots VS from downhole testing method as a function of N_{60}, distinguished by predominant sediment type. Figure 4.7 plots VS from the ReMi method as a function of N_{60}, distinguished by predominant sediment type. Regarding predominant sediment types, as mentioned previously, this dataset has mostly clay. Even sediments classified as predominantly sand have clay in them and thus possess cohesive properties, although there are some DS test results with zero and near-zero cohesion. Of the sediments with cementation, more than half are primarily clay, while 9% is fully cemented caliche. Predominance of gravel is uncommon, therefore, no general conclusions are drawn about this sediment type from this dataset.

N_{60} (Blow counts adjusted for 60% hammer efficiency)

Energy correction was applied to N to yield N_{60}, since ER was available. 70% of the 56 N_{60} values range between 0 and 50 (Fig. 4.4), and 16% have N_{60} values over 100, all but one of which were computed from data showing penetration refusal as explained earlier. Most sediments with 100-plus N_{60} are cemented. A few clays and sands (whose logs do not indicate cementation) also have N_{60} over 100. 14% of N_{60} range between 50 and 100.

Strength parameters (ϕ, c) with respect to N_{60}

ϕ As expected, samples that are predominantly sand have higher ϕ values, ranging between 25 and 35 degrees, while those for clays range between 10 and 25 degrees (Fig. 4.4 a); as stated earlier, typically ϕ from a drained test ranges from 27 to 45 degrees in sands and 5 to 30 degrees in clays (Das, 2010). The data presented here fit within the expected range of values for both clay and sand. A moderate trend of increase in N_{60} with increasing ϕ is seen in sands with N_{60} under 50 ($R^2 = 0.58$). N_{60} appears to be independent of ϕ in clays and cemented sediments. As expected, N_{60} for clays is lower than for cemented sediments, while both ϕ and N are highly variable for cemented sediments

c Most of the c values (from drained DS tests) cluster in the range of 0 to 40 kPa irrespective of sediment type (Fig. 4.4 b); typically c ranges between 10 and 105 kPa in normally consolidated clays (Geotechdata.info, 2014). Few clays have higher c than most sands. The highest value of c is observed in a cemented sandy clay; the high cohesion in this specimen is explained by the presence of both cementation and clay. Most clays have

low c and N_{60} under 20. Both N_{60} and c are highly variable in cemented sediments, while N_{60} is slightly higher in sands than clays.

VS (Shear wave velocity)

In this dataset, more VS values are available from the ReMi method than the downhole testing method. In the ReMi dataset, the slowest and fastest sediments are sand and cemented respectively (Fig. 4.7); most sands have VS in the range of ~200 m/s to ~700 m/s. VS in most clays range between 300 and 500 m/s, while most cemented sediments have VS ranging between 200 and 500 m/s. More variation in VS is observed with the ReMi method than with the downhole velocity method. The downhole measurements were obtained from two boreholes located about 170 m apart, the deepest downhole measurement was at 36 m; while the ReMi measurements were obtained from 9 ReMi arrays spread over an area of 200,000 m^2. As explained earlier, VS from the ReMi method, which provides low resolution as a function of depth, is not compared with shear strength parameters in this research. VS from downhole velocity testing is not compared with shear strength parameters for this site because only 5 comparable data pairs are available, all of which have VS of ~400 m/s (Fig. 4.6).

N_{60} with respect to VS

Most VS values from downhole velocity testing range between 400 and 450 m/s (Fig. 4.6), therefore, no general conclusions are drawn about the relationship between VS and N_{60}. VS from ReMi has a wider range, between 200 m/s and 850 m/s (Fig. 4.7). Cemented sediments have highly variable N_{60} values ranging from ~10 to 100-plus. This

large range of N_{60} is likely due to the variation in degree of cementation in sediments, as explained earlier, as well as because some cemented layers are thin (less than 12 inches). Both N_{60} and VS are highly variable within each predominant sediment type. A weak trend ($R^2 = 0.02$) of increasing N_{60} with increasing VS is observed in sands with N_{60} under 100 (Fig. 4.7). On the contrary, a weak trend ($R^2 = 0.08$) of decreasing N_{60} with increasing VS is observed in cemented sediments with N_{60} under 100. Virtually no trend ($R^2 = 0.0006$) is observed in clays with N_{60} under 100 because of high variability in both VS and N_{60}.

4.1.4. 3rd St. & Gass Ave.

In situ and laboratory test results were obtained for a project located near 3rd St. & Gass Ave., hereafter referred to as the 3rd & Gass dataset. Data from borehole logs, suspension logging, and DS tests were analyzed for this site. Clay is the dominant sediment type, of which most are cemented (Appendix B). DS test results provided ϕ and c from reconstituted samples obtained from the SPT sampler. VS values were obtained from the suspension logging method. These VS values are compared with N_{60} from the same hole, taken at the most 0.5 m above or below the suspension logging measurements.

Test results are shown in Figures 4.8 through 4.10. Figure 4.8 shows ϕ and c with respect to N_{60}, distinguished by predominant sediment type. Figure 4.9 shows Mohr-Coulomb failure envelopes from DS tests, distinguished by sediment type and N_{60}. Figure 4.10 plots VS from suspension logging as a function of N_{60}, distinguished by predominant sediment type. More than half of the specimens tested have some form of cementation.

Predominance of sand is uncommon, therefore, no general conclusions are drawn about this sediment type from this dataset.

N_{60} (Blow counts adjusted for 60% hammer efficiency)

Energy correction was applied to N to yield N_{60}, since ER was available. N_{60} for clays and sands range mostly between 0 and 50, while it ranges above 50 for most cemented sediments (Fig. 4.8).

Strength parameters (ϕ, c) with respect to N_{60}

ϕ Ten data pairs of ϕ and N_{60} are available (Fig. 4.8 a). Of those 5 are cemented specimens, three are clay and two are sand. All cemented sediments have higher ϕ and N_{60} than all clay and sand. Clays have lower ϕ than other sediments.

c c values range between about 5 and 50 kPa (Fig. 4.8 b). The highest c is observed in a cemented sediment with N_{60} over 100, while the lowest c is observed in a sand with N_{60} under 10. As expected, c is smallest for predominantly sandy sediments, intermediate for clays, and highest for most cemented sediments. This small but good quality dataset shows weak trends for increasing c with increasing N_{60} irrespective of sediment type.

VS (Shear wave velocity)

As expected, the fastest VS is in cemented sediments. VS values range widely, between about 200 and 1200 m/s. The majority of specimens are cemented and have low VS values. VS in clays range between about 200 and 600 m/s, while they range slightly

higher, between 300 and 900 m/s, in sands. VS from suspension logging is not compared with shear strength parameters because only 4 comparable data pairs are available. The shear strength parameters c and ϕ (in that order), for the comparable data pairs are 7 kPa and 24 degrees (sand), 20 kPa and 28 degrees (cemented), 25 kPa and 14 degrees (clay), and 21 kPa and 26 degrees (cemented) at depths of 7.6 m, 13.7 m, 25.9 m, and 33.5 m respectively.

N_{60} with respect to VS

Cemented sediments have highly variable N_{60} values, ranging from ~10 to over 100 (Fig. 4.10). All sediments with $N_{60} > 30$ and all but one with VS > 620 m/s are cemented. A weak trend ($R^2 = 0.06$) of increasing N_{60} with increasing VS is observed in cemented sediments for N_{60} under 100. VS appears to decrease with increasing N_{60} for clay but because the sample size was small (6), the fit was not calculated.

4.1.5. Neon

The Neon project is located along the Interstate-15 (I-15) corridor near downtown Las Vegas between the US 95 and Sahara Avenue interchanges. Data from borehole logs, PMT, DS, and UU triaxial tests were analyzed for this site. Clay is the dominant sediment type in this dataset (Appendix B). The borehole logs show that most sediments tested have some form of cementation. DS test results provided ϕ and c for three samples, 2 of which were relatively undisturbed samples obtained from Modified California samplers, while S_u was obtained from UU triaxial test results. Shear strength parameters are available for very few data pairs (under five) from DS and UU triaxial tests, therefore no

general conclusions are drawn about shear strength parameters obtained from these tests for this dataset. p_L, S_u by log method and Gibson loading S_u were obtained from PMT test results. No VS test data were available for this location, including the Optim VS ReMi dataset obtained from the CCDDS-BD (discussed later).

Test results are shown in Figures 4.11 through 4.13. Figure 4.11 shows ϕ, c, and S_u with respect to N, distinguished by predominant sediment type. Figure 4.12 shows Mohr-Coulomb failure envelopes from DS tests, distinguished by sediment type and N range. Figure 4.13 shows p_L, S_u by log method, and Gibson loading S_u with respect to N, distinguished by predominant sediment type. As mentioned previously, clay is the prevalent sediment type, of which most are cemented. Predominance of sand is uncommon, therefore, no general conclusions are drawn about this sediment type from this dataset.

N (Blow counts)

N are mostly low for clays and sands, ranging between 0 and 40 (Fig. 4.11, 4.13). High variability of N is observed in cemented sediments, ranging from 20 to over 100. All sediments with N over 100 are predominantly cemented.

Strength parameters (ϕ, c, S_u, S_u by log method and Gibson loading S_u) and surrogates for strength (p_L) with respect to N

ϕ Only three data pairs of ϕ and N are available (Figure 4.11 a), one each of a clay, a sand and a cemented sediment. All three ϕ values are about 30 degrees, with the

cemented sediment having the highest ϕ; therefore, as noted previously for the US95/CC215 interchange dataset, a distinction of soils by predominant sediment may not always be useful. Despite similar shear strength parameters, both clay and sand have N of about 20, while the cemented sediment has N over 100.

c All c are low and similar, ranging between 4 and 12 kPa (Fig. 4.11 b); as previously mentioned, typically c ranges between 10 and 105 kPa in normally consolidated clays (Geotechdata.info, 2014). The low c (12 kPa) in the cemented sediment is possibly due to cementation broken during sampling or low degree of cementation.

S_u Four data pairs of S_u are available from UU testing, all of which are clays. As expected, they fit the typical range for clays as presented by Das (2010) and range between 60 and 110 kPa (Fig. 4.11 c). Both S_u and N are variable. For example, for the same N, S_u varies by ~100% and for almost the same S_u, N varies by ~50%.

S_u by log method and Gibson loading S_u S_u by log method values range between 250 and 2000 kPa in cemented sediments, while it ranges between 300 and 700 kPa in clays and sands (Fig. 4.13 b). Gibson loading S_u values range between 200 and 1100 kPa in cemented sediments, while they range between 200 and 500 kPa in clays and sands (Fig. 4.13 c). As stated earlier, typical values of S_u range from 0 to 200 kPa for very soft to very stiff clays and more than 200 kPa in very hard clays (Das, 2010); therefore, Gibson loading S_u values are more comparable to typical S_u values than are S_u by log method

values. High variability is observed in N, S_u by log method, and Gibson loading S_u for cemented sediments.

p_L The p_L data are available mostly for cemented sediments, some clays and few sands (Fig. 4.13 a). p_L values for cemented sediments range between 1500 and 9000 kPa. As expected, for clays and sands p_L ranges lower, between 1400 and 3500 kPa; as mentioned previously, typical p_L ranges from 50 to 2500 kPa in clays and 1200 to 5000 kPa in sands and gravels (Newcomb & Birgisson, 1999). Both N and p_L are highly variable in cemented sediments. For example, for about the same N, p_L varies by ~400% and for almost the same S_u, N varies by more than 300%.

Although all three PMT outcomes (p_L, S_u by log method and Gibson loading S_u) in Fig 4.13 have a different scale on the X-axis, they exhibit similar scatter trends when compared to N. S_u from PMT is much higher than S_u from UU triaxial testing. Of the sediments that underwent PMT, most are cemented followed by predominantly sandy sediments and only about a third are predominantly clay, while all sediments that that underwent UU triaxial testing are predominantly clay. Overall, clays and sands have lower p_L, S_u by log method, and Gibson loading S_u than cemented sediments. Therefore, although the project Neon dataset is small, results follow reasonable trends and fit expectations.

4.1.6. City Center

The City Center project is located east of I-15, between Tropicana Ave. and Flamingo Rd. Data from borehole logs, suspension logging, and DS tests were analyzed for this site. Sand is the dominant sediment type in this dataset (Appendix B), although almost all have clay in them. DS test results provided ϕ and c from reconstituted samples obtained from the SPT sampler. VS values were obtained from the suspension logging method. These VS values are compared with N from the same hole, taken at the most 1 m above or below the suspension logging measurements.

Test results are shown in Figures 4.14 through 4.16. Figure 4.14 shows ϕ and c with respect to N, distinguished by predominant sediment type. Figure 4.15 shows Mohr-Coulomb failure envelopes from DS tests, distinguished by sediment type and N range. Figure 4.16 plots VS from suspension logging method as a function of N, distinguished by predominant sediment type. Some transitional sediments are found in this dataset. Predominance of gravel is uncommon, therefore no general conclusions are drawn about this sediment type from this dataset.

N (Blow counts)

N mostly range between 0 and 50, but there are many over 100 as well (Fig. 4.16). Most sediments with 100-plus N are predominantly sand. Some clays and sands (whose logs do not indicate cementation) also have N over 100.

Strength parameters (ϕ, c) with respect to N

ϕ Of the data pairs provided, only one is predominantly clay. Sands have ϕ values ranging between 25 and 35 degrees, while the clay has a ϕ value of about 10 degrees (Fig. 4.14 a). The lowest ϕ value of 7 degrees is in a transitional sediment logged as 'silty sand/sandy clay' with N value of about 35; this low ϕ value suggests that the specimen tested may be predominantly clay or silt. In cemented sediments, ϕ values range between 10 and 30 degrees. N shows high variability with respect to ϕ

c c values fall in the range of 0 to 50 kPa (Fig. 4.14 b). Most sands have low c, ranging between 0 and 20 kPa, while the clay sediment has a c value of about 40 kPa, as expected. The highest value of c is observed in the transitional sediment with the lowest ϕ value and plots adjacent to the clay. In sediments with N over 100, c is variable, ranging between 0 and 30 kPa.

VS (Shear wave velocity)

The fastest sediment is predominantly clay with VS of about 1800 m/s (possibly due to the presence of cementation); most clays have VS in the range of ~200 to 600 m/s. The slowest sediment is predominantly gravel with VS of about 200 m/s. Sands have VS ranging between 200 and 1200 m/s. In cemented sediments, VS is highly variable, ranging from 200 to ~1400 m/s, despite all specimens having N>100. VS is not compared with shear strength parameters as no comparable data pairs are available from this

project, because specimens for laboratory strength tests were not obtained from the same hole in which suspension logging was performed.

N with respect to VS

A weak trend ($R^2 = 0.04$) of increasing N with increasing VS is observed in sands for N under 100 (Fig. 4.16). A weaker trend ($R^2 = 0.02$) also shows increasing N with increasing VS in clays. In sediments with N over 100, VS is highly variable with respect to N.

4.1.7. Discussion

The major project datasets are from different locations in the LVV, therefore lithology varies from site to site. Of the different sediment specimens included in this study (Appendix B), the most prevalent predominant sediment type is clay, which accounts for 42% of sediments from all major project datasets. Cemented sediments and sands account for 28% and 25% of the predominant sediments respectively, while gravel and silt are less than 4% of the entire sediment specimens tested. Clay is the most prevalent (53%) predominant sediment type within cemented sediments listed in Appendix B, while sediments logged in borehole logs as sand and caliche account for 24% and 15% of cemented sediments category respectively. Almost no specimen tested is entirely cohesionless.

For cemented sediments in this study, the sediment type or the degree of cementation is not distinguished. As mentioned previously, the term ‘cemented sediments’ has been

applied to sediments reported to have cementation ranging from trace to fully cemented materials and/or caliche; sediments with trace cemented materials are considered 'cemented' only if they are reported to have N or N_{60} values above 50. As a result, high variability is observed in all parameters studied within cemented sediments and detection of more distinct trends is hindered. In some cases, predominant sediment types show distinction in shear strength parameters; for example, clays are observed to have higher c and lower ϕ than sands. However, different predominant sediment types are in some cases observed to have practically the same N and N_{60}, VS, shear strength parameters, and surrogates for shear strength from PMT among different specimens. A more descriptive classification of cemented sediments and sediment types might enhance determination of trends with respect to sediment constitution.

As mentioned previously, most sediments tested are predominantly clay and/or cohesive. Very few gravels and silts are observed. Most borehole logs show some form of cementation. Most cemented sediments have N or N_{60} values over 100. Surrogates of shear strength from PMT are few in number and are highly variable for sediments with similar N or N_{60} values, this can be explained by the heterogeneity of sediments in the LVV. The PMT values are distinctly higher in most cemented sediments than in sediments logged as being without cementation, whereas this is not true for N. These data suggest that PMT is a more effective tool in characterizing stiffness of cemented and uncemented sediments in the LVV than is SPT. Comparing N or N_{60} and VS, weak trends ($R^2 < 0.1$) of increasing VS with increasing N or N_{60} are observed. It is likely that more distinct trends between N or N_{60} and VS could have been identified if similar volumes of

soil tested were compared. Note that in general, better correlations of N or N_{60} with suspension logging data than with ReMi were not observed; although datasets with both suspension logging and ReMi data were not available for a more meaningful comparison. N or N_{60}, considered to be point measurements, should be more comparable to VS measurements that target smaller volumes of soil. Because PMT outcomes observed in this study mostly cluster separately for each predominant sediment type, it is hypothesized that through PMT, valuable correlation can be made of the intermediate-strain modulus from PMT with the small strain modulus from VS testing of a comparable soil volume. This hypothesis could not be tested because comparable VS and PMT data pairs were not available for the respective locations. Note that absolute strength values from PMT may not be reliable as they are considerably higher than S_u obtained from other laboratory tests, nevertheless PMT data can still be useful for understanding the shear behavior of sediments. However, in a study conducted by In Situ Engineering (2012) in the LVV, the samples acquired adjacent to the *in situ* test locations for testing did not closely represent the materials being tested due to high sediment heterogeneity, thus hindering the effectiveness of PMT for soils characterization in that setting.

4.2. Clark County valley-wide dataset

Datasets of SPT and VS from the LVV were acquired from the Clark County (Nevada) Department of Development Services - Building Division (CCDDS-BD). They are referred to as the Clark County valley-wide dataset. It has a larger sample size than the major projects datasets that were provided to the author. The author conducted a pilot study to analyze trends between N and VS for a smaller subset of their data. The *in situ*

test data acquired from the CCDDS-BD can be categorized as: (i) ESGI, and (ii) Optim VS.

4.2.1. ESGI

The CCDDS-BD has a program called the Electronic Submittal of Geotechnical Information (ESGI) wherein certain surface and subsurface geotechnical information is submitted in an electronic format by the building permit holder on all projects that require a geotechnical report in Clark County (Lynn, 2008). The types of information required to be supplied for the ESGI are shown in Table 4.3.

The entire ESGI collection is quite large and had not been fully vetted by the County, therefore a smaller batch that had already undergone preliminary QA/QC check by the CCDDS-BD was acquired by the author on behalf of CCDDS-BD from J. Bahr on October 9, 2013. The data were provided in the form of an Excel spreadsheet file with columns as mentioned in Table 4.3. The contents of this spreadsheet will be referred to as the ESGI dataset. The dataset includes about 2200 N values.

4.2.2. Optim VS

Some government entities in Clark County, NV contracted with Optim SDS to have mapped seismic hazard class systematically through about 550 square miles of the LVV (Louie et al., 2011). The average VS for the top 30 m of the ground surface, also known as VS30, is used for seismic site classification. Optim SDS performed VS measurements as a function of depth using the ReMi method, yielding a VS profile at each array

location. The average spacing between ReMi array center points was about 0.3 km (1000 ft) (Louie et al., 2011). Locations of VS30 measurements referenced by latitude and longitude were made available to the author by the CCDDSS-BD in an ArcGIS file, along with VS profiles for each of VS30 measurement location in individual Excel spreadsheets. The VS profiles and their corresponding location information, hereafter referred to as the Optim VS dataset, were provided to the author on behalf of CCDDS-BD by W. Hellmer on October 9, 2013. Figure 4.17 shows Optim VS dataset test locations overlaid on a map of the LVV.

4.2.3. Methodology

Both ESGI and Optim VS data are refined based on availability of usable data.

4.2.3.1. ESGI

Although a rich assortment of data as shown in Table 4.3 might be available from the ESGI dataset for each N, complete information is not available. Under further inspection of the acquired dataset, some inaccuracies and misprints were found. Some of these were addressed on consultation with J. Bahr, the point-of-contact at CCDDS-BD. Entries that were erroneous and could not be corrected, could not be verified, or had insufficient information were eliminated from further consideration. A little fewer than 1000 usable N values in about 60 boreholes were identified; this dataset and its associated information will hereon be referred to as the ‘select ESGI’ dataset. Very few N are reported above 100, these values are plotted at N=100 as described earlier (Ch. 3). Note that penetration refusal is not recorded, because N is reported as a single numerical value in this dataset. Each N from the select ESGI dataset was input into ArcGIS along with its geographical

location and depth. Figure 4.18 shows the select ESGI dataset overlaid on a map of the LVV. Most of the select ESGI data are concentrated in the western and south-western parts of the LVV.

In the select ESGI dataset, columns titled 'USCS ID' and 'Description' provide information on sediment type of specimen on the basis of the Unified Soil Classification System (USCS) and a brief explanation respectively. Most entries have information in these columns, while some have one or the other, and a few have neither. Table 4.4 provides information on sediment grouping for this study. The USCS group symbols referred to as the 'USCS ID' in the ESGI dataset and their USCS Group names are broadly classified into their general description based on percent fines content (ASTM D2487-11). For clarity of portrayal in plots, these USCS designations are further simplified into their predominant sediment types in Table 4.4 as gravel, sand, silt and clay. The most prevalent predominant sediment type in the select ESGI dataset is clay. Sediments with cementation stated in their 'Description' and/or checked 'true' in the 'Cemented' column in the Excel spreadsheet are considered cemented. A Few specimens without sediment information are present; these are termed as 'unclassified'.

Sampler information is not available in the dataset, therefore all N are assumed to be obtained from standard split-spoon samplers. ER is available for about 10% of N. Energy correction is applied to this small portion of N to yield N_{60}. Because N_{60} constitutes a very small portion of the select ESGI data it is not distinguished from N, therefore N and N_{60} are referred together as 'N' from here on for this dataset. As mentioned previously,

most of the sediments in the ESGI dataset are predominantly clay, and even the predominantly sand and gravel sediments also have clay in them.

4.2.3.2. Optim VS

Although the Optim VS data collection is quite dense (Fig. 4.17), the VS test locations do not coincide with the locations of the N values from the ESGI dataset. In order to reduce the large Optim VS dataset to a smaller relevant subset in the vicinities of the select ESGI dataset locations, all VS test locations no less than about 610 m (2000 feet) in all directions from each N location were taken into consideration. This smaller set of VS will be referred to as the 'select Optim VS' dataset. Figure 4.19 shows select ESGI dataset along with select Optim VS dataset. The VS data for each of the select Optim VS locations were input into ArcGIS.

4.2.4. Processing and analysis

Because the select Optim VS dataset locations do not coincide with the select ESGI locations, a comparison of N and VS for the same location is not possible. Consequently, an interpolation of VS to generate an expected VS value for each select ESGI data location is conducted. At each select ESGI data location, a 2D spatial interpolation of VS was performed for each depth where N values were available. The Inverse Distance Weighting (IDW) Method from the Geostatistical Analyst tool in ArcGIS was used for VS interpolation. According to ArcGIS, the IDW tool interpolates by estimating cell values by an averaging process, where values closer to the cell being interpolated are weighted more in the averaging process than the farther ones. VS was interpolated as

contour plots at each depth of N for all select ESGI data locations. The interpolated VS values were identified visually in ArcGIS and tabulated along with corresponding N values from the select ESGI dataset. Figure 4.20 shows the process of obtaining interpolated VS for a select ESGI data point.

Figure 4.21 shows N plotted with respect to their corresponding VS values, distinguished by predominant sediment type. Figure 4.21 is further classified separately for gravels, sands, clays and silts, and cemented sediments in Figures 4.22, 4.23, 4.24 and 4.25 respectively; these figures are distinguished on the basis of percent fines present in gravels and sands, plasticity in clays and silts, and sediment types in cemented sediments. Regarding predominant sediment types, this dataset has mostly clay closely followed by sand. Predominance of silt is uncommon, therefore, no general conclusions are drawn about this sediment type from this dataset.

N range from 0 to 100; many sediments have N=50 (Fig. 4.21). VS clusters almost entirely between 200 and 1000 m/s. N are highly variable in all predominant sediment types with respect to VS, ranging between almost 0 and more than 100. N reported are obtained from depths ranging to about 30 m in this dataset. Gravels have VS ranging mostly between 600 and 1000 m/s; typically VS for gravelly soils range between 350 and 700 m/s (refer to Table 3.2), therefore local gravels have higher than expected values. In clays, VS values mostly range between 200 and 400 m/s, while in sands they mostly range between 300 and 600 m/s; typical VS values for stiff clays range between 200 and 400 m/s, while for sands they range between 100 and 600 m/s (refer to Table 3.2),

therefore local clays and sands are in agreement with expected values. Comparison of VS from this dataset with LVV site-specific VS correlations by Murvosh et al. (2013b) (Ch. 3) show that clays and sands are in agreement with the site specific correlations, while the gravels have higher VS values than suggested by Murvosh et al. (2013b). Most cemented sediments have surprisingly low VS, ranging between 200 and 300 m/s. Unclassified sediments have N ranging from 10 to 50. Most unclassified sediments have VS ranging between 600 and 900 m/s, which is higher than most sediments classified by their predominant sediment type.

Figures 4.22 and 4.23 indicate that VS is influenced by the percent fines present in sediments. Higher VS mostly corresponds to sediments with lower fines content. For example, VS of gravels with low (< 5%) fines content ranges mostly between 600 and 1000 m/s, while in gravels with higher (> 12%) fines content VS is lower, ranging between 200 and 600 m/s (Fig. 4.21). Similarly, VS of sands with low (< 12%) fines content ranges mostly between 600 and 900 m/s, while in gravels with higher (> 12%) fines content VS is lower, ranging between 200 and 400 m/s (Fig. 4.23). Clays with high plasticity have higher VS compared to most clays with low plasticity, while clays with no subclass have a higher range of VS, between 700 m/s and 900 m/s (Fig. 4.24). Within cemented sediments (Fig. 4.25), caliche has the highest VS (~500 m/s), while the lowest VS of about 200 m/s is exhibited by all other sediment types; most sands have an intermediate VS value higher than most clays and lower than most gravels (Fig. 4.25). Within cemented sediments from this dataset, caliche and gravels have higher than expected VS values, while clays and sands are in agreement with expected VS values

(refer to Table 3.2). Comparison of VS in cemented sediments with LVV site-specific VS correlations by Murvosh et al. (2013b) (Ch. 3) show that contrary to expectation clays, sands and gravels all have lower VS values than the representative profile).

4.2.5. Discussion

The sediments from the select ESGI dataset are from different locations in the LVV, therefore lithology varies from site to site; despite this, several trends emerged. Clay is the most prevalent of the predominant sediment types and constitutes ~40% of the select ESGI dataset, closely followed by sand at 38%. Most sediments classified as predominantly sand have clay in them, and therefore are not purely cohesionless. Gravels and cemented sediments account for 13% and 7% of the select ESGI dataset, respectively. A little over half of the cemented sediments are predominantly sand. As noted earlier, the degree of cementation in sediments is not specified in this dataset. High N and VS in some specimens for all sediment types suggests that some cementation might have been present in specimens not labeled as such. Sediments logged as cemented have much lower VS than expected. This low VS in cemented sediments implies low degrees of cementation. Overall, in this dataset, VS has no obvious correlation to N. However, VS is quite sensitive to percent fines content in gravels and sands. Note that this dataset cannot be used for comparison of either N or VS with shear strength parameters, because shear strength data were not available for the respective locations.

There are several sources of uncertainty in this dataset. VS data available for this dataset are obtained by the ReMi method which, as explained earlier, averages large soil volumes

unlike the much more localized measurements for N. Note that VS was interpolated at select ESGI locations, therefore the interpolated VS might not be representative of the N and sediment type tested. As mentioned previously, the ESGI dataset did not address refusal, many sediments have N=50; this high concentration of N at 50 is not reasonable, and is possibly because N-values of 50 and above were taken as refusal and reported as 50. It is reasonable to assume that different types of samplers were used to conduct SPT for such a large dataset, but sampler types used are not reported in the select ESGI dataset. As such, N from non-standard samplers could not be corrected to SPT-equivalent N. Energy correction is only available for about 10% of N, therefore few N are converted to N_{60}. Regarding cemented sediments, the degree of cementation is not reported; it is also possible that some sediments with cementation may not have been reported as having cementation in the ESGI dataset. And despite all this, some trends emerged. Classification of cemented sediments based on their degree of cementation might prove more effective in observing trends within cemented sediments, which may have gone unnoticed.

Summary This chapter analyses relationships between shear parameters and *in situ* tests for the LVV using two datasets: a) major-projects dataset and b) Clark County valley-wide dataset. The major-projects dataset provides *in situ* and laboratory strength data, while the Clark County dataset provides randomized N and VS. Overall, clay is the predominant sediment type within the datasets analyzed in this chapter; cementation is prevalent as well. No strong general correlations between laboratory strength tests and *in situ* tests are observed for the LVV. Although laboratory strength data is sparse, some

weak trends are observed between shear parameters and *in situ* tests within the major projects dataset. As expected, sand mostly has higher friction angles and lower cohesion than clay, while clay and cemented sediments usually have higher undrained shear strength and cohesion than sand. Generally, shear parameters c and ϕ increase with increasing blow counts. Blow counts are highly variable in all predominant sediment types with respect to shear wave velocity within both datasets; very weak trends of increasing shear wave velocity with increasing blow counts are observed, if any. Comparison of local data and global correlations relevant to deep foundations are conducted in the upcoming chapter.

Table 4.1 – List of available data used for shear parameter comparisons in the major projects dataset

	Availability by Project				
Test data	**Mc-Carran**	**Tropicana & I-15**	**3rd St. & Gass Ave.**	**Neon**	**City Center**
Borehole logs*	x	x	x	x	x
VS – Surface wave (ReMi)	x	x			
VS – Downhole velocity		x			
VS – Suspension logging			x		x
Pressuremeter test	x	x		x	
Direct shear (DS) test		x	x	x	x
Single point DS test	x				
Unconfined compression test	x				
UU triaxial test				x	
Map showing approximate boring locations	x	x			

* - Borehole logs provide sediment description, blow count and sampler information

Table 4.2 – McCarran – Upper-bound friction angles from single-point direct shear tests

Borehole	Test depth (m)	Sediment description	Estimated friction angle (deg.)
C-1	13.7	Sandy fat clay	34
C-11	12.2	Fat clay	44
C-12	6.1	Sandy lean clay	51
C-14	17.5	Silty sand	32
C-19	15.2	Clayey sand	32
C-20	3.8	Sandy lean clay	50
C-22	13.7	Sandy fat clay	46
C-23	3.8	Clayey sand	50
C-26	18.3	Clayey sand	34
C-26	3.8	Silty sand	41
C-4	16.0	Clayey sand	46
C-5	21.8	Sandy fat clay	32
C-6	9.8	Sandy elastic silt	34
C-7	7.6	Sandy lean clay	41
CP-3	3.0	Clayey sand	48
CP-3	4.6	Poorly graded sand with clay	54
MSE-3	6.7	Clayey sand	41
PSB-1	10.7	Fat clay	36
PSB-11A	18.3	Fat clay	33
PSB-14	10.7	Silty sand	59
PSB-15	12.2	Fat clay	38
PSB-18	12.2	Poorly graded sand	45
PSB-21	6.4	Sandy fat clay	47
PSB-7	4.6	Fat clay	48
R-11	17.5	Sandy lean clay	36
R-4	19.8	Sandy fat clay	34
R-8	24.4	Fat clay	29
RSB - 1E	7.6	Sandy lean clay	40
RSB -1B	13.7	Fat clay	28
RSB -1C	22.9	Fat clay	35
RSB -1C	6.1	Fat clay	36
RSB -2C	9.8	Sandy fat clay	39
S-1	11.1	Fat clay	35
S-2	3.0	Clayey sand	51

Table 4.3 – Summary of ESGI data types (Lynn, 2008)

Report Information	Exploration Information	Layer Information	Layer Attributes	Index, Geotechnical and Chemical Properties
Report date	Exploration name	Start layer	Fill	Sample depth
Report no.	Exploration type	Stop layer	Non-plastic	Sample thickness
Agency name	Exploration location (State grid format)	Shear wave velocity**	Cemented	Moisture content**
Project type*	Exploration location accuracy*	Soil classification	Non-cemented	Dry density**
Site class	Exploration elevation	Visual description*	Organics	Standard penetration test**
	Exploration method*		Porous	Percentage passing #200 sieve**
	Depth of groundwater table**		Bedrock	Plastic limit**
				Liquid limit**
				Plasticity index**
				Swell**
				Sulfates** (SO_4^{-2})
				Solubility**

Notes: * Non-mandatory ** Where applicable, or performed

Table 4.4 – Sediment groupings

USCS group symbol	USCS group name	USCS general description	Predominant sediment type
GC	Clayey gravel	Gravel with more than 12% fines	Gravel
GM	Silty gravel		
GP	Poorly graded gravel	Poorly-graded gravel with less than 5% fines	
GP-GC	Poorly graded gravel with clay	Poorly-graded gravel with 5 to 12% fines	
GP-GM	Poorly graded gravel with silt		
GW	Well graded gravel	Well-graded gravel with less than 12% fines	
GW-GM	Well graded gravel with silt		
SC	Clayey sand	Sand with more than 12% fines	Sand
SC-SM	Silty, clayey sand		
SM	Silty sand		
SP	Poorly graded sand	Poorly-graded sand with less than 12% fines	
SP-SC	Poorly graded sand with clay		
SP-SM	Poorly graded sand with silt		
SW	Well graded sand	Well-graded sand with less than 12% fines	
SW-SC	Well graded sand with clay		
MH	Elastic silt	Silt	Silt
ML	Silt		
CH	Fat clay	High plasticity clay	Clay
CL	Lean clay	Low plasticity clay	
CL-ML	Silty clay		

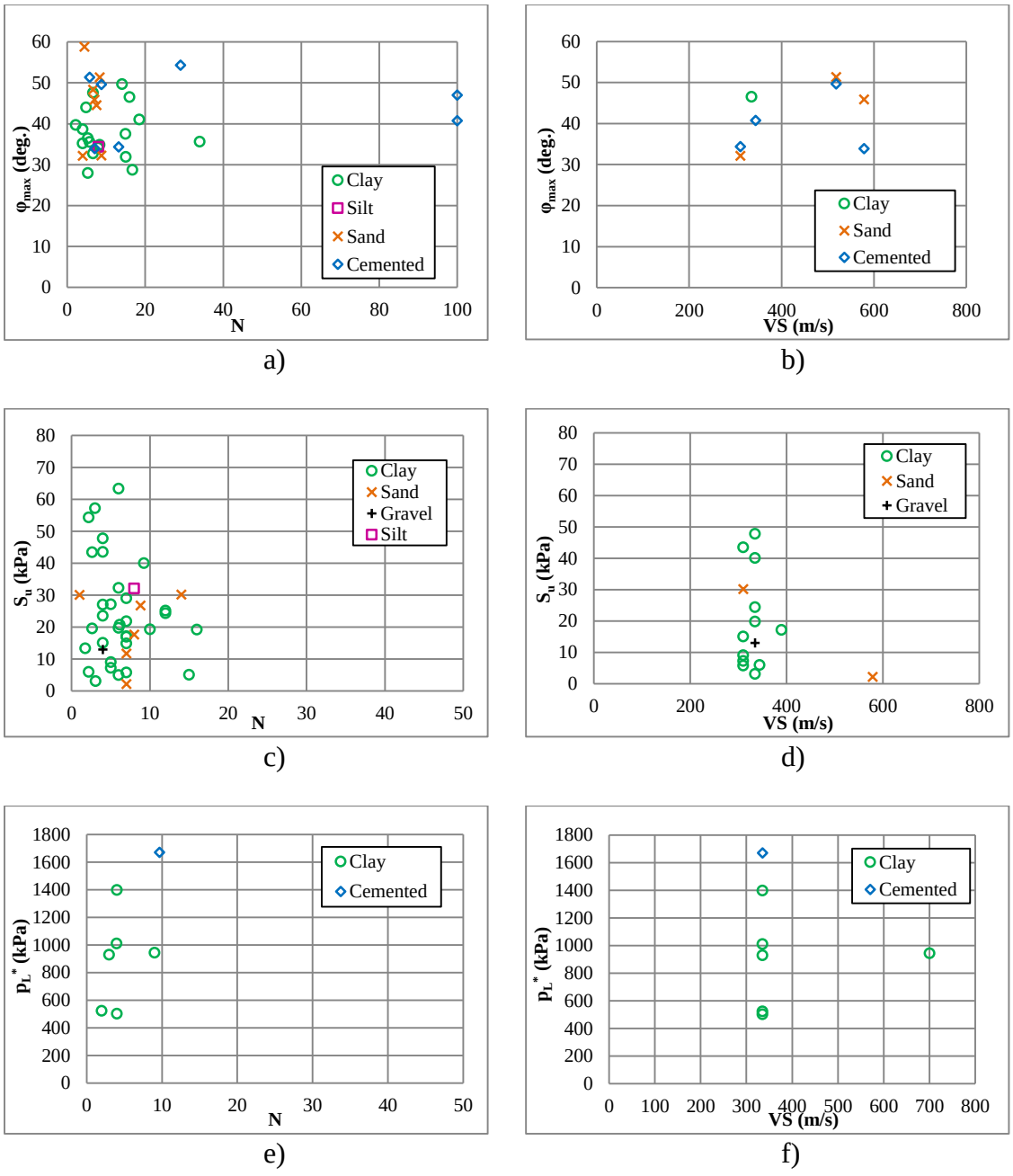

Figure 4.1: McCarran – Calculated upper bound friction angles (ϕ_{max}) from single point DS tests compared with a) N, and b) VS; undrained shear strength (S_u) compared with c) N, and d) VS; net limit pressure (p_L^*) from PMT compared with e) N, and f) VS. All plots distinguished by predominant sediment type.

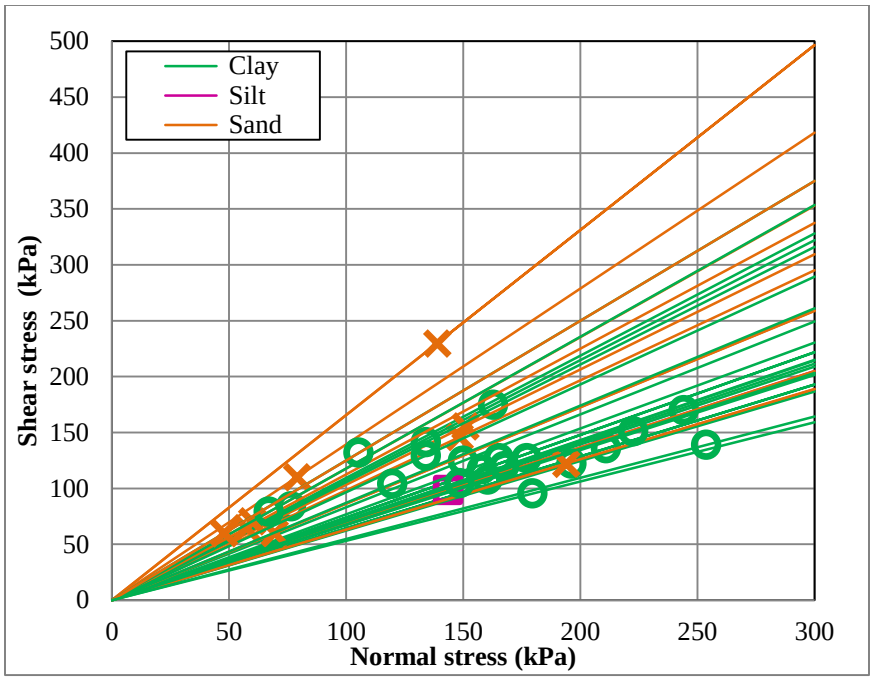

a)

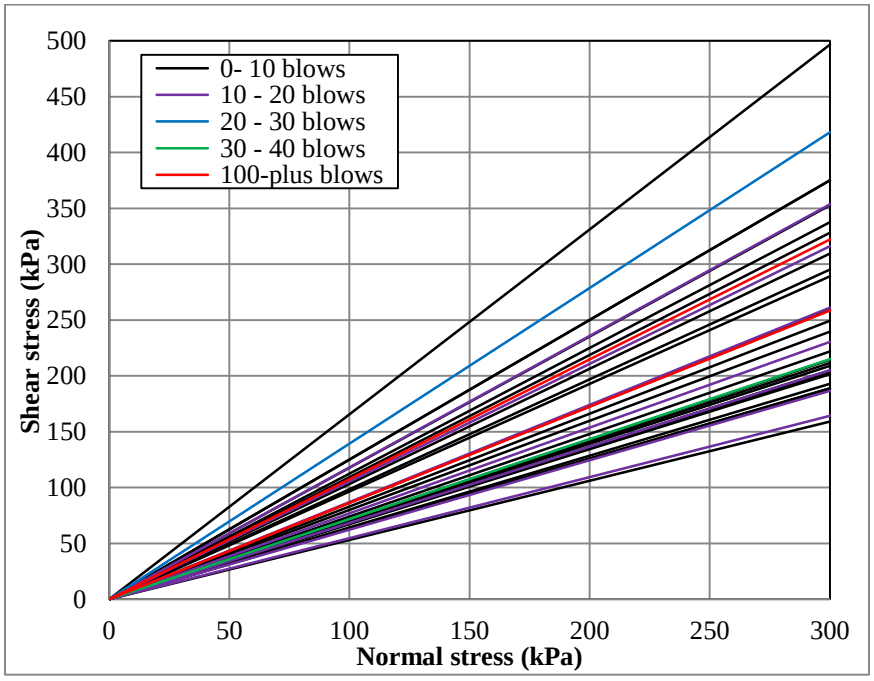

b)

Figure 4.2: McCarran – Mohr-Coulomb failure envelopes from single point DS tests assuming zero cohesion, distinguished by a) predominant sediment type (symbols show each test), and b) N ranges.

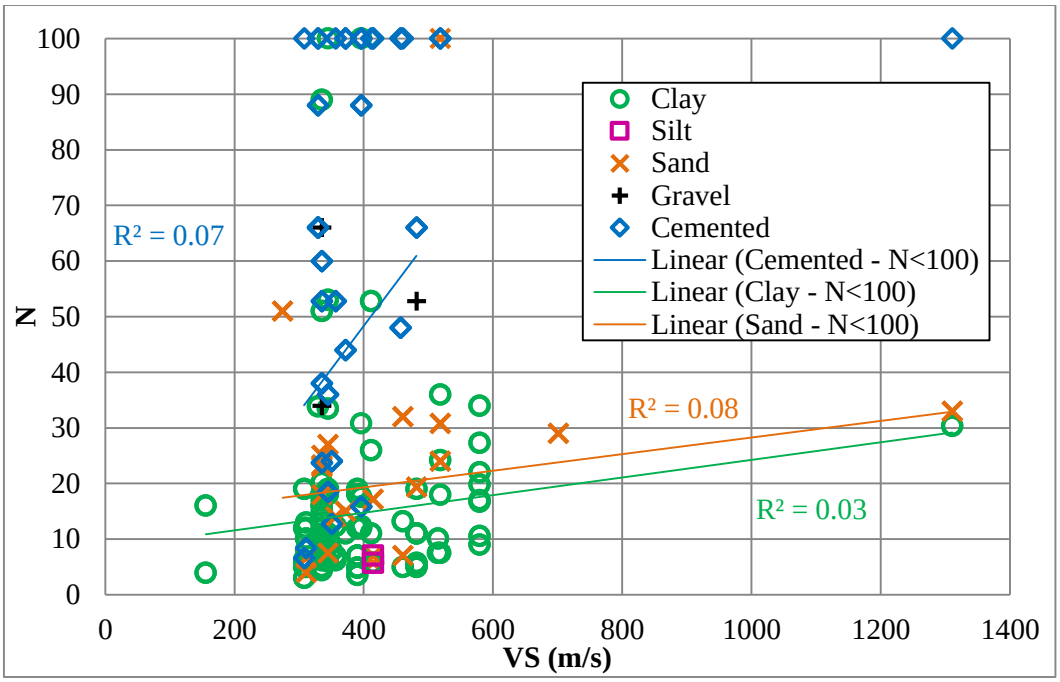

Figure 4.3: McCarran – VS from ReMi lines compared with N from nearby boreholes; distinguished by predominant sediment type.

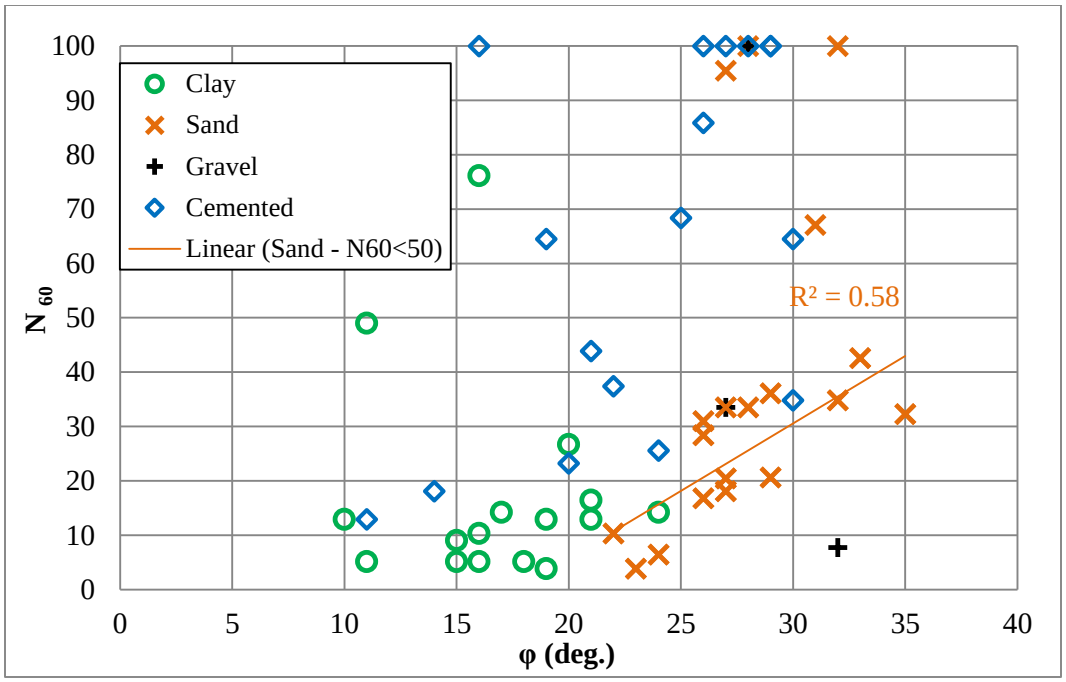

a)

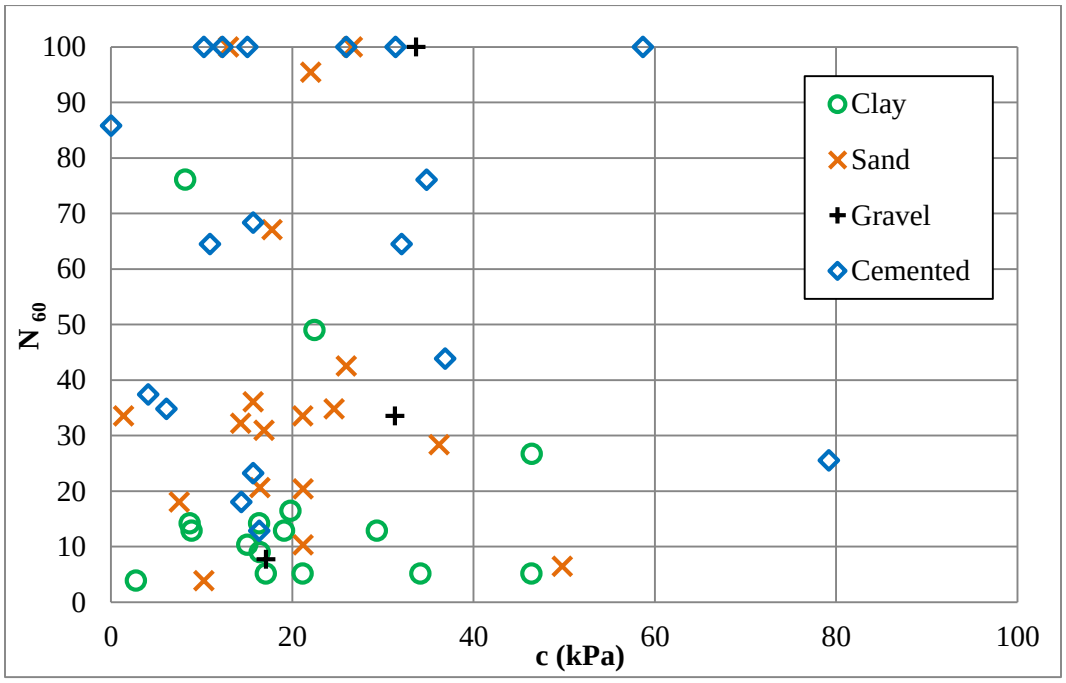

b)

Figure 4.4: Tropicana & I-15 – Shear strength parameters from DS tests a) friction angle (ϕ) and b) cohesion (c) compared with N_{60}; distinguished by predominant sediment type.

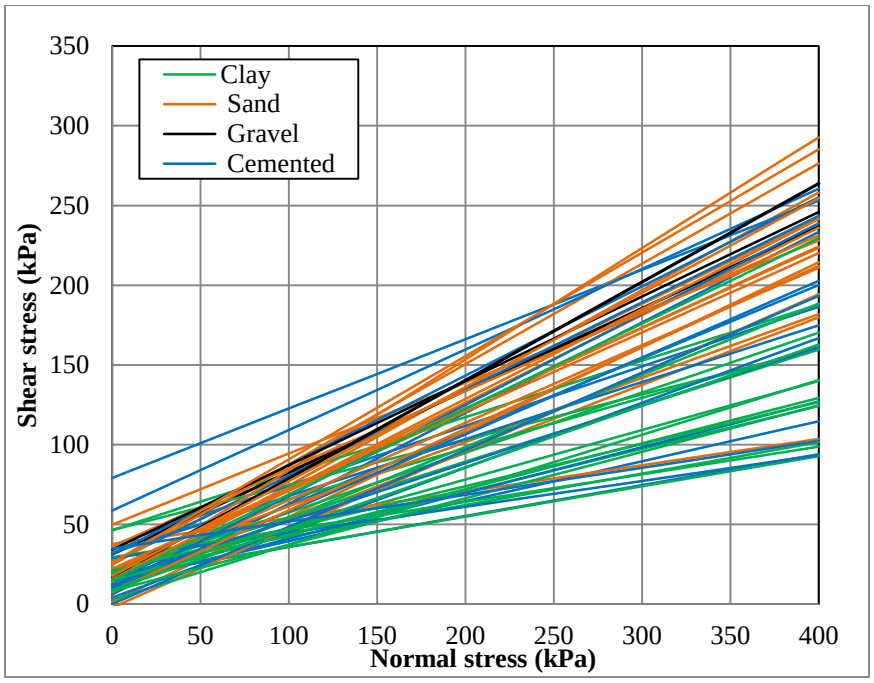

a)

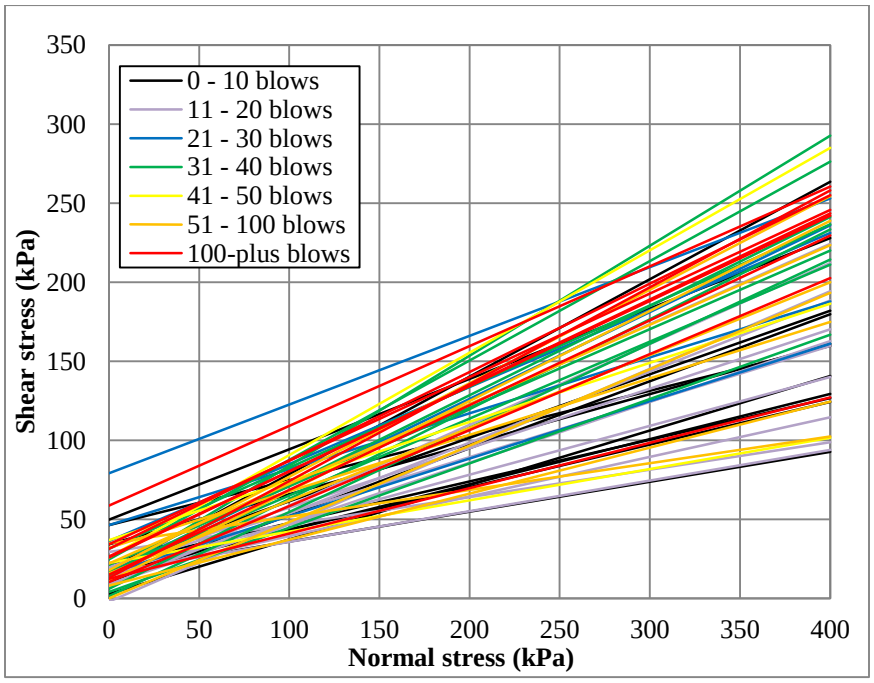

b)

Figure 4.5: Tropicana & I-15 – Mohr-Coulomb failure envelopes from DS tests, distinguished by a) predominant sediment type, and b) N_{60} ranges.

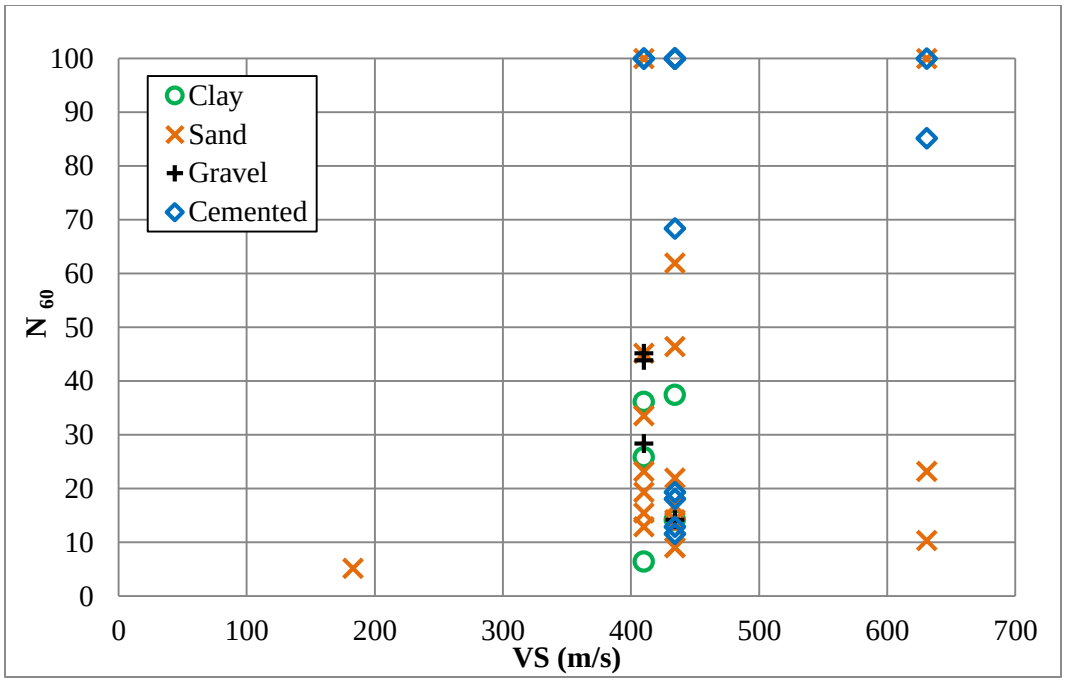

Figure 4.6: Tropicana & I-15 – VS from downhole velocity testing compared with N_{60}.

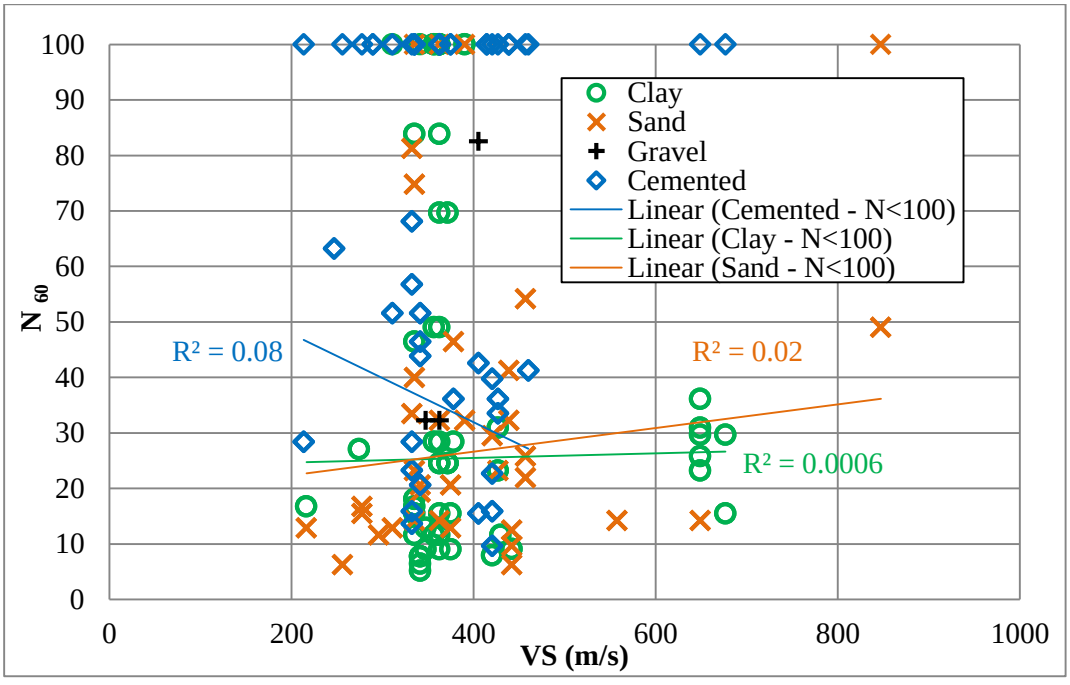

Figure 4.7: Tropicana & I-15 – VS from ReMi lines compared with N_{60} from nearest boreholes.

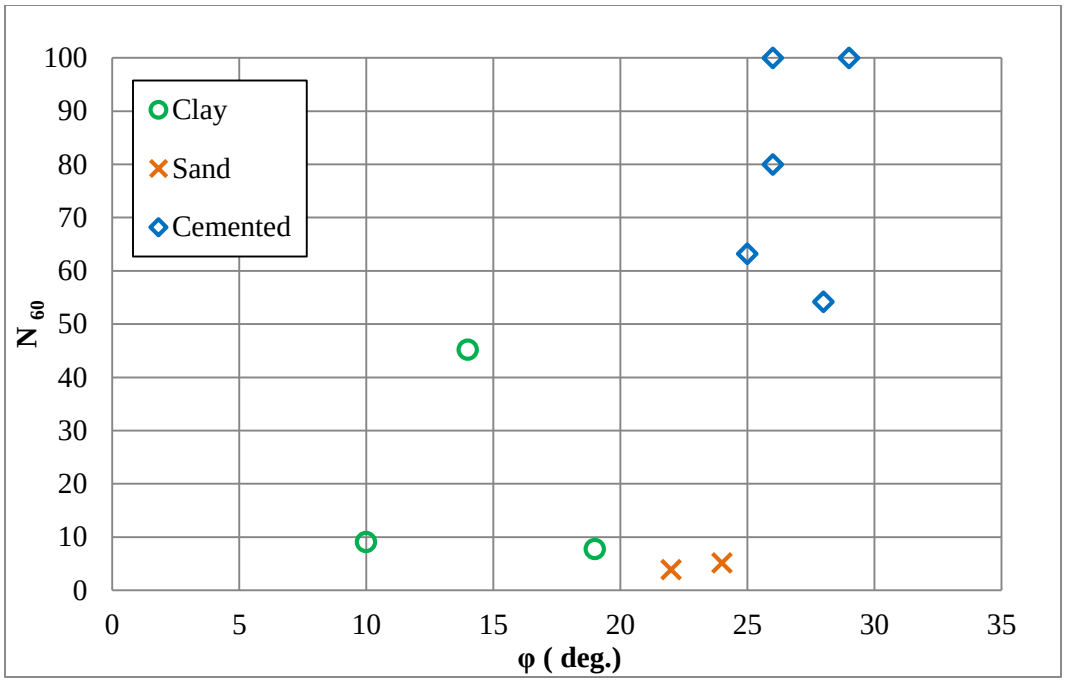

a)

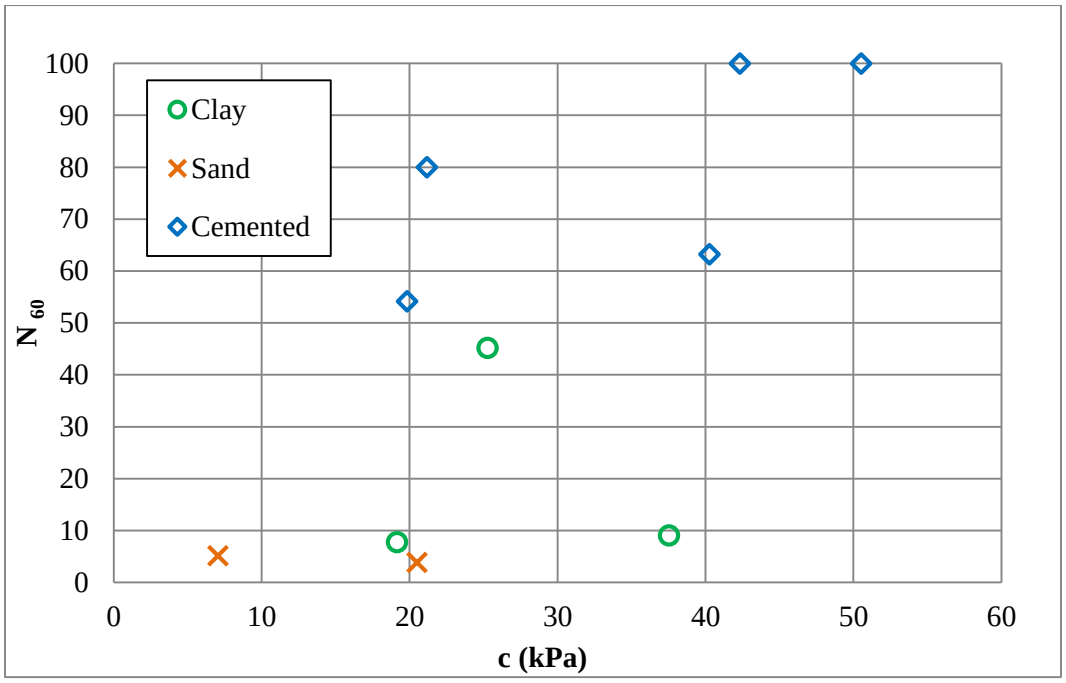

b)

Figure 4.8: 3rd & Gass – Shear strength parameters from DS tests a) friction angle (ϕ) and b) cohesion (c) compared with N_{60}.

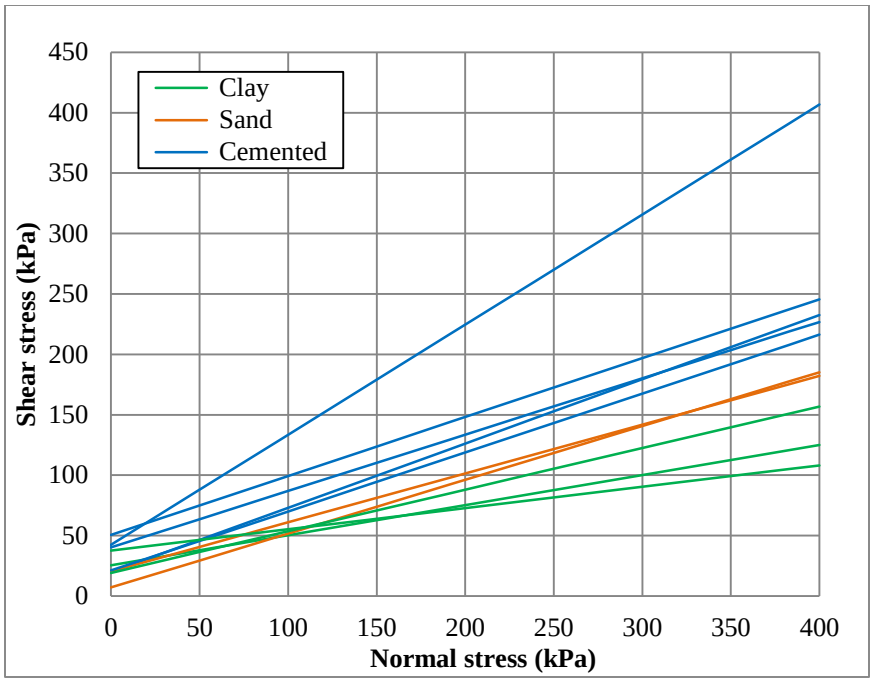

a)

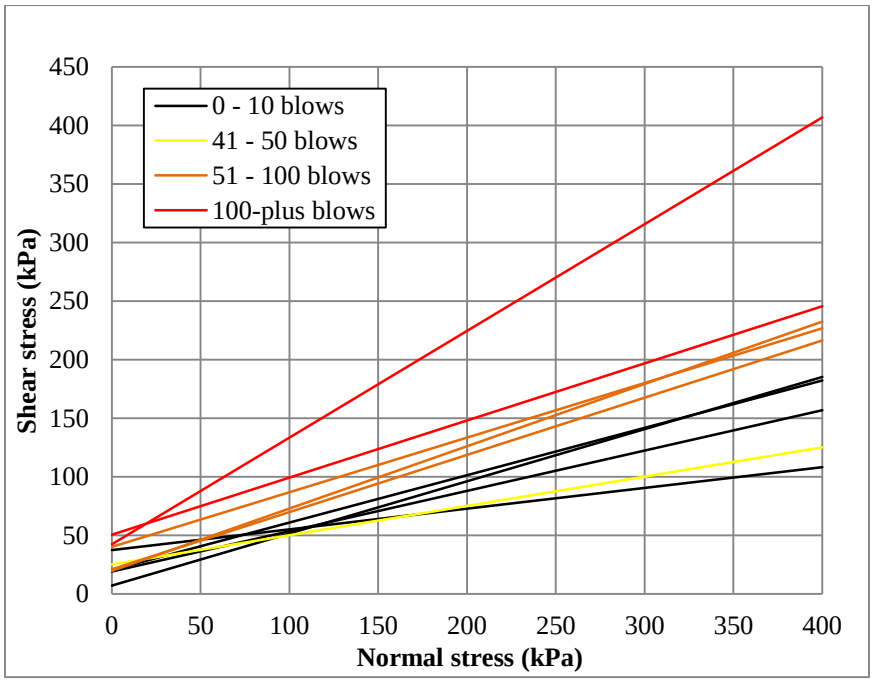

b)

Figure 4.9: 3rd & Gass – Mohr-Coulomb failure envelopes from DS tests, distinguished by a) sediment type, and b) N_{60} ranges.

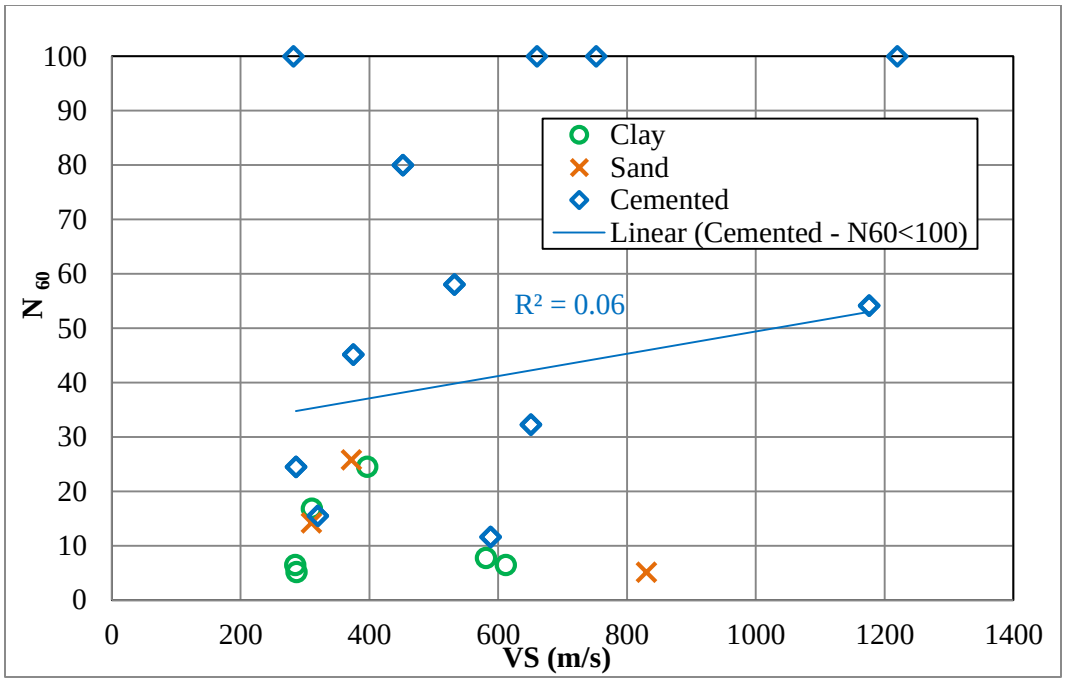

Figure 4.10: 3rd & Gass – VS from suspension logging compared with N_{60} for the same borehole.

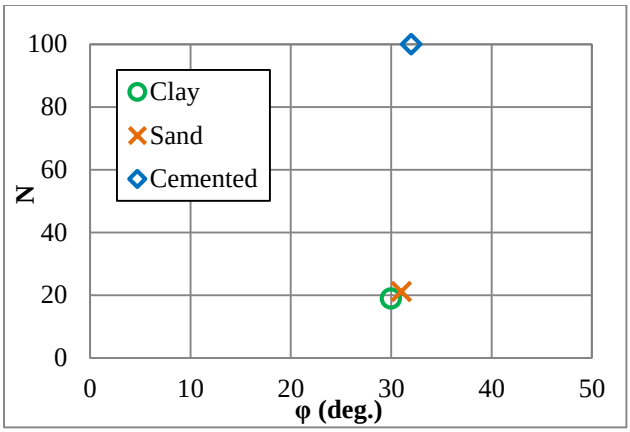

a)

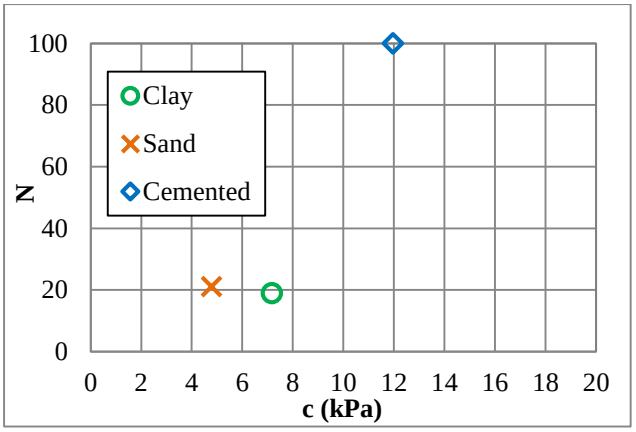

b)

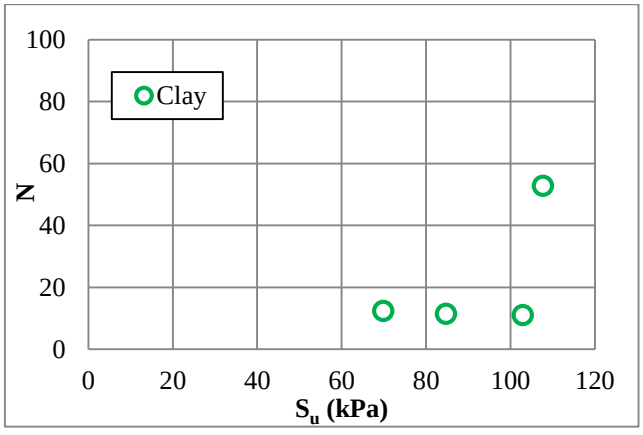

c)

Figure 4.11: Neon – Shear strength parameters a) friction angle (ϕ) and b) cohesion (c) from DS tests, and c) undrained shear strength (S_u) from Unconsolidated Undrained (UU) triaxial tests compared with N.

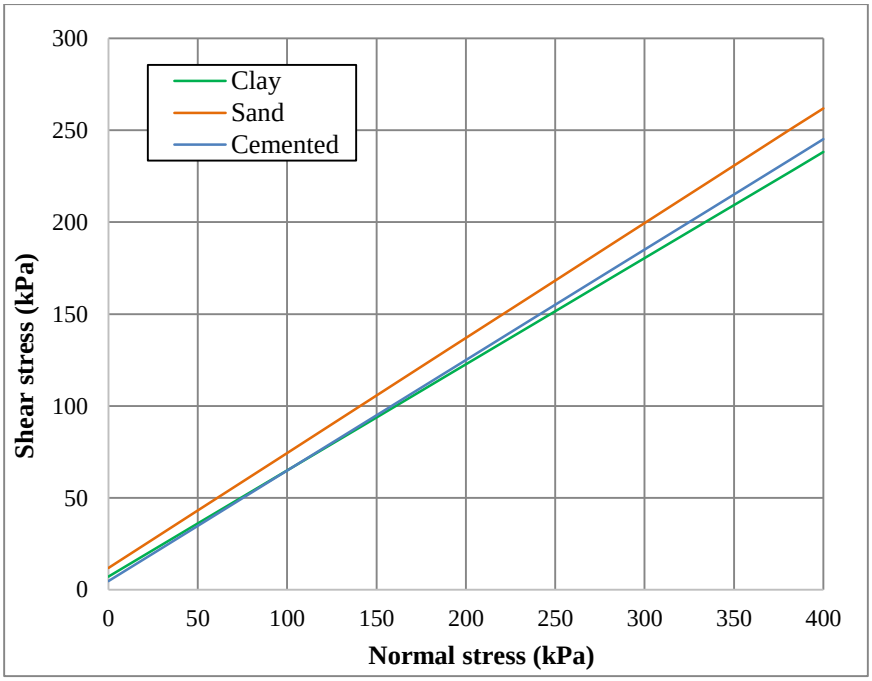

a)

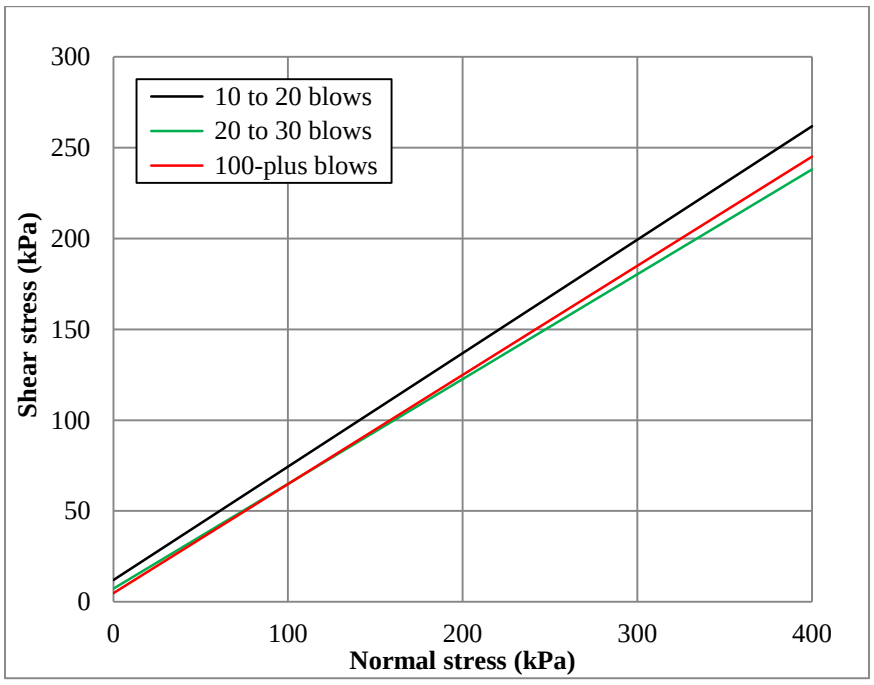

b)

Figure 4.12: Neon – Mohr-Coulomb failure envelopes from DS tests, distinguished by a) sediment type, and b) N ranges.

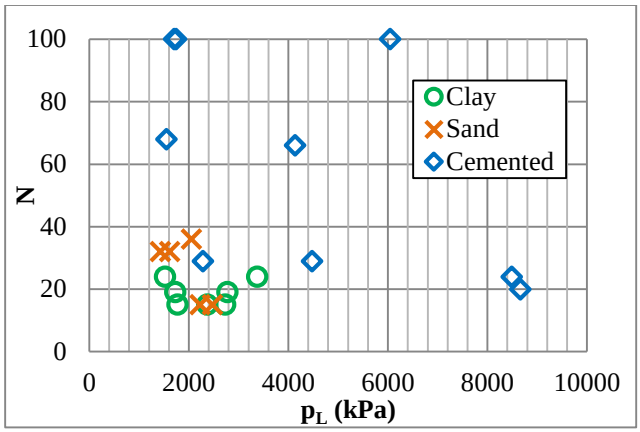

a)

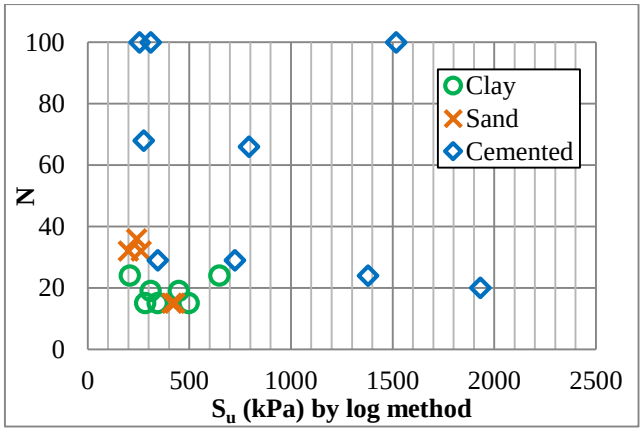

b)

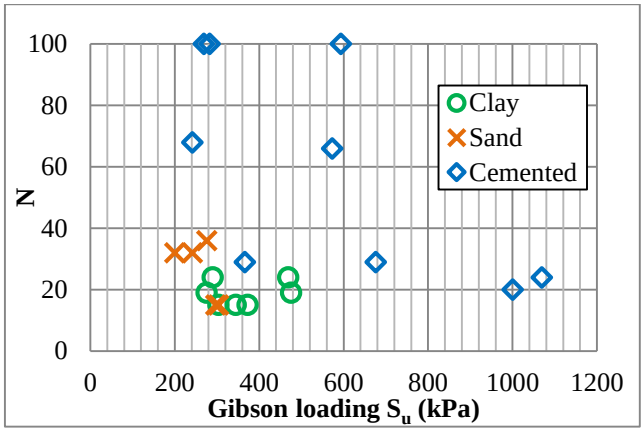

c)

Figure 4.13: Neon – Outcomes of PMT a) limit pressure (p_L), b) S_u by log method, and c) Gibson loading S_u compared with N.

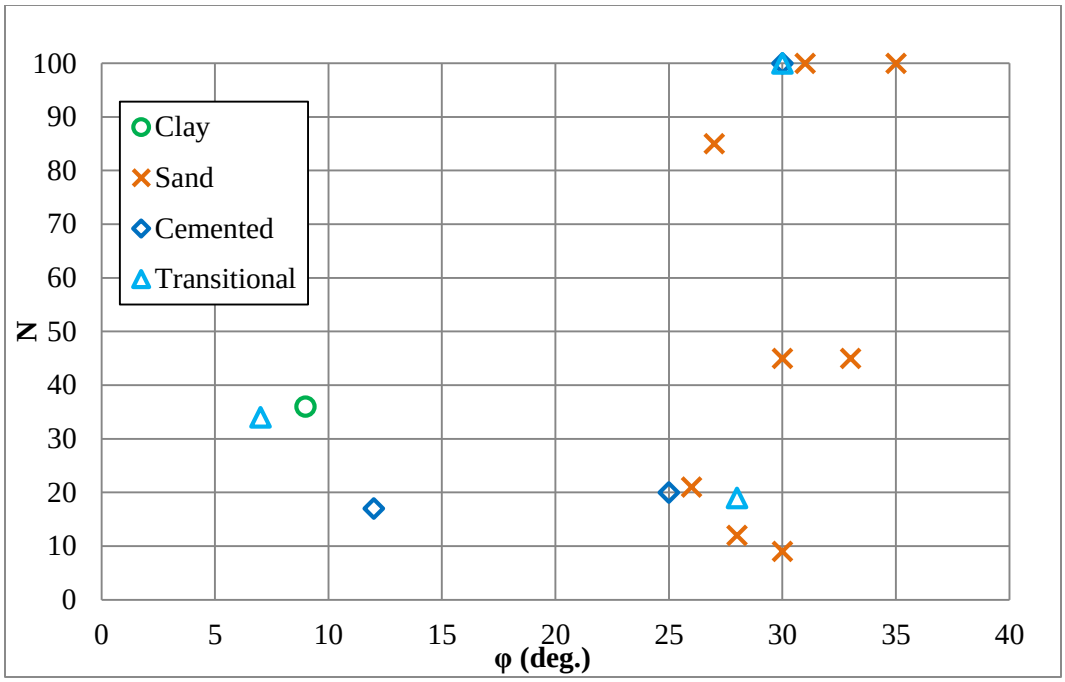

a)

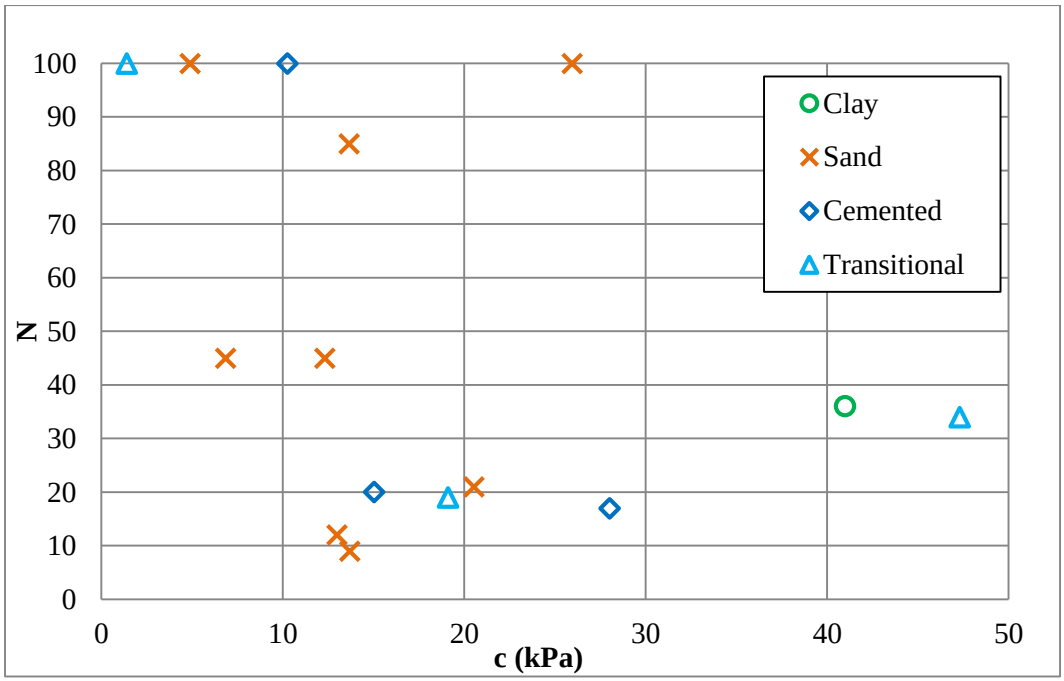

b)

Figure 4.14: City Center – Shear strength parameters from DS tests a) friction angle (ϕ) and b) cohesion (c) compared with N.

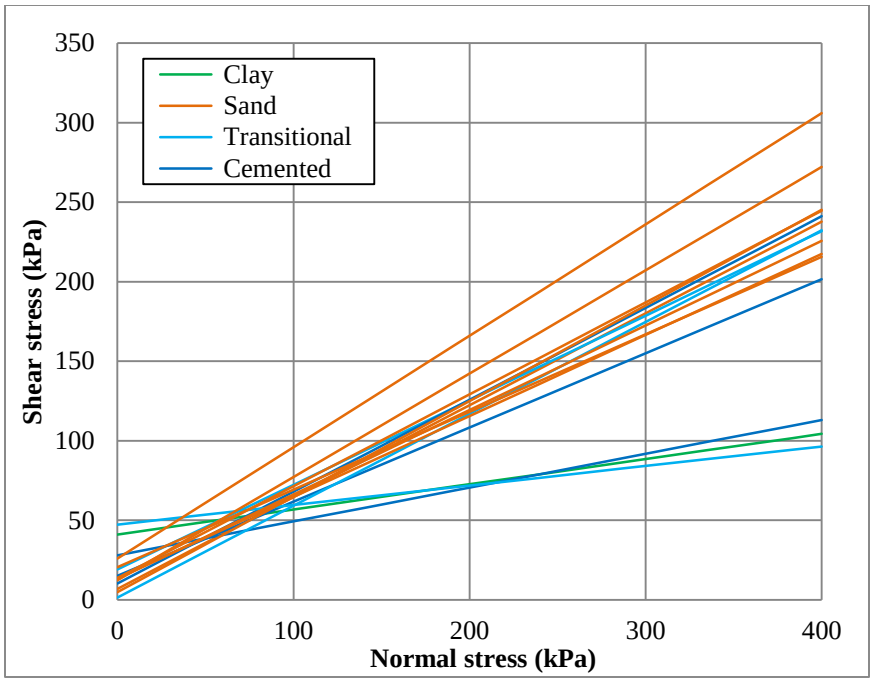

a)

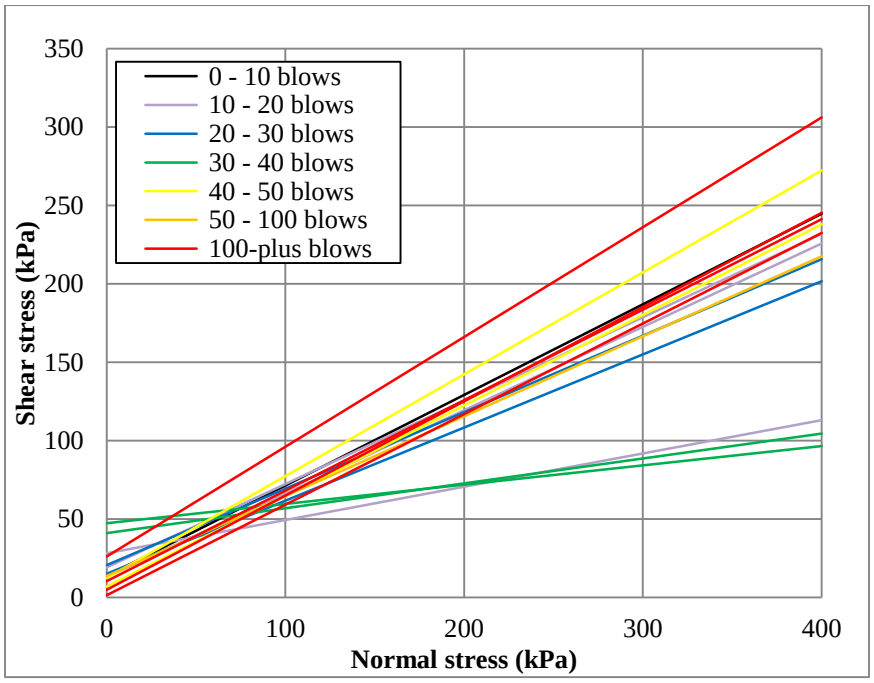

b)

Figure 4.15: City Center – Mohr-Coulomb failure envelopes from DS tests, distinguished by a) sediment type, and b) N ranges.

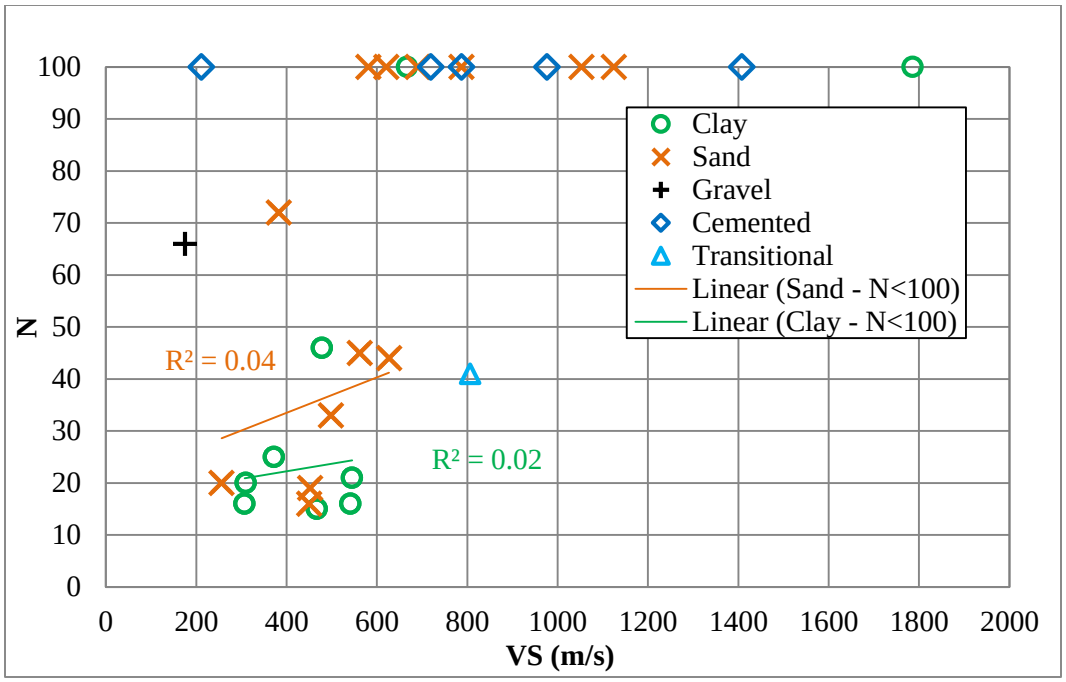

Figure 4.16: City Center – VS from suspension logging compared with N for the same borehole.

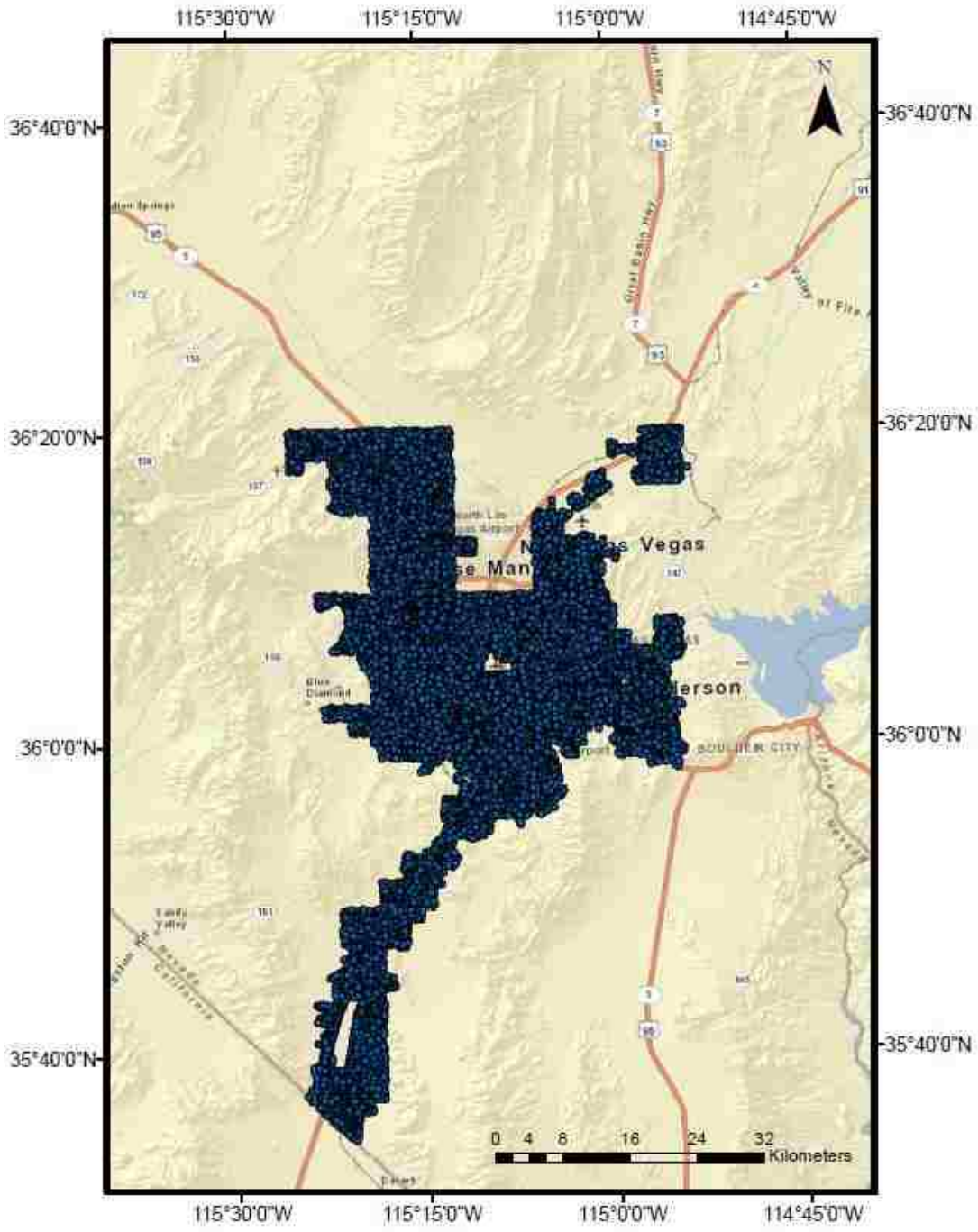

Figure 4.17: Optim VS dataset overlaid on the LVV.

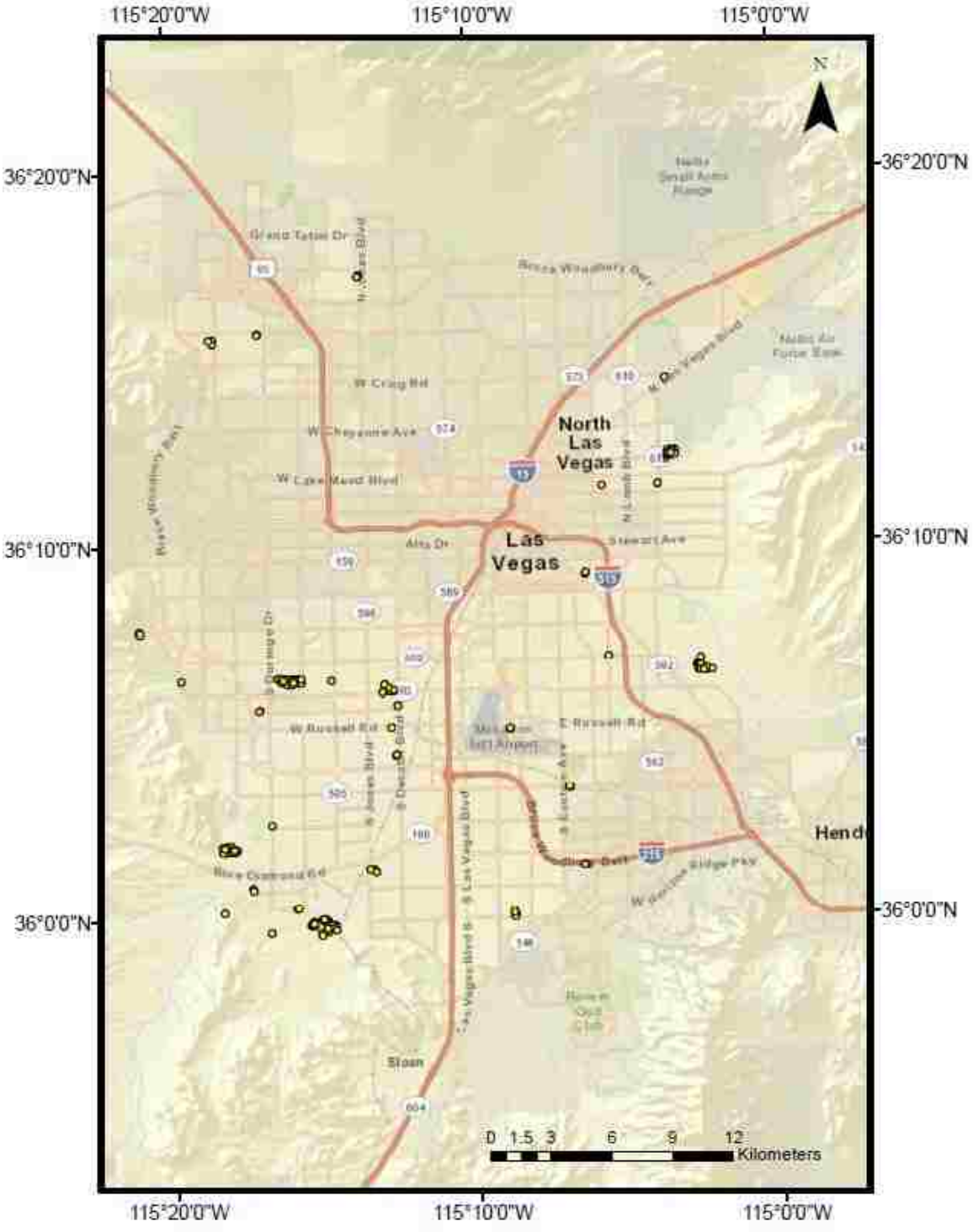

Figure 4.18: Select ESGI data points (yellow) overlaid on the LVV. Note that all N obtained from testing at different depths in the same borehole is represented by one location on the map.

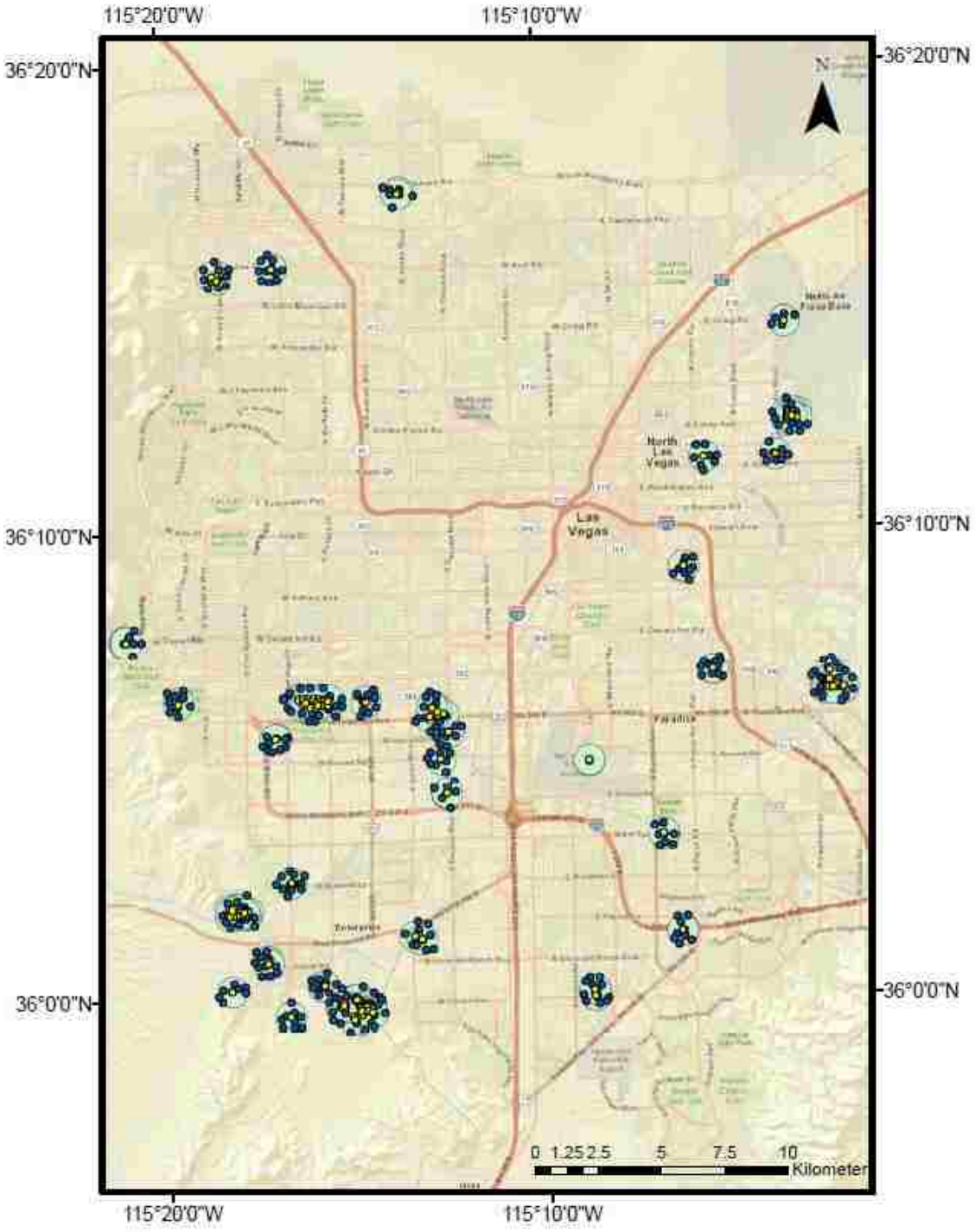

Figure 4.19: Select ESGI SPT data points (yellow) along with select Optim VS data point (dark blue) located within the 610-m (2000-ft) radius of select ESGI SPT locations (light blue).

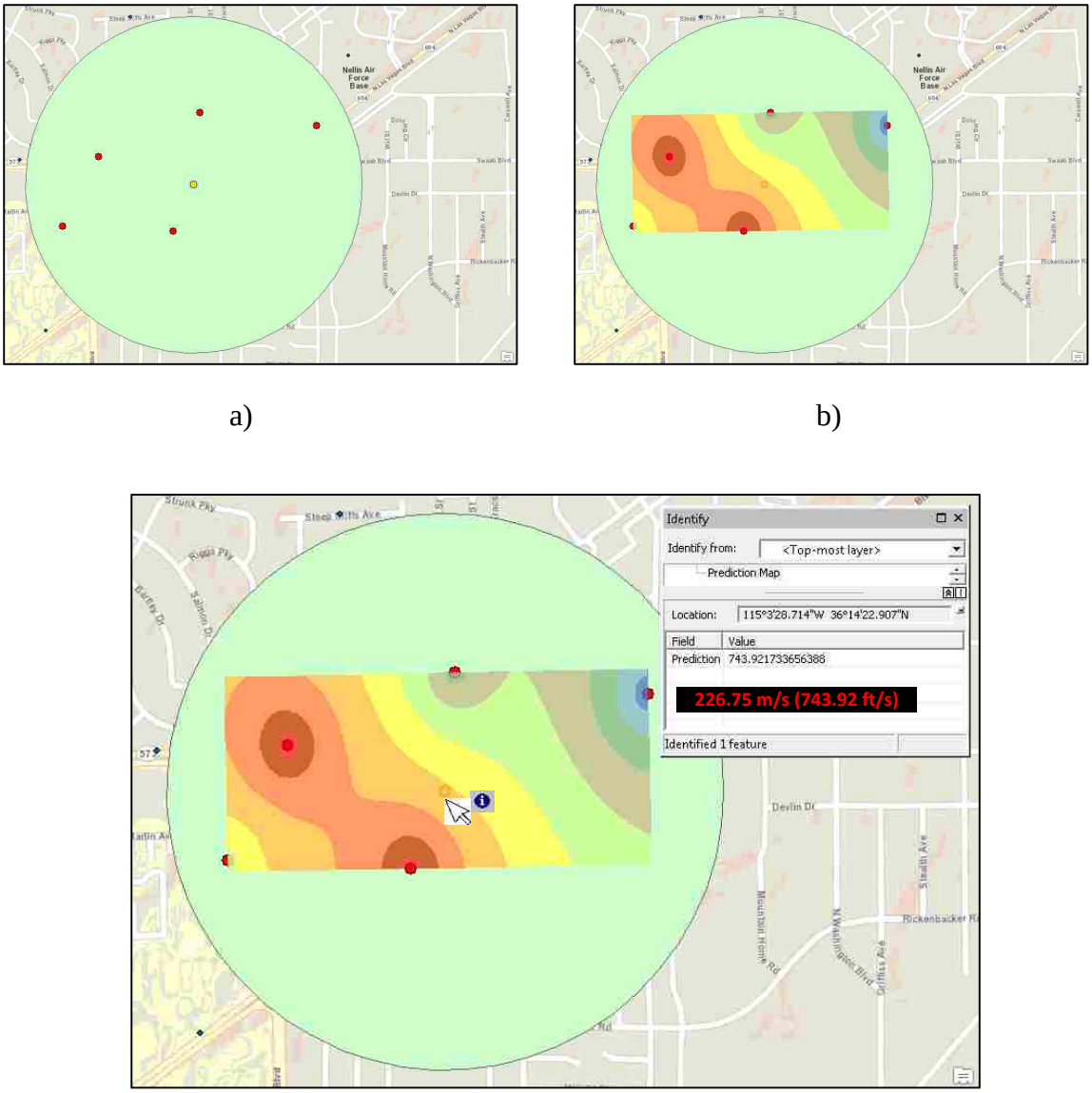

a) b)

c)

Figure 4.20: Process of obtaining interpolated VS at a specific depth for a select ESGI data point in ArcGIS. a) A select ESGI data point (yellow) along with select Optim VS data points (red) located within 610-m (2000-ft) radius of the select ESGI data point. b) A 2D spatial interpolation of VS at the depth of an N measurement is performed by the IDW tool using VS values from the select Optim VS data points at the specified depth. c) The 'Identify' tool is used to visually identify the interpolated VS at the select ESGI data point for the specified depth.

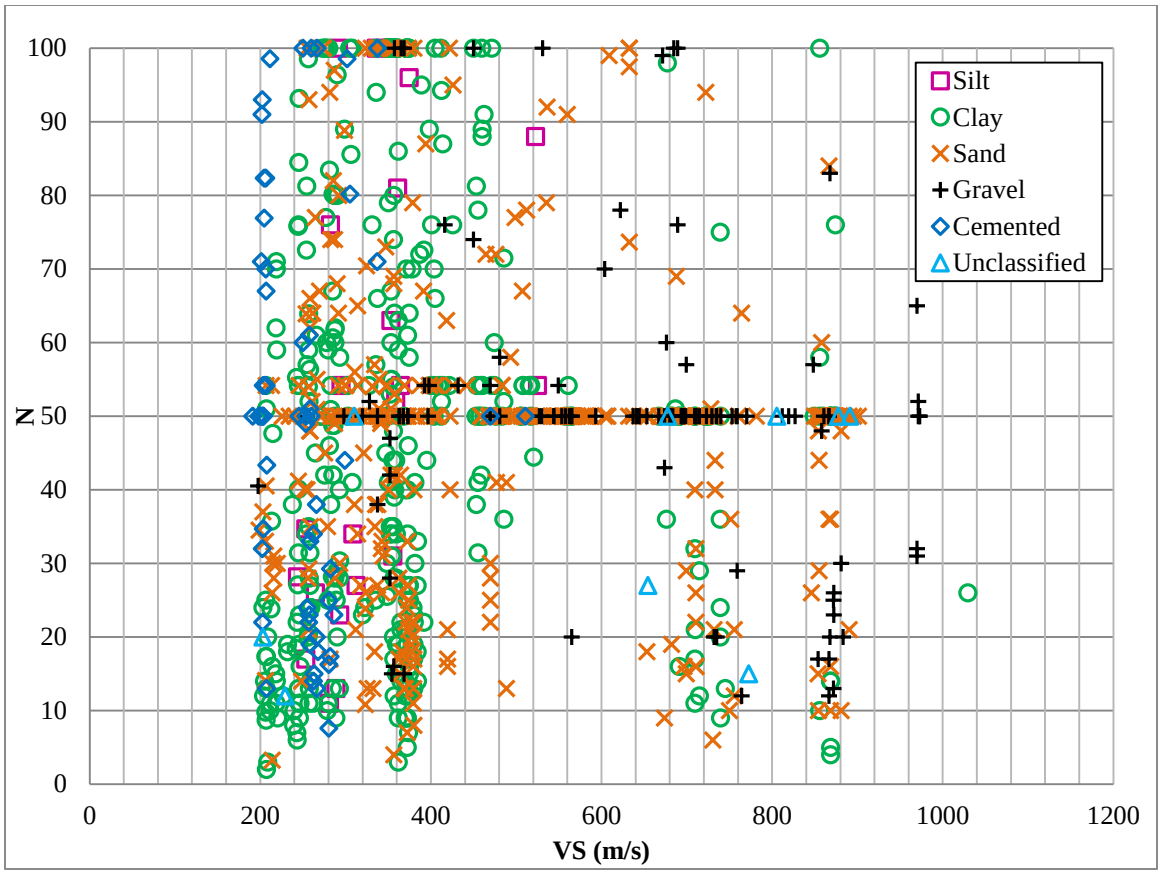

Figure 4.21: Clark County - Select ESGI N plotted with respect to VS interpolated using Select Optim VS dataset; distinguished by predominant sediment types.

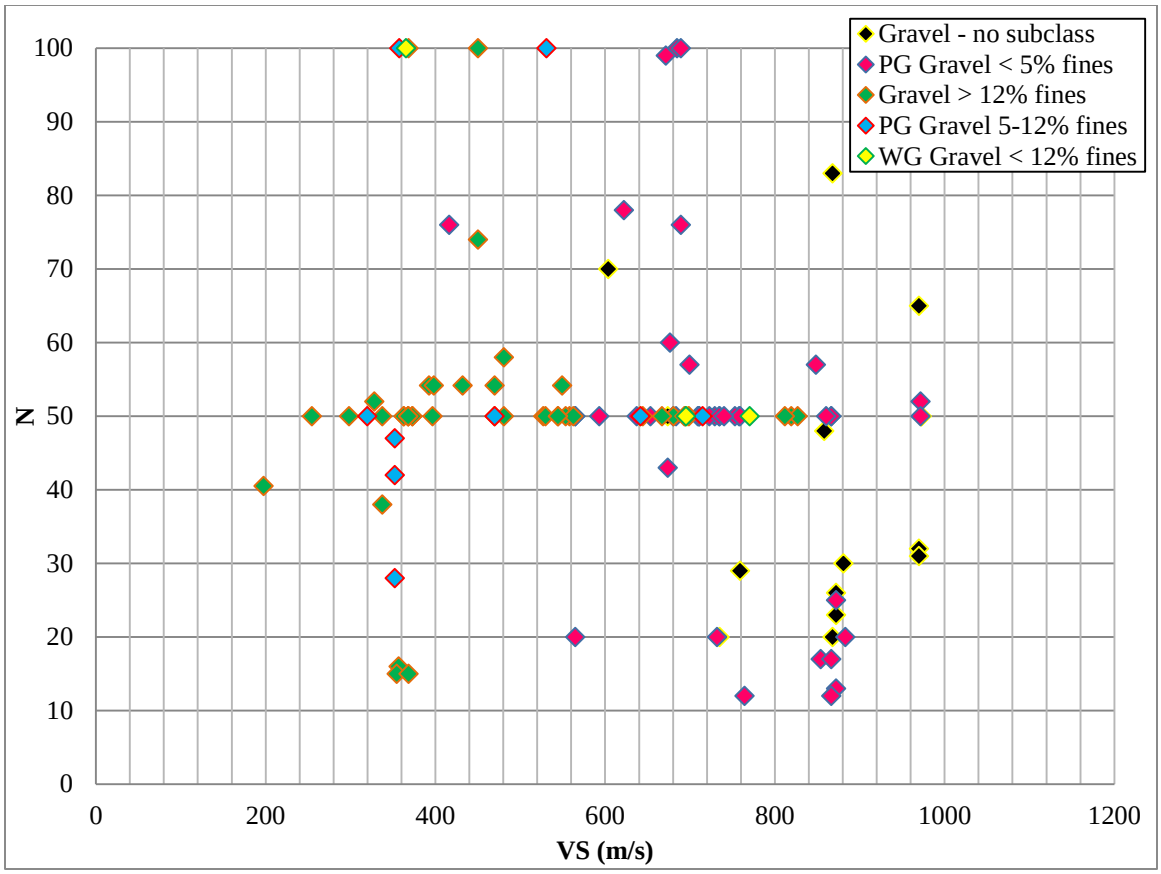

Figure 4.22: Clark County - Subset of dataset from Fig. 4.21 for gravel; distinguished by percent fines content. PG: poorly graded; WG: well graded.

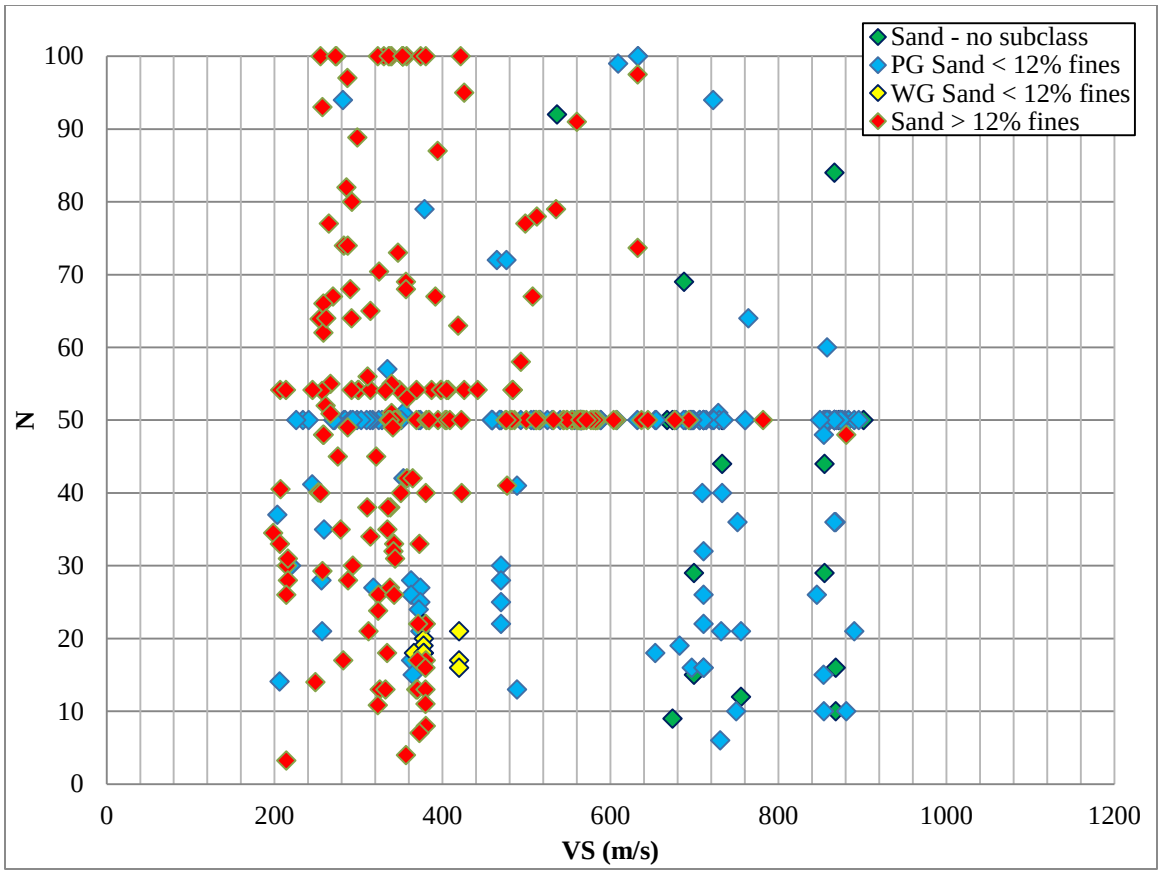

Figure 4.23: Clark County - Subset of dataset from Fig. 4.21 for sand; distinguished by percent fines content. PG: poorly graded; WG: well graded.

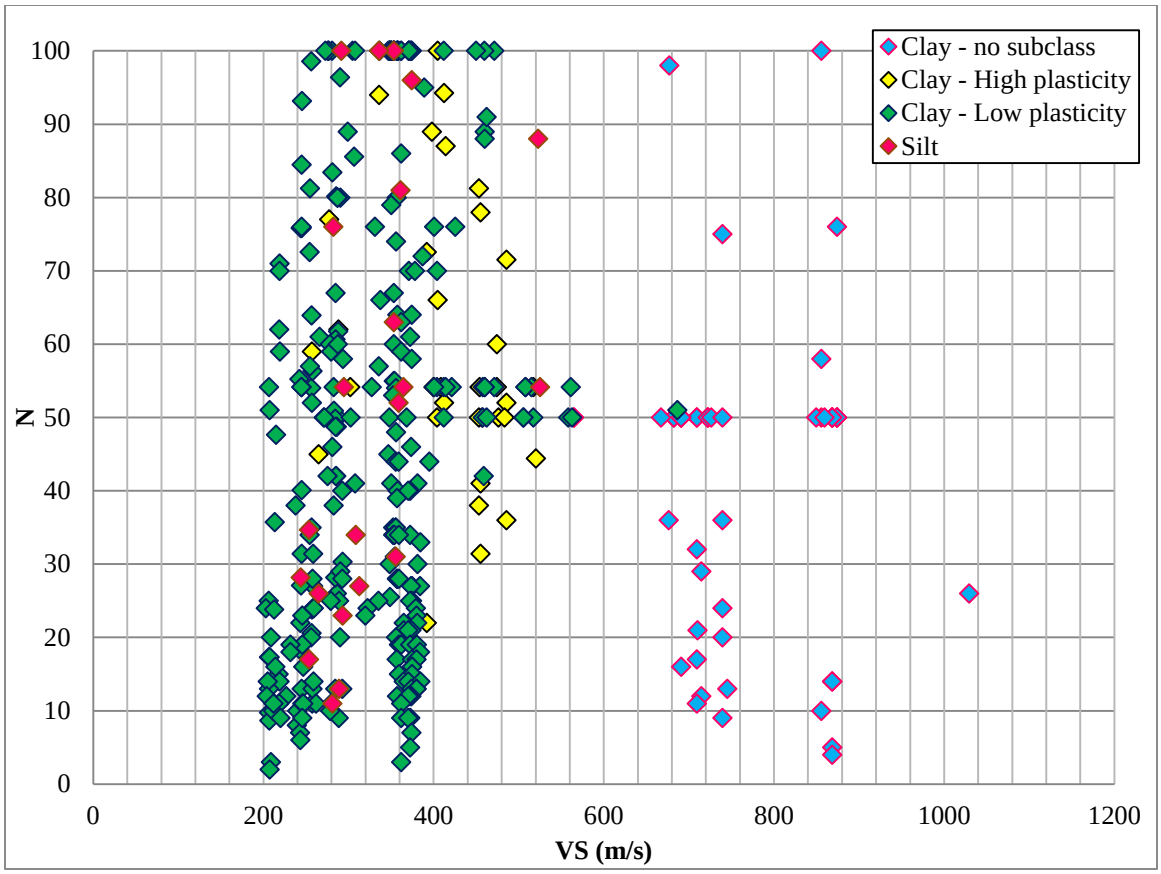

Figure 4.24: Clark Clark County - Subset of dataset from Fig. 4.21 for clay and silt; distinguished by plasticity

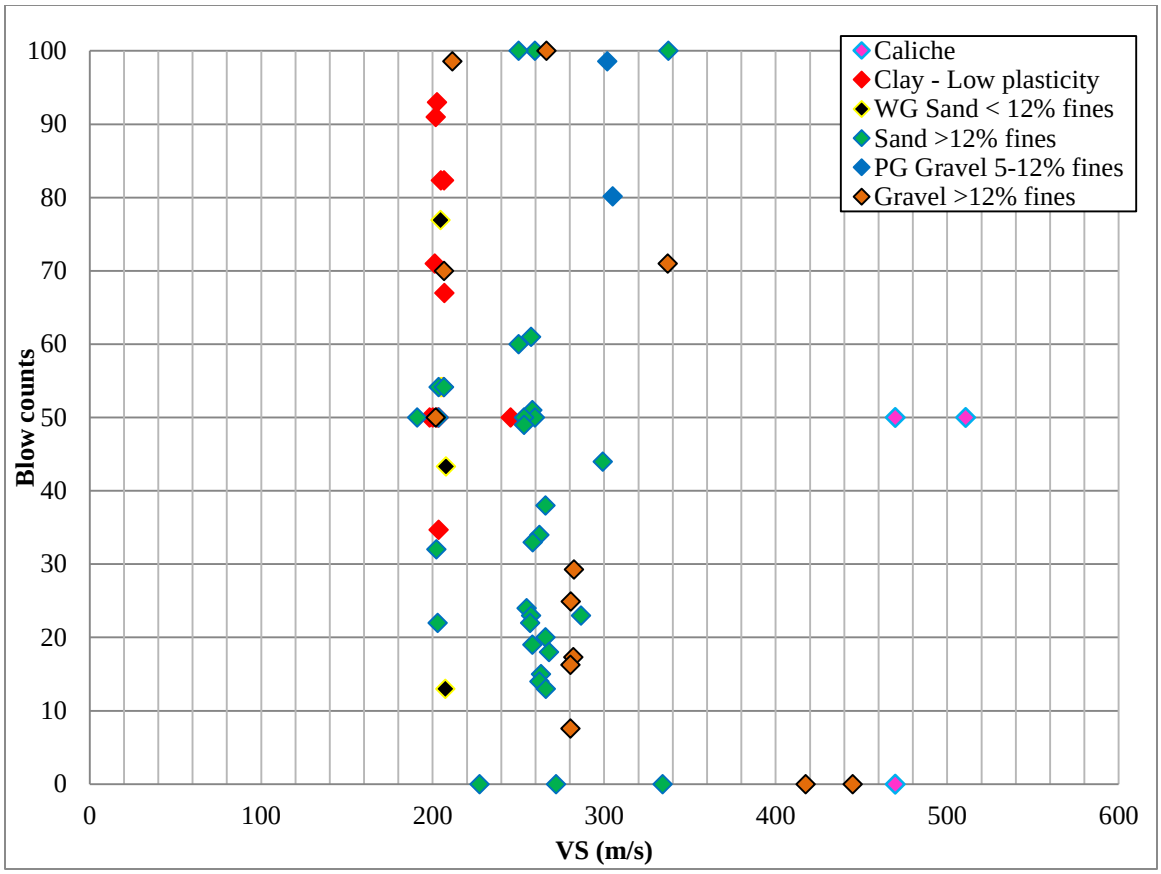

Figure 4.25: Clark County - Subset of dataset from Fig. 4.21 for cemented sediments; distinguished by percent fines content in sands and gravels, and plasticity in clays. PG: poorly graded; WG: well graded.

CHAPTER 5

DISCUSSION

Datasets from readily measured *in situ* tests and laboratory tests from the LVV were obtained from direct measurements, local consultants and government entities to study relationships with stress-strain characteristics of sediments from the LVV. In this chapter, all data obtained for this study irrespective of projects or locations (Chapters 3 and 4) are overlaid on the global plots of shear strength parameters and VS with respect to N or N_{60} that were introduced in Ch. 2. Comparisons of local data with global correlations test the representativeness of the LVV soils with respect to soils from different sites around the world and, therefore, the applicability of such global correlations in the LVV.

Figure 5.1 shows ϕ plotted with respect to N or N_{60}. As stated earlier, the global correlations are for cohesionless soils while LVV data comprises mostly of cohesive soils (Appendix B), therefore it is not surprising that most local ϕ values are lower than the ranges suggested by the global correlations. Local ϕ values are highly variable, particularly with respect to N or N_{60} under 20, ranging between 10 to 60 degrees. A trend ($R^2 = 0.15$) of increasing ϕ with increasing N and N_{60} is observed, for values including N and N_{60} of 100. The exponential trend line ($y = 7.7594\ e^{0.0555\ x}$) generated shows a similar growth curve like most global correlations, except with much lower ϕ; in fact, it scales particularly well with JRA's study of sandy soils in 1990 (as cited in Baxter et al., 2005) offset by about 13 degrees at N or N_{60} value of 30. It is important to note that most local ϕ values over 35 degrees are the ϕ_{max} values calculated from the McCarran SDS test

results (Ch. 4), are higher than typical ϕ observed in the LVV, and were therefore not included in the exponential fit.

Figure 5.2 shows S_u plotted with respect to N or N_{60}. Variability among global correlations increases with increasing N or N_{60} and S_u. For example, at N or N_{60} = 20, S_u ranges from ~50 to ~250 kPa; while at N or N_{60} =100, S_u ranges from ~100 to 1200 kPa. Local S_u values range from 0 to 2000 kPa, although most local values have N or N_{60} under 20 and S_u below 200 kPa. A trend (R^2 = 0.29) of increasing S_u with increasing N or N_{60} is observed. Figure 5.3 shows the subset of Figure 5.2 for N or N_{60} under 20. Most LVV data with N or N_{60} under 13 are comparable to some global correlations. Half of those with N or N_{60} above 10 have much higher S_u than predicted by global correlations. Very low S_u (under 25 kPa) is observed for some N and N_{60} in 37% of cases. While most S_u values are obtained from laboratory tests, most of the S_u values over 100 kPa are obtained from PMT of the Neon dataset (Ch. 4) and are suspect. A low trend (R^2 = 0.11) of increasing S_u with increasing N or N_{60} is observed by excluding the high S_u values obtained from PMT. Unlike laboratory tests that are performed on disturbed soil samples, PMT are conducted on relatively intact sediments and therefore might be a more accurate indicator of the *in situ* S_u of soils, particularly dense, hard to sample LVV soils. Note that soil heterogeneity can hinder the effectiveness of PMT in sediments occurring in the LVV (In Situ Engineering, 2012).

Figure 5.4 shows VS plotted with respect to N or N_{60}. Most local VS values are higher than those predicted by global correlations, especially for low N or N_{60}. These higher

local VS suggest that most global correlations used to estimate VS from N or N_{60} are overconservative for the LVV, particularly for low blow counts. Many local VS-N/N_{60} data pairs have N/N_{60} over 100, whose VS values range between 200 and 1800 m/s. Recall that some of the N or N_{60} over 100 are extrapolated from refusal reported in borehole logs. Overall, N or N_{60} is highly variable with respect to local VS; this high variability in N or N_{60} is possibly because of several reasons such as the presence of varying degrees of cementation, lack of standardization of SPT testing method and refusal criteria, and the wide geographical range of data. A weak trend ($R^2 = 0.01$) of increasing VS with increasing N or N_{60} is observed, including values with N or N_{60} =100. Figure 5.5 shows the data from Figure 5.4 distinguished by predominant sediment type. Some local VS-N/N_{60} data pairs are comparable to global correlations plotted, while most local data pairs have higher VS than predicted by global correlations. Local VS tends to increase with increasing grain size of predominant sediment type. As stated earlier, neither N nor VS are straight surrogates for shear strength of sediments (Ch. 3), nevertheless they provide useful information regarding relative density and shear modulus of the sediment respectively.

A similar study conducted by Bellana (2009) generated equations of VS as a function of N_{60} and σ'_v. The equations were generated by statistical regression of datasets collected at various bridge sites in California. According to Bellana (2009), σ'_v is an important factor in predicting VS, although published correlations typically do not consider the influence of overburden. Bellana (2009) obtained VS values solely from suspension logging tests and regression analysis was conducted only on combinations of N_{60} and VS values

recorded at the same depth. Note that the work of Bellana (2009) was not complicated by the presence of cemented soils, which are key factors in the LVV. In contrast, this author's work considers a much broader range of tests to understand the highly variable sediments in the LVV. VS available for this study is primarily obtained from the non-intrusive ReMi method; restricting comparisons by depth for a non-point-based measurement is not reasonable, would further decrease the sample size of the useful dataset and possibly exclude the challenging sediments in question. Therefore, the more exacting correlations developed for California bridge sites by Bellana (2009) could not be replicated for the Las Vegas dataset.

Prevalent *in situ* tests in the LVV include SPT, VS and, to a lesser extent, PMT, although there are variations in testing procedures and equipment used. VS from passive source surface waves is available for most of the LVV. Laboratory test results that yield shear strength parameters are sparse in the LVV and when available may not be representative of the strength across the area in consideration due to material heterogeneity. The lab data are unavailable especially in cemented sediments and dense sands possibly due to expensive coring techniques required or difficulty in recovering undisturbed samples [note that even the DS test data from SPT samplers are reported on reconstituted specimens]. The author was unable to compare local VS with S_u due to the scarcity of lab strength data that when available, as explained earlier, was not comparable to the VS with low resolution per depth. Regarding comparisons with N and N_{60}, some trends with respect to predominant sediment types are observed when shear strength parameters c, ϕ and S_u are compared with N or N_{60}. On the contrary, comparisons of VS with N or N_{60}

yield only very weak correlations ($R^2 < 0.09$), therefore comparisons of VS with N or N_{60} do not yield useful trends that relate to the shear behavior of soil. Comparisons of local data and global correlations with respect to N or N_{60} show that most LVV soils have different ranges of shear strength parameters and VS than predicted by global correlations. Global correlations with N or N_{60} over predict ϕ (Fig. 5.1), while they under predict S_u and VS (Fig. 5.2 and 5.4); therefore global correlations of shear parameters with N or N_{60} are not representative of the LVV soils. Note that uncertainty in the data used to generate the global correlations are not provided here, certainly some of our data fall within the scatter ranges. This study shows that SPT alone may not be effective in analyzing shear behavior of sediments. As discussed earlier, comparisons of PMT outcomes with VS of comparable soil volumes might prove to be more effective in understanding the shear behavior of soil. However, the heterogeneity of sediments in the LVV results in high variability in the strength and stiffness of sediments tested and limits the usefulness of PMT for the LVV.

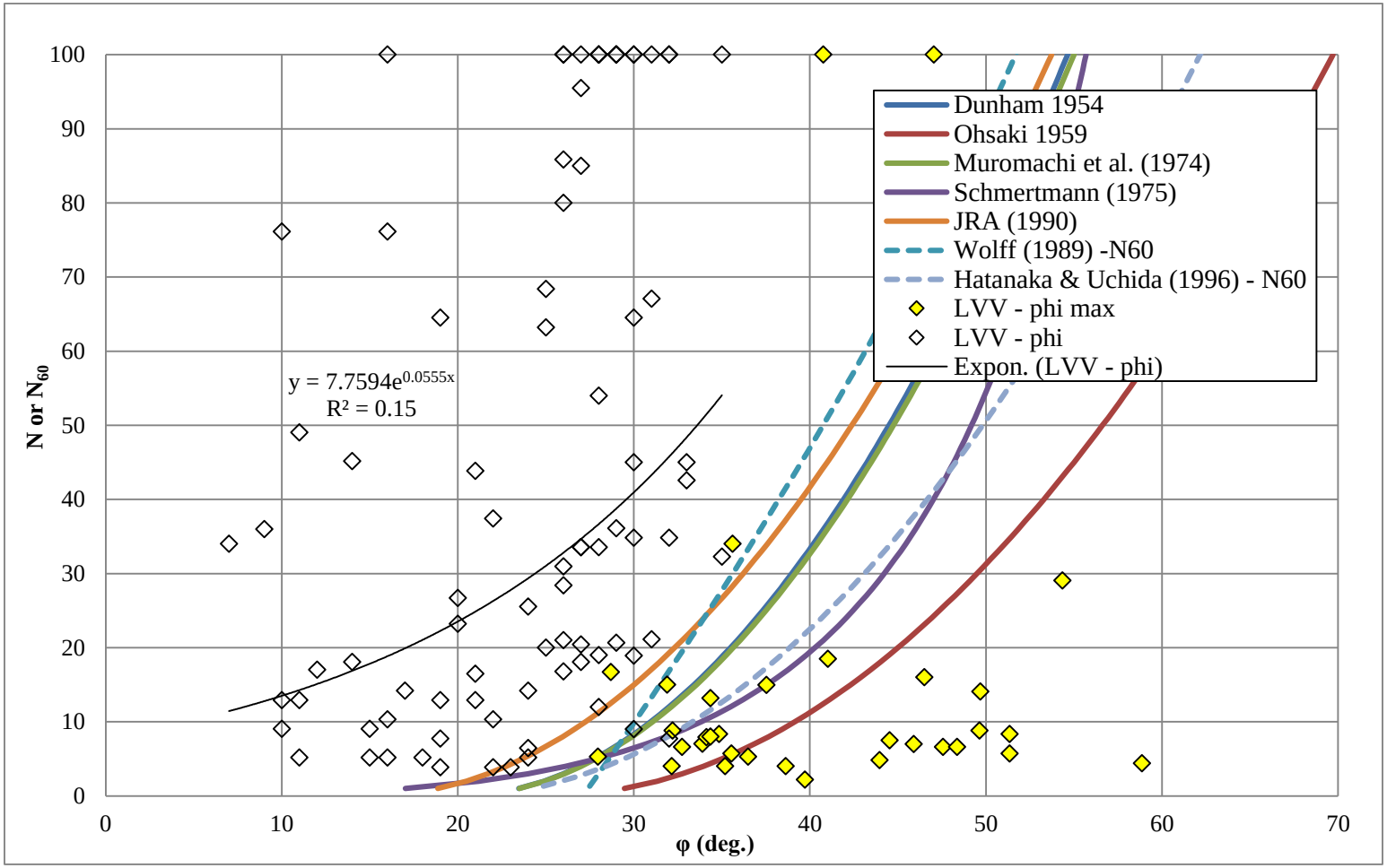

Figure 5.1: N or N_{60} versus friction angle (ϕ); global correlations from Table 2.2 for cohesionless soils (lines) shown together with LVV data (symbols).

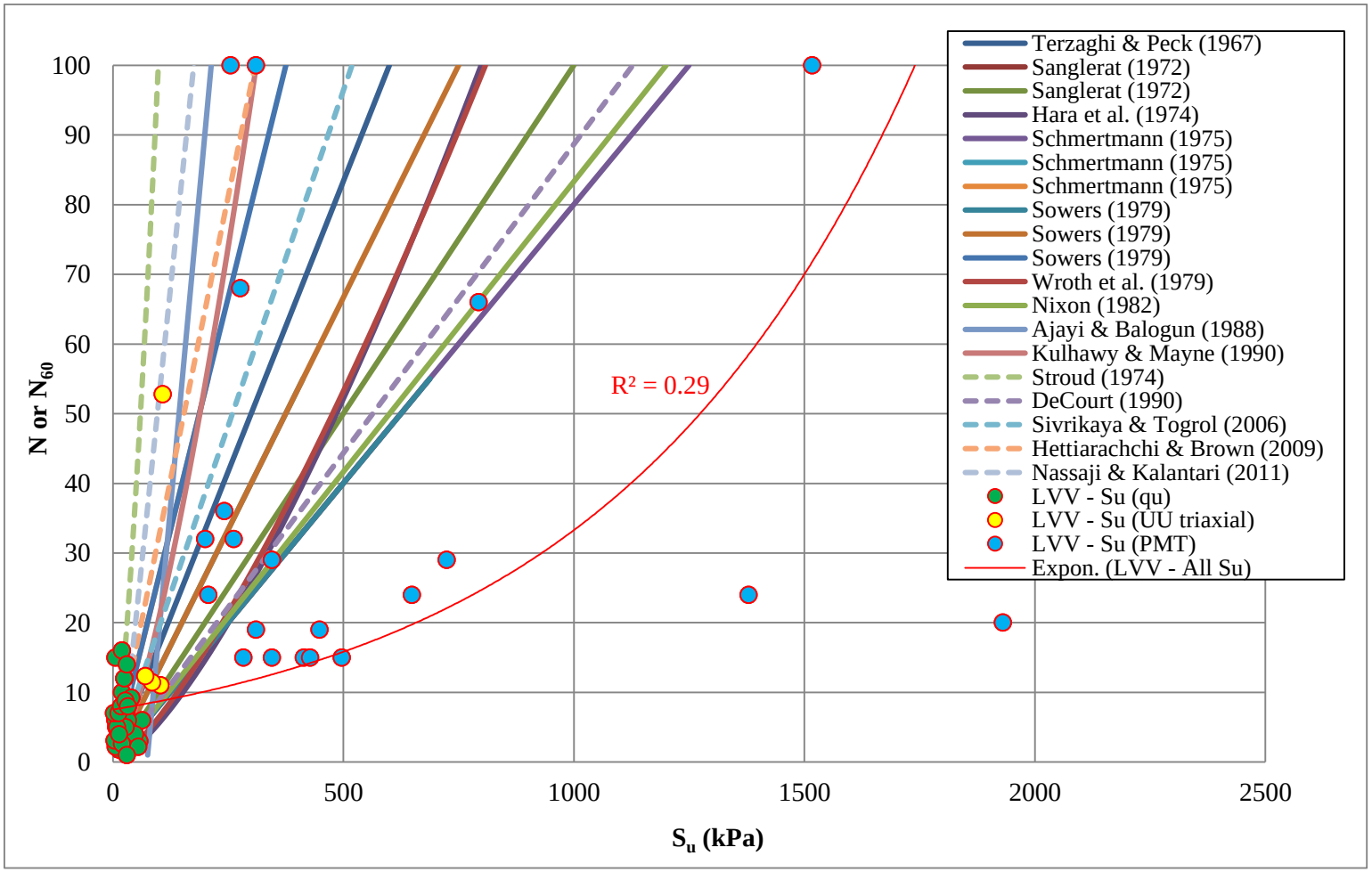

Figure 5.2: N or N_{60} versus undrained shear strength (S_u); global correlations from Table 2.4 for cohesive soils (lines) shown together with LVV data (symbols). Dashed lines represent global correlations using N_{60} as opposed to those using N (solid lines).

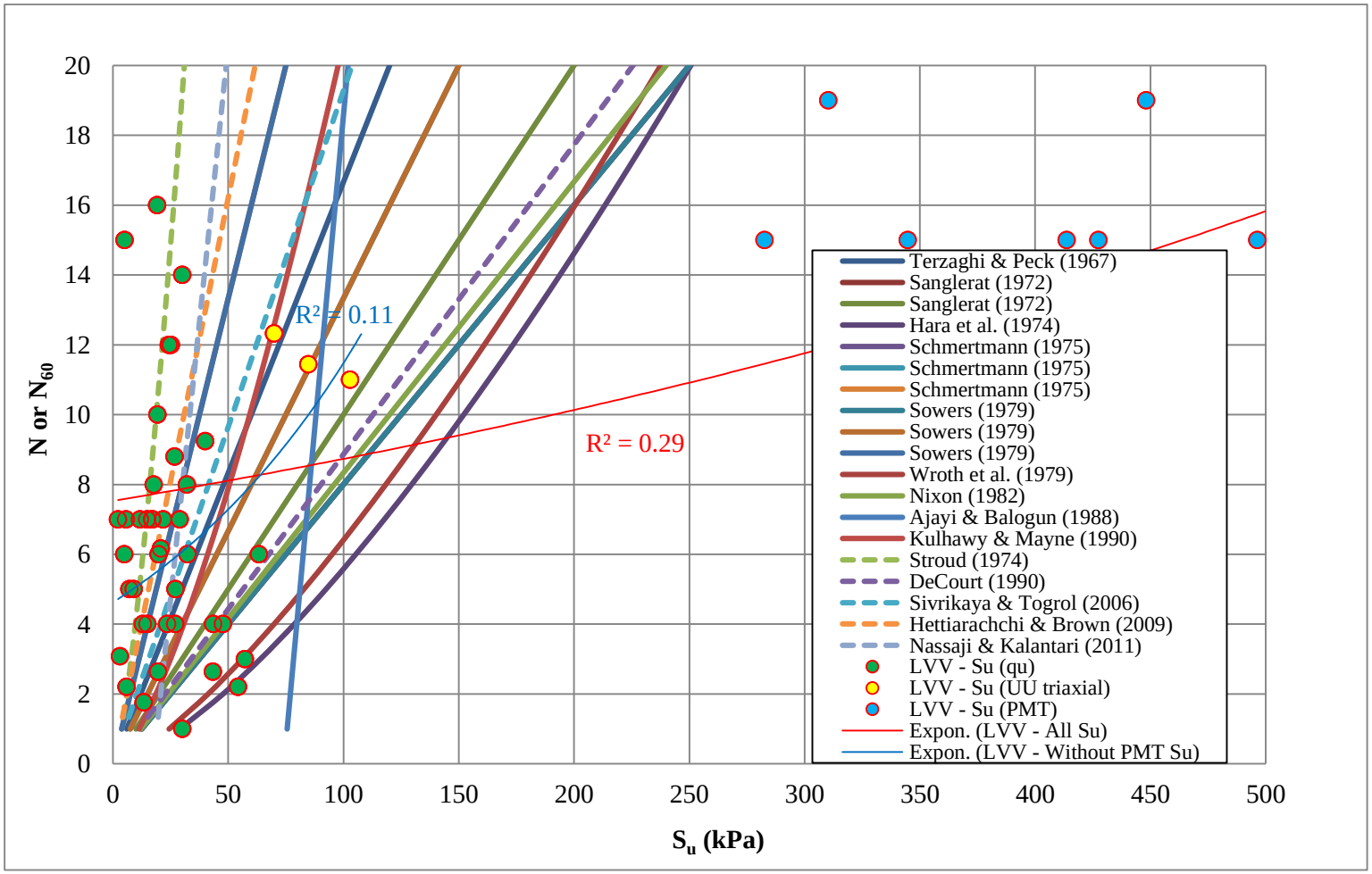

Figure 5.3: Subset of Figure 5.2. N or N_{60} versus undrained shear strength (S_u); global correlations from Table 2.4 for cohesive soils (lines) shown together with LVV data (symbols). Dashed lines represent global correlations using N_{60} as opposed to those using N (solid lines).

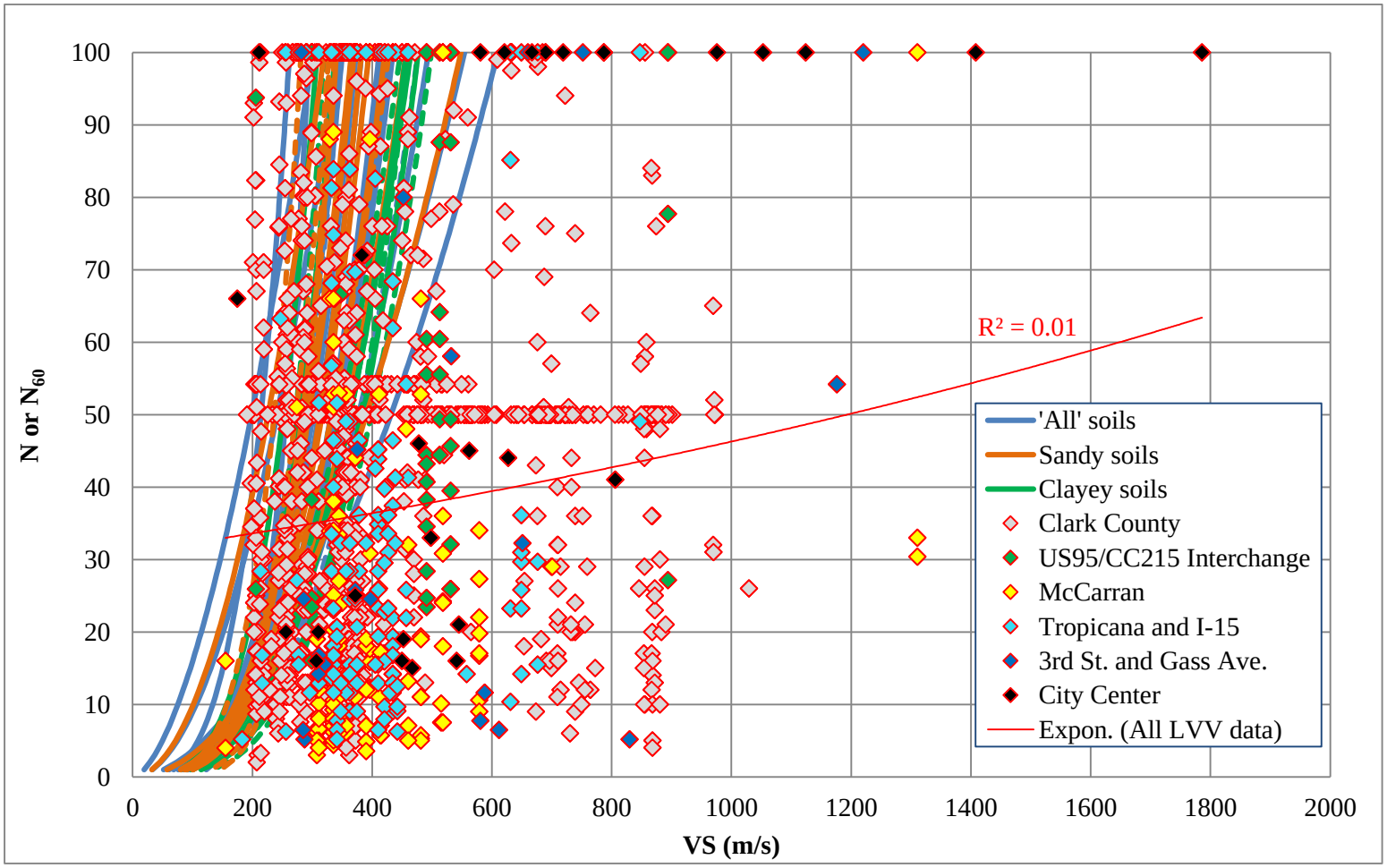

Figure 5.4: N or N_{60} versus VS; global correlations from Tables 2.8, 2.9, and 2.10 for 'all', sandy, and clayey soils shown together with LVV data (symbols); distinguished by datasets.

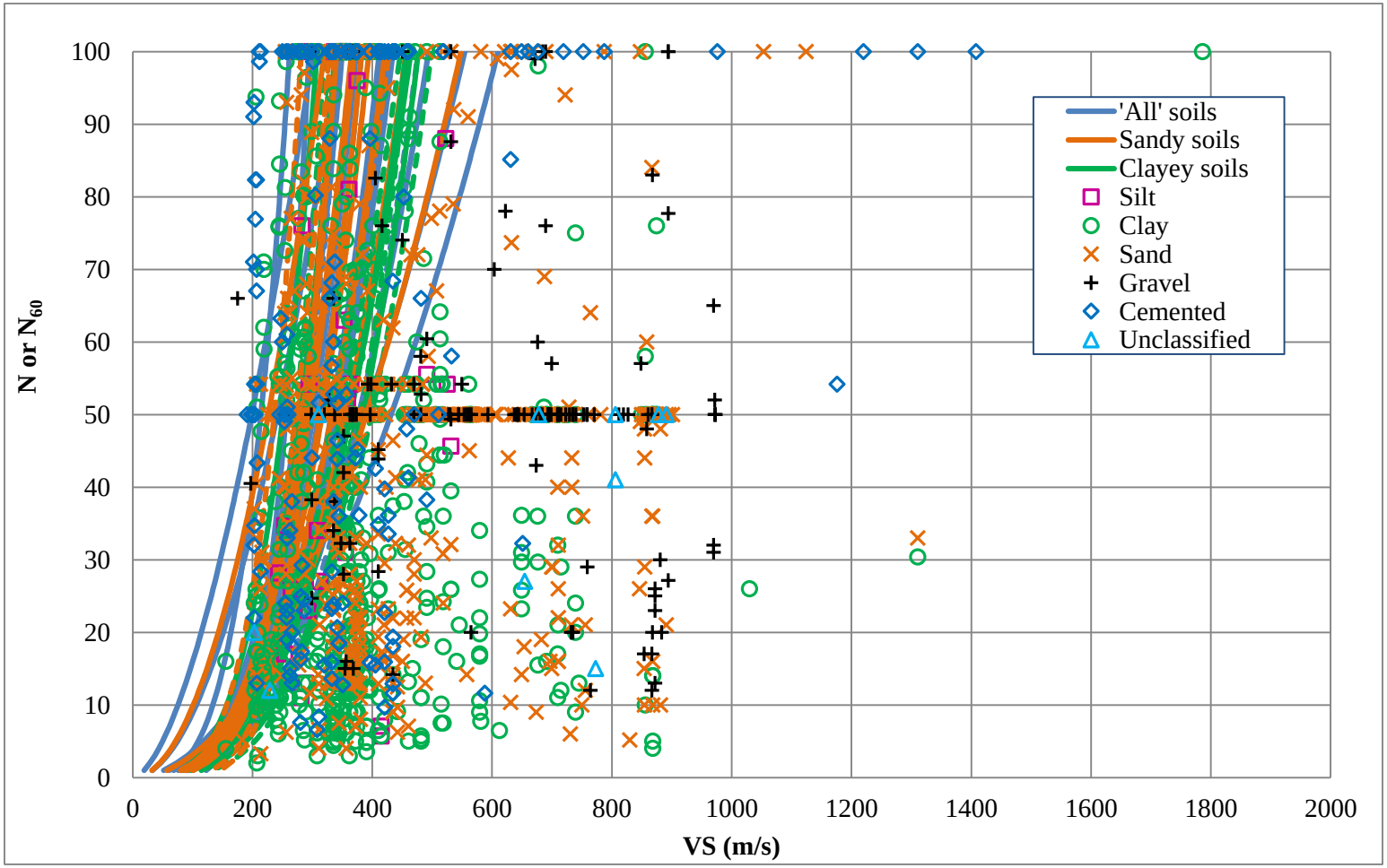

Figure 5.5: Figure 5.4 wherein local data is distinguished by predominant sediment types.

CHAPTER 6

CONCLUSIONS AND RECOMMENDATIONS

This study was undertaken to investigate trends between readily measured *in situ* test data and shear strength parameters as a means to help assess the shear behavior of sediments that occur in the LVV in working ranges of stress/strain for the purpose of enhancing deep foundation design. Downhole velocity testing was conducted at a major highway interchange in the LVV to obtain direct measurements of VS for comparison against other data collected on the same site. Local datasets of *in situ* tests and laboratory data were obtained from local geotechnical consultants and government entities. Global correlations of *in situ* test data with shear strength parameters were reviewed, and local data were compared with global correlations to test their applicability in the LVV. Despite the high sediment heterogeneity across the LVV, variations in testing, and lack of sufficient laboratory data, some trends emerged between shear parameters and *in situ* tests. Although no strong correlations were uncovered between *in situ* test data and shear parameters for the LVV, *in situ* tests are found to be valuable for deep foundation design in the LVV when complemented with other available data. Employing multiple *in situ* tests in addition to standard subsurface investigation and laboratory tests gives a better understanding of sediment conditions and variability than is available from a smaller suite of tests.

The following observations are made from this study:

1) Of the LVV datasets analyzed in this study, clay is the most prevalent predominant sediment type. Most sands and gravels also have clay in them, which lends cohesion even in predominantly granular sediments.
2) Of the datasets analyzed in this study, cementation of sediments is common. The sediments classified as 'cemented' in this study are not distinguished by the degrees of cementation present; they range from trace to partially cemented to fully cemented caliche. A better system of classification of sediments and their degrees of cementation could prove useful to identifying trends that would otherwise go unnoticed
3) *In situ* downhole seismic measurements were conducted at the US95/CC215 Interchange site (Ch.3). In that dataset, VP reflects the depth to moist soil, which was well above the observed groundwater table. VS mostly complements sediment lithology of boreholes and VS reference profiles for local sediments, while it mostly does not correspond with N_{60} reported in the borehole logs. The downhole VS profiles for the interchange site tracked with the VS from the local MASW measurement and local reference profiles by Murvosh et al. (2013b) in the upper ~15 m.
4) Regarding shear strength parameters c, ϕ, and S_u with respect to N or N_{60}: As expected, sands mostly have higher ϕ and lower c than clays, while higher S_u and c are mostly in clays and cemented sediments. Generally, ϕ and c increase with increasing N or N_{60}. Analysis of the relationship of S_u with N or N_{60} is inconclusive due to the small dataset size for S_u.

5) Overall, local N or N_{60} are highly variable, irrespective of whether they are distinguished by predominant sediment type, location, test type or VS. This high variability of local N or N_{60} is conjectured to be a result of soil heterogeneity but also lack of standardization in SPT testing, which hindered comparisons with other parameters. Furthermore, the ESGI dataset which provides most of the local N or N_{60} data had not undergone complete QA/QC check by the CCDDS-BD by the time of the author's research. Therefore, further analysis of the Clark County dataset using SPT data from the ESGI dataset provided for the assessment of shear behavior of sediments in the LVV might not prove beneficial.
6) Detecting trends is hindered when comparing datasets that obtain test data based on vastly different volumes of soil. For example, N or N_{60}, which apply to a depth interval of 0.3 m (12 in.), and ReMi, which represent VS averaged over much larger volumes of soil (tens or hundreds of cubic meters), are not comparable if the sediments under consideration are not homogenous, which is generally the case in the LVV. Therefore, it is important to analyze comparable sediment volumes to decrease the errors due to soil heterogeneity and increase the reliability of any trends observed. For example, when comparing N or N_{60} with VS, it would be more beneficial to compare N or N_{60} with VS from the suspension logging method than ReMi, as conducted by Bellana (2009).
7) The comparisons of the few large-strain PMT data available in the study dataset show that PMT outcomes (p_L, S_u) are distinctly higher in cemented sediments than non-cemented sediments. PMT data also cluster according to non-cemented predominant sediment type. It is hypothesized that analysis of PMT outcomes

with VS of comparable soil volumes may be useful in detecting trends that are meaningful to deep foundation design, although sediment heterogeneity prevalent in the LVV can hinder the effectiveness of PMT for sediment characterization.

8) Weak trends ($R^2 = 0.01$) are observed when local VS are compared with local N or N_{60}. The weak trends in the local data are attributed to factors such as the heterogeneity of sediments across LVV, varying degrees of cementation, and the disparity in soil volumes tested. Variability is observed among global correlations. These global correlations of N or N_{60} with shear parameters are not representative of the shear behavior of sediments in LVV. Local shear parameter values are significantly higher than most of the global correlations of shear parameters with N or N_{60} according to sediment type that were studied in this research. This outcome implies that a design that was based on shear strength parameters obtained from most global correlations for generic sediment types would be over-conservative for the LVV.
9) Due to the heterogeneity of sediments, varying degrees of cementation, sampling difficulty, variability in volumes of sediments tested, and lack of standardization in testing in the LVV, joint sets of *in situ* and lab test results should be analyzed with careful consideration. Neither seismic velocities nor N_{60} is more informative than the other, but when complemented with each other provide valuable insight regarding stiffness and relative density of sediments and their variability with respect to depth. Any test by itself may not be representative of the soils in the area, or may not be the best tool to understand the shear strength properties of the sediments in question. Therefore, the use of readily measured *in situ* test data is

valuable for deep foundation design in the LVV as long as it is complemented with other data; the *in situ* data provide a general trend of the shear behavior of some sediments common to the LVV such as dense, difficult-to-sample and/or cemented sediments. However, there are limitations associated with quantifying correlations of readily-measured *in situ* test data with shear behavior of sediments due to reasons such as high sediment heterogeneity, lack of standardization in testing, and differences in sediment volumes tested.

It is important to note that the datasets considered in this study are not comprehensive and therefore limit the author in drawing conclusions for the entire LVV.

Recommendations for future research include the following:

1) Processing of downhole velocity data by taking into account the refracted ray paths based on Snell's law of refraction rather than a straight-line path may help determine velocities closer to real values for sediments particularly at depths.
2) Comparing downhole velocity test results with Osterberg cell® load test results for co-located drilled shafts in the same site can be done at the US95/CC215 interchange site, as planned by NDOT and UNLV. This comparison can demonstrate how seismic velocities measured *in situ* compare to load test results and can improve characterization of the sediment stress-strain response in stiff, variable, difficult-to-sample sediments, in order to better predict the capacity of drilled shafts.
3) The author suggests the following method for improved sediment classification for the LVV. Use the USCS method (ASTM D2487-11) for basic sediment

classification, as is typically done by all. In addition, the degree of cementation in sediments can be represented by letters following the USCS symbols ranging from – no cementation (N), trace cementation (T), weakly cemented (W), partially cemented (P) to fully cemented (F). Degree of cementation can be assessed during drilling, using universal, simple visual and physical methods. Then, for example, a well-graded clean gravel with less than 5% fines and partial cementation can be represented using the suggested system as ‘GW-P’, while a silty sand with more than 12% fines and trace cementation can be represented as ‘SM-T’.

APPENDIX – A

US95/CC215 NDOT BOREHOLE LOGS

Note: Hole 1 is Boring TS-1-2, and Hole 2 is Boring TS-3A

NEVADA DEPARTMENT OF TRANSPORTATION
GEOTECHNICAL ENGINEERING

EXPLORATION LOG

START DATE 9/9/13
END DATE 9/10/13
JOB DESCRIPTION US95 / CC-215 System-to-System Interchange
LOCATION Northwest Las Vegas - Clark County
BORING TS-1-2
E.A. # 73518
GROUND ELEV. 2406.10 (ft)
HAMMER DROP SYSTEM Automatic

GROUNDWATER LEVEL		
DATE	DEPTH ft	ELEV. ft

STATION "XP" 189+88
OFFSET 313' Right
ENGINEER Boomhower/Lawrence
EQUIPMENT Diedrich D-120 (Unit 1627)
OPERATOR Beus/Pypkowski
DRILLING METHOD 6" H.S.A.
BACKFILLED _____ DATE _____

ELEV. (ft)	DEPTH (ft)	SAMPLE NO.	SAMPLE TYPE	BLOW COUNT 6 inch Increments	BLOW COUNT Last 1 foot	Percent Recov'd	LAB TESTS	USCS Group	MATERIAL DESCRIPTION	REMARKS
									Asphaltic Concrete	
	3.00									
		A	CMS	12 12 12	24	100		CL ML	**SILTY CLAY** Dry, medium dense, very pale brown (10 YR 7/4)	
	4.50									
2401.1	5	B	SPT	6 5 14	19	85			**LEAN CLAY with SAND** Dry, medium dense, very pale brown to white (10 YR 7/4 to 10 YR 8/1)	
	6.00									
	6.50									
		C	CMS	11 15 22	37	95			**LEAN CLAY** Dry, very stiff, light gray to white (10 YR 7/2 to 10 YR 8/1)	
	8.00									
		D	SPT	11 11 17	28	85		CL	**LEAN CLAY with SAND** Dry, very stiff, light gray to white (10 YR 7/2 to 10 YR 8/1)	
	9.50									
2396.1	10	E	CMS	18 15 16	31	85			**LEAN CLAY with SAND** Dry, very stiff, light gray to white (10 YR 7/2 to 10 YR 8/1)	
	11.00									
		F	SPT	8 10 13	23	85			**SANDY LEAN CLAY** Dry, very stiff, light gray to white (10 YR 7/2 to 10 YR 8/1)	
	12.50									
		G	CMS	11 16 22	38	95			**SANDY LEAN CLAY** Dry, very stiff, light gray (2.5 Y 7/2)	
	14.00									
		H	SPT	12 15 21	36	85		SC	**CLAYEY SAND** Dry, very stiff, light gray (2.5 Y 7/2)	
2391.1	15 15.50									
		I	CMS	20 35 15/0.1'	15/0.1'	80			**CLAYEY SAND with GRAVEL** Dry, very hard, light gray (10 YR 7/2)	(I) Last 10 blows; no progress.
	16.80									
	17.00									
		J	CMS	31 38 50/0.4'	50/0.4'	95		GM	**SILTY GRAVEL with SAND** Dry, very dense, light gray (10 YR 7/2)	
	18.40									
	19.00									
	20.00									
2386.1	20									
		K	CMS	20 33 41	74	95		SC	**CLAYEY SAND with GRAVEL** Dry, very dense, light gray (10 YR 7/2)	
	21.50									
		L	SPT	15 21 28	49	80		GC	**CLAYEY GRAVEL with SAND** Dry, dense, yellow to very pale brown (10 YR 7/6 to 10 YR 8/2)	
	23.00									
		M	CMS	25 23 31	54	95				
	23.80									
	24.50							CH	**FAT CLAY with SAND** Dry, dense, yellowish brown to very pale brown (10 YR 5/6 to 10 YR 7/3)	
2381.1	25	N	CMS	1 6 26	32	55		SC	**CLAYEY SAND with GRAVEL** Dry, dense, yellowish brown to very pale brown (10 YR 5/6 to 10 YR 7/3)	(N) Loose sample recovered.
	26.00									
		O	SPT	14 16 19	35	80		CH	**SANDY FAT CLAY** Dry, hard, very pale brown to white (10 YR 7/3 to 10 YR 8/1)	
	27.50									
		P	SPT	25 35 53	88	95		SC	**CLAYEY SAND with GRAVEL** Dry, very dense, white (7.5 YR 8/1)	End day 1 drilling @ 27.5'.
	29.00									
	30.00									

NV_DOT GINT FILES.GPJ NV_DOT.GDT 1/17/14

NEVADA DEPARTMENT OF TRANSPORTATION — GEOTECHNICAL ENGINEERING

EXPLORATION LOG

START DATE 9/9/13
END DATE 9/10/13
JOB DESCRIPTION US95 / CC-215 System-to-System Interchange
LOCATION Northwest Las Vegas - Clark County
BORING TS-1-2
E.A. # 73518
GROUND ELEV. 2406.10 (ft)
HAMMER DROP SYSTEM Automatic

GROUNDWATER LEVEL		
DATE	DEPTH ft	ELEV. ft

STATION "XP" 189+88
OFFSET 313' Right
ENGINEER Boomhower/Lawrence
EQUIPMENT Diedrich D-120 (Unit 1627)
OPERATOR Beus/Pypkowski
DRILLING METHOD 6" H.S.A.
BACKFILLED _____ DATE _____

ELEV. (ft)	DEPTH (ft)	SAMPLE NO.	SAMPLE TYPE	BLOW COUNT 6 inch Increments	BLOW COUNT Last 1 foot	Percent Recov'd	LAB TESTS	USCS Group	MATERIAL DESCRIPTION	REMARKS
				19					**GRAVELLY LEAN CLAY with SAND** Dry, hard, light gray (10 YR 7/2) with white (10 YR 8/1) nodules	(Q) Nodules lightly to strongly cemented.
	31.50	Q	CMS	26 55	81	100			**LEAN CLAY** Dry to moist, very hard, white (10 YR 8/1)	
		R	SPT	18 30 50/0.3'	50/0.3'	100				
	32.80 33.00									
		S	CMS	27 17 21	38	95		CL	**SANDY LEAN CLAY** Dry to moist, medium dense to dense, white to very pale brown (10 YR 8/1 to 10 YR 7/4)	
	34.50									
2371.1	35	T	SPT	10 9 11	20	75			**SANDY LEAN CLAY** Moist, very stiff, very pale brown to brown (10 YR 8/2 to 7.5 YR 5/4)	
	36.00									
	37.50									
		U	CMS	10 15 30	45	95		CH	**FAT CLAY with SAND** Moist, very stiff, pale brown to brown (10 YR 6/3 to 7.5 YR 5/4)	
	39.00									
2366.1	40	V	SPT	11 13 18	31	60		GC	**CLAYEY GRAVEL with SAND** Moist, hard, pale brown (10 YR 6/3) with white (10 YR 8/1) nodules	(V) Nodules lightly to strongly cemented.
	40.50									
		W	CMS	11 23 30	53	100		CL	**SANDY LEAN CLAY with GRAVEL** Moist, hard, pale brown (10 YR 6/3) with white (10 YR 8/1) nodules	(W) Nodules lightly to strongly cemented.
	42.00									
		X	SPT	9 13 32	45	95		ML	**SANDY SILT with GRAVEL** Moist, hard, pale brown (10 YR 6/3) with white (10 YR 8/1) nodules	
	43.50									
		Y	CMS	13 14 22	36	85			**LEAN CLAY with SAND** Moist, hard, pale brown (10 YR 6/3) with white (10 YR 8/1) nodules	
2361.1	45.00 45									
		Z	SPT	7 12 21	33	85		CL	**LEAN CLAY** Dry to moist, hard, light brown (7.5 YR 6/4)	
	46.50									
		AA	CMS	18 18 24	42	95			**SANDY LEAN CLAY with GRAVEL** Moist, dense, light gray to light yellowish brown (2.5 Y 7/2 to 10 YR 6/4)	
	48.00									
		BB	SPT	2 7 24	31	65		GC	**CLAYEY GRAVEL with SAND** Moist, stiff to very stiff, light yellowish brown (10 YR 6/4)	(BB) Sample strongly cemented in sampler shoe.
	49.50									
2356.1	50	CC	CMS	11 24 20	44	95		CH	**SANDY FAT CLAY** Moist, very stiff, mottled light gray to brown (10 YR 7/2 to 7.5 YR 5/4)	(CC) Nodules lightly to strongly cemented.
	51.00									
		DD	SPT	7 9 11	20	65			**CLAYEY GRAVEL with SAND** Moist, medium dense, brown (7.5 YR 5/4)	
	52.50									
		EE	CMS	11 11 34	45	85		GC	**CLAYEY GRAVEL with SAND** Moist, very stiff, mottled light gray to brown (10 YR 7/2 to 7.5 YR 5/4)	
	54.00									
2351.1	55	FF	SPT	9 14 50/0.3'	50/0.3'	60			**CLAYEY GRAVEL with SAND** Moist, very hard, very pale brown (10 YR 8/3)	
	55.50									
	56.30	GG	CMS	41 50/0.3'	50/0.3'	90			**CLAYEY GRAVEL with SAND** Dry to moist, very hard, very pale brown to light gray (10 YR 8/2 to 10 YR 7/2)	(GG) Sample strongly cemented lenses.
									57.00	Very hard drilling from 56.5' to 60.0'. Progress 3.5'/30 minutes @ 250
	60.00 60.10									

NV_DOT GINT FILES.GPJ NV_DOT.GDT 1/17/14

NEVADA DEPARTMENT OF TRANSPORTATION — GEOTECHNICAL ENGINEERING

EXPLORATION LOG

START DATE 9/9/13
END DATE 9/10/13
JOB DESCRIPTION US95 / CC-215 System-to-System Interchange
LOCATION Northwest Las Vegas - Clark County
BORING TS-1-2
E.A. # 73518
GROUND ELEV. 2406.10 (ft)
HAMMER DROP SYSTEM Automatic

GROUNDWATER LEVEL		
DATE	DEPTH ft	ELEV. ft

STATION "XP" 189+88
OFFSET 313' Right
ENGINEER Boomhower/Lawrence
EQUIPMENT Diedrich D-120 (Unit 1627)
OPERATOR Beus/Pypkowski
DRILLING METHOD 6" H.S.A.
BACKFILLED _____ DATE _____

ELEV. (ft)	DEPTH (ft)	SAMPLE NO.	SAMPLE TYPE	BLOW COUNT 6 inch Increments	BLOW COUNT Last 1 foot	Percent Recov'd	LAB TESTS	USCS Group	MATERIAL DESCRIPTION	REMARKS
		HH	SPT	15/0.1'	15/0.1'	0			**Hard Drilling - Moderate to Strongly Cemented Materials - "Caliche"**	psi down pressure. (HH) Last 10 blows; no progress. No sample recovered.
	62.00									
	64.50							CL		Very hard drilling from 60.1' to 60.3'. Progress 0.2'/25 minutes @ 300 psi down pressure.
2341.1	65	A2	CMS	6 10 25	35	100			**LEAN CLAY** Moist, very stiff to hard, very pale brown (10 YR 7/3)	
	66.00									
	66.00							CL		
		B2	SPT	8 7 6	13	100			**LEAN CLAY with SAND** Moist, stiff, very pale brown (10 YR 6/3)	Very hard drilling from 60.3' to 60.6'. Progress 0.3'/30 minutes @ 300 psi down pressure.
	67.50									
	69.50									
	69.00							CL		
2336.1	70	C2	CMS	7 50/ 0.45'	50/ 0.45'	0			**C-CMS-NO RECOVERY**	Drilling with clean water
	70.50									
	71.00	D2	SPT	50/ 0.45'	50/ 0.45'	100			**LEAN CLAY** Moist, hard, very pale brown (10 YR 6/3)	(D) SPT full, poor sample
	72.00									
	74.50									
2331.1	75	E2	CMS	18 14 12	26	105				
	76.00									
		F2	SPT	4 7 12	19	95		CL	**LEAN CLAY with SAND** Moist ,very stiff ,very pale brown (10 YR 6/4) mottled 10% brownish yellow (10 YR 6/6)	
	77.50									
	79.50									
2326.1	80	G2	CMS	8 9 54	63	100				
	81.00									
	81.00									
	81.80	H2	SPT	34 50/0.30'	50/0.30'	100		CL	**GRAVELLY LEAN CLAY with SAND** Moist, very hard , very pale brown (10 YR 7/4)	
	83.50									
	84.50								**SANDY LEAN CLAY** Moist, very hard, brown (7.5 YR 5/4)	
2321.1	85	I2	CMS	14 51 50/ 0.15'	50/ 0.15'	75		CL		
	85.70									
	86.50	J2	SPT	28 50/ 0.30'	50/ 0.30'	100		CL		
	86.50								**SANDY LEAN CLAY with GRAVEL** Moist, very hard, very pale brown (10 YR 7/4)	
	88.00									
	89.50								**GRAVELLY LEAN CLAY** Moist, hard, very pale brown (10 YR 7/4)	
				20						

NV_DOT_GINT FILES.GPJ NV_DOT.GDT 1/17/14

NEVADA DEPARTMENT OF TRANSPORTATION
GEOTECHNICAL ENGINEERING

EXPLORATION LOG

START DATE 9/9/13
END DATE 9/10/13
JOB DESCRIPTION US95 / CC-215 System-to-System Interchange
LOCATION Northwest Las Vegas - Clark County
BORING TS-1-2
E.A. # 73518
GROUND ELEV. 2406.10 (ft)
HAMMER DROP SYSTEM Automatic

GROUNDWATER LEVEL		
DATE	DEPTH ft	ELEV. ft

STATION "XP" 189+88
OFFSET 313' Right
ENGINEER Boomhower/Lawrence
EQUIPMENT Diedrich D-120 (Unit 1627)
OPERATOR Beus/Pypkowski
DRILLING METHOD 6" H.S.A.
BACKFILLED _____ DATE _____

ELEV. (ft)	DEPTH (ft)	SAMPLE NO.	SAMPLE TYPE	BLOW COUNT 6 inch Increments	BLOW COUNT Last 1 foot	BLOW COUNT Percent Recov'd	LAB TESTS	USCS Group	MATERIAL DESCRIPTION	REMARKS
	91.00	K2	CMS	30 30	60	0			**K-CMS-NO RECOVERY**	
	92.50	L2	SPT	5 9 27	36	55		CL	**GRAVELLY LEAN CLAY** Moist, hard, very pale brown (10 YR 7/4)	(L) 2' + in SPT, CMS sample?
	93.00									
	94.50							CL		
2311.1	95	M2	CMS	12 20 45	65	115			**LEAN CLAY** Moist, hard, very pale brown (10 YR 7/4)	
	96.00									
	97.50	N2	SPT	26 30 55	85	100		CL ML	**SANDY SILTY CLAY** Moist, hard, very pale brown (10 YR 7/4)	
	98.00									
	99.50									
2306.1	100	O2	CMS	12 19 50/ .40'	50/ .40'	120			**LEAN CLAY with SAND** Moist, very hard, light yellowish brown (10 YR 6/4) mottled 10% brownish yellow (10 YR 6/6)	(O) CMS full, not draining pressure
	100.90									
	102.40	P2	SPT	28 25 20	45	75		CL	**LEAN CLAY with SAND** Moist, hard, very pale brown (10 YR 6/4)	
	103.00									
	104.50								**Q-CMS- NO RECOVERY**	
	104.80	Q2	CMS	50/ .30'	50/ .30'	0				
2301.1	105			30					**LEAN CLAY** Moist, hard, light yellowish brown (10 YR 6/4)	(Q) 1.3' cuttings in CMS sample, No recovery
	106.30	R2	SPT	17 19	36	120		CL		
	108.00									
	109.50									
2296.1	110	S2	CMS	33 31 60	91	100		CL ML	**SILTY CLAY** Very hard, moist, light yellowish brown (10 YR 6/4)	
	111.00									
	112.50	T2	SPT	18 26 45	71	100				
	113.00									
	114.50							ML		
2291.1	115	U2	CMS	18 28 40	68	100			**SILT** Hard, moist, light yellowish brown (10 YR 6/4)	
	116.00									
	117.50	V2	SPT	11 14 26	40	115		CL ML	**SILTY CLAY** Hard, moist, light yellowish brown (10 YR 6/4)	
	118.00									
	119.50								**LEAN CLAY** Moist, very stiff, light yellowish brown (10 YR 6/4)	
				38						

NV_DOT GINT FILES.GPJ NV_DOT.GDT 1/17/14

NEVADA DEPARTMENT OF TRANSPORTATION — GEOTECHNICAL ENGINEERING

EXPLORATION LOG

START DATE 9/9/13
END DATE 9/10/13
JOB DESCRIPTION US95 / CC-215 System-to-System Interchange
LOCATION Northwest Las Vegas - Clark County
BORING TS-1-2
E.A. # 73518
GROUND ELEV. 2406.10 (ft)
HAMMER DROP SYSTEM Automatic

GROUNDWATER LEVEL		
DATE	DEPTH ft	ELEV. ft

STATION "XP" 189+88
OFFSET 313' Right
ENGINEER Boomhower/Lawrence
EQUIPMENT Diedrich D-120 (Unit 1627)
OPERATOR Beus/Pypkowski
DRILLING METHOD 6" H.S.A.
BACKFILLED _____ DATE _____

ELEV. (ft)	DEPTH (ft)	SAMPLE NO.	SAMPLE TYPE	BLOW COUNT 6 inch Increments	BLOW COUNT Last 1 foot	Percent Recov'd	LAB TESTS	USCS Group	MATERIAL DESCRIPTION	REMARKS
	121.00	W2	CMS	22 20	42	115		CL	**LEAN CLAY** Moist, very stiff, light yellowish brown (10 YR 6/4)	
	122.50	X2	SPT	5 19 30	49	105			**LEAN CLAY WITH SAND** Moist, hard, light yellowish brown (10 YR 6/4)	
	124.50							CL		
2281.1	125 125.90	Y2	CMS	32 40 50/.40'	50/.40'	100			**LEAN CLAY WITH SAND** Moist, very stiff, light yellowish brown (10 YR 6/4)	
	127.40	Z2	SPT	24 24 28	52	85			**LEAN CLAY WITH SAND** Moist, hard, light yellowish brown (10 YR 6/4) to very pale brown (10 YR 8/2)	
									END TS-2 @ 127.4'	
2276.1	130									
2271.1	135									
2266.1	140									
2261.1	145									

NV_DOT GINT FILES.GPJ NV_DOT.GDT 1/17/14

NEVADA DEPARTMENT OF TRANSPORTATION
GEOTECHNICAL ENGINEERING

EXPLORATION LOG

START DATE 10/9/13
END DATE 10/21/13
JOB DESCRIPTION US95 / CC-215 System-to-System Interchange
LOCATION Northwest Las Vegas - Clark County
BORING TS-3A
E.A. # 73518
GROUND ELEV. 2425.30 (ft)
HAMMER DROP SYSTEM Automatic

GROUNDWATER LEVEL		
DATE	DEPTH ft	ELEV. ft

STATION "A" 65+30
OFFSET 227' Right
ENGINEER Boomhower/ Lawrence
EQUIPMENT Diedrich D-120(Unit 1627)
OPERATOR Pypkowski
DRILLING METHOD 6" H.S.A. /4" Rotary
BACKFILLED Wash DATE

ELEV. (ft)	DEPTH (ft)	SAMPLE NO.	SAMPLE TYPE	BLOW COUNT 6 inch Increments	BLOW COUNT Last 1 foot	Percent Recov'd	LAB TESTS	USCS Group	MATERIAL DESCRIPTION	REMARKS
									SANDY GRAVEL, tan, dry	
2420.3	5.00							GC		
	5	A	CMS	15 30 50/0.4'	50/0.4'	100			**CLAYEY GRAVEL with SAND** Dry, very dense, very pale brown (10 YR 7/4)	
	6.40									
	6.50	B	SPT	20/0.1'	20/0.1'	0				(B) Last 10 blows; no progress. No sample recovered.
	7.50								7.00	
	7.80	C	CMS	50/0.3'	50/0.3'	0				
	8.00							GW GC		
		D	CMS	37 60 50/0.4'	50/0.4'	85			**WELL-GRADED GRAVEL with SILTY CLAY and SAND** Dry, very dense, very pale brown (10 YR 7/4)	(C) Last 10 blows; no progress; No sample recovered.
	9.40								9.70	
	10.00									
2415.3	10			9				SW SM	**WELL-GRADED SAND with SILT and GRAVEL** Dry, very dense, very pale brown (10 YR 7/4)	
		E	CMS	45 63	108	95				
	11.50								11.50	
	12.20	F	SPT	50 35/0.2'	35/0.2'	100			**CLAYEY SAND with GRAVEL** Dry, very dense, very pale brown (10 YR 7/4)	(F) Last 10 blows; no progress.
	13.00							SC		
		G	CMS	20 32 71	103	80				
	14.50								13.80	
2410.3	15	H	SPT	39 30 41	71	80		GC	**CLAYEY GRAVEL with SAND** Dry, very dense, very pale brown (10 YR 7/4)	
	16.00									
	17.50								17.50	
	17.70	I	CMS	30/0.2'	30/0.2'	0				(I) Last 10 blows; no progress.
	19.00									
2405.3	20	J	CMS	16 22 27	49	100			**LEAN CLAY with SAND** Dry, very stiff, very pale brown (10 YR 7/3)	
	20.50									
		K	SPT	15 17 15	32	80		CL	**SANDY LEAN CLAY** Dry, hard, mottled light yellowish brown to very pale brown (10 YR 6/4 to 10 YR 8/2)	
	22.00									
		L	CMS	12 14 29	43	95			**LEAN CLAY with SAND** Dry, hard, mottled light yellowish brown to very pale brown (10 YR 6/4 to 10 YR 8/2)	
	23.50									
		M	SPT	16 10 11	21	85			**SANDY LEAN CLAY** Dry, very stiff, light brown (7.5 YR 6/4)	
	25.00								25.00	
2400.3	25									
		N	CMS	13 26 30	56	95			**CLAYEY SAND with GRAVEL** Dry to moist, dense, mottled pale brown to white (10 YR 6/3 to 10 YR 8/1)	
	26.50									
		O	SPT	9 12 14	26	80		SC	**CLAYEY SAND with GRAVEL** Dry to moist, dense, mottled pale brown to white (10 YR 6/3 to 10 YR 8/1)	
	28.00									
	30.00								30.00	

NV_DOT GINT FILES.GPJ NV_DOT.GDT 1/17/14

NEVADA DEPARTMENT OF TRANSPORTATION — GEOTECHNICAL ENGINEERING

EXPLORATION LOG

START DATE 10/9/13
END DATE 10/21/13
JOB DESCRIPTION US95 / CC-215 System-to-System Interchange
LOCATION Northwest Las Vegas - Clark County
BORING TS-3A
E.A. # 73518
GROUND ELEV. 2425.30 (ft)
HAMMER DROP SYSTEM Automatic

GROUNDWATER LEVEL		
DATE	DEPTH ft	ELEV. ft

STATION "A" 65+30
OFFSET 227' Right
ENGINEER Boomhower/ Lawrence
EQUIPMENT Diedrich D-120(Unit 1627)
OPERATOR Pypkowski
DRILLING METHOD 6" H.S.A. /4" Rotary
BACKFILLED Wash DATE

ELEV. (ft)	DEPTH (ft)	SAMPLE NO.	SAMPLE TYPE	BLOW COUNT 6 inch Increments	BLOW COUNT Last 1 foot	Percent Recov'd	LAB TESTS	USCS Group	MATERIAL DESCRIPTION	REMARKS
				12						
		P	CMS	30	77	100		GC GM	**SILTY CLAYEY GRAVEL with SAND** Dry to moist, dense, mottled pale brown to white (10 YR 6/3 to 10 YR 8/1)	
	31.50			47					31.50	
				9					**FAT CLAY with SAND** Dry to moist, very stiff, mottled light brown to pale yellow (7.5 YR 6/3 to 2.5 Y 8/3)	
		Q	SPT	8	21	85				
	33.00			13				CH		
									34.00	
	35.00									
2390.3	35									
				22					**CLAYEY GRAVEL with SAND** Dry to moist,	
		R	CMS	26	58	100			dense, mottled pale brown to white (10 YR 6/3	
	36.50			32					to 10 YR 8/1)	
				16				GC	**CLAYEY GRAVEL with SAND** Dry to moist,	
		S	SPT	16	40	75			dense, mottled pale brown to white (10 YR 6/3	
	38.00			24					to 10 YR 8/1)	
				17					**CLAYEY GRAVEL with SAND** Dry to moist,	
		T	CMS	21	57	100			dense, mottled pale brown to white (10 YR 6/3	
	39.50			36					39.50 to 10 YR 8/1)	
				11					**GRAVELLY ELASTIC SILT with SAND** Dry	
2385.3	40	U	SPT	20	37	75			to moist, dense, mottled pale brown to white (10	
	41.00			17				MH	YR 6/3 to 10 YR 8/1)	
									41.50	
	42.00									
	42.40	V	CMS	50/0.4'	50/0.4'	100		GM	42.70 **SILTY GRAVEL with SAND** Dry to moist,	
	43.00								dense, mottled pale brown to white (10 YR 6/3 to 10 YR 8/1)	
				16						
		W	SPT	24	50/0.4'	70		SC	**CLAYEY SAND with GRAVEL** Dry, very	
	44.40			50/0.4'					dense, light brown to pinkish white (7.5 YR 6/3	
	45.00								44.70 to 7.5 YR 8/2)	
2380.3	45									
	45.40	X	CMS	50/0.4'	50/0.4'	100			**CLAYEY GRAVEL with SAND** Dry to moist, very dense, light brown (7.5 YR 6/3)	
	47.00									
				28						
		Y	CMS	15	40	100			**CLAYEY GRAVEL with SAND** Dry to moist, medium dense to dense, light brown to reddish yellow (7.5 YR 6/4 to 7.5 YR 6/6)	
	48.50			25						
				17					**CLAYEY GRAVEL with SAND** Dry to moist,	
		Z	SPT	23	63	85			very dense, multicolored	
	50.00			40						
2375.3	50			45						
		AA	CMS	32	60	100			**CLAYEY GRAVEL with SAND** Dry to moist, very dense, multicolored	
	51.50			28						
				17						
		BB	SPT	10	22	75		GC	**CLAYEY GRAVEL with SAND** Moist, very stiff, light brown (7.5 YR 6/4)	
	53.00			12						
										End day 1 drilling @ 53.0'.
	55.00									
2370.3	55									
		CC	CMS	25	25/0.2'	90			**CLAYEY GRAVEL with SAND** Moist, very dense, yellowish brown (10 YR 5/6)	(CC) Last 10 blows; no progress.
	56.20			23						
	56.60	DD	SPT	25/0.2'	25/0.2'	0				(DD) Last 10 blows; no progress. No sample recovered.
										Hard drilling at 57.5' to 60.0'.
	60.00								60.00	

NV_DOT GINT FILES.GPJ NV_DOT.GDT 1/17/14

EXPLORATION LOG

NEVADA DEPARTMENT OF TRANSPORTATION — GEOTECHNICAL ENGINEERING

START DATE 10/9/13
END DATE 10/21/13
JOB DESCRIPTION US95 / CC-215 System-to-System Interchange
LOCATION Northwest Las Vegas - Clark County
BORING TS-3A
E.A. # 73518
GROUND ELEV. 2425.30 (ft)
HAMMER DROP SYSTEM Automatic

GROUNDWATER LEVEL		
DATE	DEPTH ft	ELEV. ft

STATION "A" 65+30
OFFSET 227' Right
ENGINEER Boomhower/ Lawrence
EQUIPMENT Diedrich D-120(Unit 1627)
OPERATOR Pypkowski
DRILLING METHOD 6" H.S.A. /4" Rotary
BACKFILLED Wash DATE

ELEV. (ft)	DEPTH (ft)	SAMPLE NO.	SAMPLE TYPE	BLOW COUNT 6 inch Increments	BLOW COUNT Last 1 foot	Percent Recov'd	LAB TESTS	USCS Group	MATERIAL DESCRIPTION	REMARKS
	60.20	EE	SPT	35/0.2'	35/0.2'	0			***Continue TS-3 down same hole, use 4" Mud rotary**	Progress 3.5'/30 minutes @ 250 psi down pressure.
									End Hard Drilling @ 62.8'	(EE) Last 10 blows; no progress. No sample recovered.
									62.80	
2360.3	65									Very hard drilling at 62.0'. Progress 0.3'/20 minutes @ 350 psi down pressure.
								CL ML		Very hard drilling at 62.5'. Progress 0.1'/20 minutes @ 350 psi down pressure.
	69.50									
2355.3	70	FF	CMS	56 30 28	58	100			**SILTY CLAY with SAND** Hard ,moist, light yellowish brown (10 YR 6/4)	
	71.00									
		GG	SPT	21 43 33	76	100			**SILTY CLAY with SAND** Very hard ,moist, light yellowish brown (10 YR 6/4)	
	72.50									
									73.00	
	74.50									
2350.3	75	HH	CMS	8 11 16	27	100		CL	**LEAN CLAY** Very stiff ,moist, light yellowish brown (10 YR 6/4)	
	76.00									
		II	SPT	6 8 13	21	100			**LEAN CLAY** Very stiff ,moist, light yellowish brown to brownish yellow (10 YR 6/4 to 10 YR 6/6) mottled black 1%-5%	
	77.50									
									78.00	
	79.50									
2345.3	80	JJ	CMS	19 31 26	57	100			**GRAVELLY LEAN CLAY** Hard ,moist, light yellowish brown (10 YR 6/4)	
	81.00									
		KK	SPT	9 15 27	42	100			**LEAN CLAY with GRAVEL** Hard ,moist, light yellowish brown (10 YR 6/4)	
	82.50							CL		
	84.50									
2340.3	85	LL	CMS	56 50-.40'	50-.40'	0				CMS(LL)- No Recovery; gouge in side of sampler-Hung up on rock?, no progress last 20 blows
	85.40									
		MM	SPT	12 24 30	54	100			**GRAVELLY LEAN CLAY** Hard, moist, light yellowish brown (10 YR 6/4), angular gravel	
	86.90									
									87.30	
									MODERATELY CEMENTED MATERIALS	CMS(NN)- No recovery;No progress last 40 blows
	89.50 89.67	NN	CMS	50-.17'	50-.17'	0				

NV_DOT_GINT FILES.GPJ NV_DOT GDT 1/17/14

NEVADA DEPARTMENT OF TRANSPORTATION — GEOTECHNICAL ENGINEERING

EXPLORATION LOG

START DATE 10/9/13
END DATE 10/21/13
JOB DESCRIPTION US95 / CC-215 System-to-System Interchange
LOCATION Northwest Las Vegas - Clark County
BORING TS-3A
E.A. # 73518
GROUND ELEV. 2425.30 (ft)
HAMMER DROP SYSTEM Automatic

GROUNDWATER LEVEL		
DATE	DEPTH ft	ELEV. ft

STATION "A" 65+30
OFFSET 227' Right
ENGINEER Boomhower/ Lawrence
EQUIPMENT Diedrich D-120(Unit 1627)
OPERATOR Pypkowski
DRILLING METHOD 6" H.S.A. /4" Rotary
BACKFILLED Wash DATE

ELEV. (ft)	DEPTH (ft)	SAMPLE NO.	SAMPLE TYPE	BLOW COUNT 6 inch Increments	BLOW COUNT Last 1 foot	Percent Recov'd	LAB TESTS	USCS Group	MATERIAL DESCRIPTION	REMARKS
									MODERATELY CEMENTED MATERIALS	
	92.00									
	94.50									
2330.3	95		OO	CMS	37 50-.28'	50-.28'	100		CL ML	**GRAVELLY SILTY CLAY** Very hard, moist, very pale brown (10 YR 7/3)
	95.30									
			PP	SPT	35 39 53	92	100			**GRAVELLY SILTY CLAY** Very hard, moist, very pale brown (10 YR 7/3)
	96.80									
	98.00									
	99.50									CMS(QQ)-No recovery; sampler ball valve, not relieving pressure during sampling? no negtive pressure to retain sample, to many cuttings?
2325.3	100		QQ	CMS	16 9 32	41	0			
	101.00				3				CL	**LEAN CLAY with GRAVEL** Very hard, moist, brownish yellow (10 YR 6/6) to very pale brown (10 YR 7/3)
			RR	SPT	6 50-.42'	50-.42'	150			***INTERBEDDED HARD GRAVELLY CLAY? AND WEAKLY CEMENTED MATERIALS FROM 102.5' to 106.0'**
	102.50									
	104.50									
	105.00		SS	CMS	50-.5'	50-.5'	40			**GRAVELLY LEAN CLAY with SAND** Very hard, moist, brownish yellow (10 YR 6/6) to very pale brown (10 YR 7/3) CMS(SS)- add brass leaf catcher, .2' recovery in shoe, sampler full of mud/cuttings, no tests
2320.3	105.40		TT	SPT	50-.35'	50-.35'	100			
	106.00									**WEAKLY TO STRONGLY CEMENTED MATERIALS** SPT(TT)- angular cemented materials in sampler, broken up by driving?
	109.50									
	109.65		UU	SPT	50-.15'	50-.15'	0			
2315.3	110									
	110.50									SPT(UU)-No recovery
	114.50								CL ML	Depth 106.0'-110.5' .08ft/min to .15 ft/min drilling rate 250psi down
2310.3	115		VV	CMS	31 56 50-.3'	50-.3'	95			**SILTY CLAY** Hard, moist, light yellowish brown (10 YR 6/4)
	115.80									
			WW	SPT	19 32 50	82	95			**SILTY CLAY** Hard, moist, light yellowish brown (10 YR 6/4)
	117.10									
	118.00									
	119.50									**LEAN CLAY** Hard, moist, reddish yellow (7.5 YR 6/6)
					22					

NV_DOT GINT FILES.GPJ NV_DOT.GDT 1/17/14

NEVADA DEPARTMENT OF TRANSPORTATION
GEOTECHNICAL ENGINEERING

EXPLORATION LOG

SHEET 5 OF 5

START DATE 10/9/13
END DATE 10/21/13
JOB DESCRIPTION US95 / CC-215 System-to-System Interchange
LOCATION Northwest Las Vegas - Clark County
BORING TS-3A
E.A. # 73518
GROUND ELEV. 2425.30 (ft)
HAMMER DROP SYSTEM Automatic

GROUNDWATER LEVEL		
DATE	DEPTH ft	ELEV. ft

STATION "A" 65+30
OFFSET 227' Right
ENGINEER Boomhower/ Lawrence
EQUIPMENT Diedrich D-120(Unit 1627)
OPERATOR Pypkowski
DRILLING METHOD 6" H.S.A. /4" Rotary
BACKFILLED Wash DATE

ELEV. (ft)	DEPTH (ft)	SAMPLE NO.	SAMPLE TYPE	BLOW COUNT 6 inch Increments	BLOW COUNT Last 1 foot	Percent Recov'd	LAB TESTS	USCS Group	MATERIAL DESCRIPTION	REMARKS
	121.00	XX	CMS	26 45	71	75			**LEAN CLAY** Hard, moist, reddish yellow (7.5 YR 6/6)	
	122.50	YY	SPT	6 10 32	42	115			**LEAN CLAY** Hard, moist, reddish yellow (7.5 YR 6/6)	
	124.50							CL		
2300.3	125	ZZ	CMS	14 22 39	61	80			**LEAN CLAY** Hard, moist, reddish yellow (7.5 YR 6/6)	
	126.00									
	127.50	AB	SPT	13 20 34	54	140			**LEAN CLAY with GRAVEL** Hard, moist, reddish yellow (7.5 YR 6/6)	
									127.50	
									END TS3A @ 127.5'	
2295.3	130									
2290.3	135									
2285.3	140									
2280.3	145									

NV_DOT GINT FILES.GPJ NV_DOT.GDT 1/17/14

APPENDIX – B

SPT INFORMATION OF SPECIMENS USED FOR COMPARISONS FROM THE MAJOR PROJECTS DATASET

Note: Sampler types: SPT – Standard SPT sampler, MC – Modified California sampler

Table 1: McCarran - Borehole blow counts and their conversion

Borehole name	Blow count depth (m)	Sediment description	Sampler type*	Field blow count	'Equivalent total' blow count for samples at refusal*	SPT-equivalent blow count	Final blow count (N)
RSB-1H	1.5	Cemented - Caliche	SPT	50/4"	150		100
RSB-1H	4.6	Cemented - Caliche	SPT	50/2"	300		100
RSB-4H	1.5	Cemented - Caliche	SPT	50/2"	300		100
RSB-5A	1.5	Cemented - Caliche	SPT	50/4"	150		100
RSB-5A	4.6	Cemented - Caliche	MC	50/1"	600	264	100
RSB-7F	3.0	Cemented - Caliche	SPT	50/1"	600		100
B-15	1.5	Cemented - Caliche	MC	50/0"	6000	2640	100
B-15	3.0	Cemented - Caliche	MC	50/1.5"	400	176	100
RSB-4H	0.8	Cemented - Clayey sand	MC	50/1"	600	264	100
C-2	4.6	Cemented - Sand and gravel	SPT	50/2"	300		100
PSB-21	6.4	Cemented - Sandy fat clay	SPT	50/4"	150		100
C-2	22.9	Cemented - Sandy fat clay	SPT	50/0"	6000		100
RSB-7A	21.3	Cemented - Sandy fat clay	SPT	50/1"	600		100
C-2	3.8	Cemented - Sandy lean clay	SPT	50/3"	200		100
RSB-5A	22.9	Cemented - Sandy lean clay	SPT	50/5"	120		100
RSB-7A	13.7	Cemented - Sandy lean clay	MC	50/1"	600	264	100
RSB-5A	19.8	Cemented - Sandy silt	SPT	50/4"	150		100
RSB-1H	22.9	Fat clay with sand	SPT	50/5"	120		100
C-14	1.5	Sandy lean clay	MC	50/4"	150	132	100
C-26	3.8	Silty sand	MC	50/1"	600	264	100
C-2	1.5	Silty sand	SPT	50/1"	600		100
B-15	0.8	Cemented - Caliche	MC	50/5.5"	109	48	48
RSB-4H	4.6	Cemented - Caliche	MC	50/3"	200	88	88
C-23	3.8	Cemented - Clayey sand	MC	20		9	9
C-26	18.3	Cemented - Clayey sand	MC	30		13	13

Borehole name	Blow count depth (m)	Sediment description	Sampler type*	Field blow count	'Equivalent total' blow count for samples at refusal*	SPT-equivalent blow count	Final blow count (N)
RSB-1H	0.8	Cemented - Clayey sand	MC	36		16	16
C-22	4.6	Cemented - Clayey sand	SPT	38			38
C-14	4.6	Cemented - Clayey sand	SPT	36			36
C-21	7.6	Cemented - Clayey sand	MC	22		10	10
RSB-1H	6.1	Cemented - Fat clay	MC	54		24	24
C-14	21.3	Cemented - Fat clay	SPT	24			24
RSB-4H	19.8	Cemented - Fat clay	SPT	50/6"	100		100
RSB-7F	22.9	Cemented - Fat clay	MC	50/4"	150	66	66
RSB-4H	6.1	Cemented - Fat clay	MC	50/4"	150	66	66
RSB-1H	21.3	Cemented - Fat clay with sand	MC	50/3"	200	88	88
RSB-4H	9.1	Cemented - Fat clay with sand	MC	50/5"	120	53	53
C-14	5.3	Cemented - Lean clay	MC	42		18	18
C-14	15.2	Cemented - Lean clay	MC	19		8	8
RSB-5A	3.0	Cemented - Lean clay	MC	50/6"	100	44	44
CP-3	4.6	Cemented - Poorly graded sand with clay	MC	66		29	29
C-1	13.7	Cemented - Sandy fat clay	MC	16		7	7
C-22	16.8	Cemented - Sandy fat clay	SPT	60			60
RSB-4H	3.0	Cemented - Sandy fat clay	MC	50/4"	150	66	66
C-12	6.1	Cemented - Sandy lean clay	MC	13		6	6
C-14	19.8	Cemented - Sandy lean clay	MC	29		13	13
RSB-7A	16.8	Cemented - Sandy lean clay	MC	15		7	7
RSB-7A	22.9	Cemented - Silty sand	MC	50/5"	120	53	53
RSB-7A	0.8	Cemented - Silty sand with gravel	MC	42		18	18
C-08	9.1	Clayey gravel	SPT	4			4
C-22	5.3	Clayey gravel with sand	MC	50/4"	150	66	66
C-22	6.1	Clayey gravel with sand	SPT	34			34

Borehole name	Blow count depth (m)	Sediment description	Sampler type*	Field blow count	′Equivalent total′ blow count for samples at refusal*	SPT-equivalent blow count	Final blow count (N)
C-04	15.2	Clayey sand	SPT	7			7
C-19	15.2	Clayey sand	MC	20		9	9
C-4	16.0	Clayey sand	SPT	7			7
CP-3	3.0	Clayey sand	MC	15		7	7
S-2	3.0	Clayey sand	MC	19		8	8
C-27	10.7	Clayey sand	SPT	1			1
PSB-2	7.6	Clayey sand	SPT	8			8
S-04	7.6	Clayey sand	SPT	7			7
C-2	2.4	Clayey sand	SPT	24			24
C-2	3.0	Clayey sand	MC	70		31	31
RSB-4H	7.6	Clayey sand	SPT	23			23
RSB-5A	0.8	Clayey sand	MC	34		15	15
RSB-5A	24.4	Clayey sand	MC	39		17	17
RSB-7F	16.8	Clayey sand	MC	44		19	19
C-14	7.6	Clayey sand	MC	15		7	7
MSE-2	24.4	Clayey sand with caliche nodules	MC	32		14	14
C-22	1.1	Clayey sand with gravel	SPT	51			51
C-22	1.5	Clayey sand with gravel	SPT	29			29
RSB-7F	0.8	Clayey sand with gravel	SPT	32			32
RSB-7F	1.5	Clayey sand with gravel	MC	16		7	7
RSB-1H	3.0	Fat clay	MC	70		31	31
C-14	12.2	Fat clay	MC	23		10	10
C-14	13.7	Fat clay	SPT	8			8
C-14	22.9	Fat clay	MC	18		8	8
C-2	6.1	Fat clay	MC	55		24	24
C-2	10.7	Fat clay	SPT	9			9
C-2	12.2	Fat clay	MC	45		20	20

Borehole name	Blow count depth (m)	Sediment description	Sampler type*	Field blow count	'Equivalent total' blow count for samples at refusal*	SPT-equivalent blow count	Final blow count (N)
C-2	13.7	Fat clay	SPT	17			17
C-2	15.2	Fat clay	MC	24		11	11
C-2	16.8	Fat clay	SPT	22			22
C-2	18.3	Fat clay	MC	62		27	27
C-21	9.1	Fat clay	SPT	3			3
C-21	15.2	Fat clay	SPT	2			2
C-21	18.3	Fat clay	SPT	4			4
C-22	22.9	Fat clay	SPT	10			10
RSB-4H	21.3	Fat clay	MC	50/5"	120	53	53
RSB-4H	22.9	Fat clay	SPT	26			26
RSB-4H	24.4	Fat clay	MC	25		11	11
RSB-7A	6.1	Fat clay	SPT	11			11
RSB-7A	7.6	Fat clay	MC	14		6	6
RSB-7A	9.1	Fat clay	SPT	3			3
RSB-7A	27.4	Fat clay	SPT	7			7
RSB-7A	29.0	Fat clay	MC	11		5	5
RSB-7A	30.5	Fat clay	MC	17		7	7
RSB-7F	9.1	Fat clay	SPT	16			16
RSB-7F	10.7	Fat clay	MC	12		5	5
RSB-7F	12.2	Fat clay	SPT	11			11
RSB-7F	15.2	Fat clay	SPT	5			5
RSB-7F	18.3	Fat clay	SPT	11			11
RSB-7F	19.8	Fat clay	MC	13		6	6
RSB-7F	21.3	Fat clay	SPT	19			19
RSB-7F	24.4	Fat clay	SPT	7			7
RSB-7F	25.9	Fat clay	MC	18		8	8
RSB-7F	27.4	Fat clay	SPT	18			18

Borehole name	Blow count depth (m)	Sediment description	Sampler type*	Field blow count	'Equivalent total' blow count for samples at refusal*	SPT-equivalent blow count	Final blow count (N)
RSB-7F	29.0	Fat clay	MC	16		7	7
RSB-7F	30.5	Fat clay	SPT	89			89
C-10	7.6	Fat clay	SPT	6			6
C-11	12.2	Fat clay	MC	11		5	5
C-14	9.1	Fat clay	SPT	5			5
PSB-1	10.7	Fat clay	MC	12		5	5
PSB-11A	18.3	Fat clay	MC	15		7	7
PSB-15	12.2	Fat clay	MC	34		15	15
PSB-7	4.6	Fat clay	MC	15		7	7
R-8	24.4	Fat clay	MC	38		17	17
RSB -1B	13.7	Fat clay	MC	12		5	5
RSB -1C	6.1	Fat clay	SPT	34			34
RSB -1C	22.9	Fat clay	MC	19		8	8
S-1	11.1	Fat clay	SPT	4			4
RSB-4C	24.4	Fat clay with caliche nodules	SPT	4			4
C-26	10.7	Fat clay with sand	SPT	4			4
RSB-1H	10.7	Fat clay with sand	SPT	13			13
RSB-1H	12.2	Fat clay with sand	MC	17		7	7
RSB-1H	13.7	Fat clay with sand	SPT	5			5
RSB-1H	16.8	Fat clay with sand	SPT	14			14
RSB-1H	18.3	Fat clay with sand	MC	28		12	12
RSB-1H	19.8	Fat clay with sand	SPT	12			12
RSB-1H	24.4	Fat clay with sand	MC	40		18	18
RSB-4H	10.7	Fat clay with sand	MC	10		4	4
RSB-4H	12.2	Fat clay with sand	SPT	17			17
RSB-4H	13.7	Fat clay with sand	MC	14		6	6
RSB-4H	15.2	Fat clay with sand	MC	32		14	14

Borehole name	Blow count depth (m)	Sediment description	Sampler type*	Field blow count	'Equivalent total' blow count for samples at refusal*	SPT-equivalent blow count	Final blow count (N)
RSB-4H	16.8	Fat clay with sand	SPT	51			51
RSB-4H	18.3	Fat clay with sand	MC	21		9	9
RSB-5A	25.9	Fat clay with sand	MC	13		6	6
RSB-5A	27.4	Fat clay with sand	MC	23		10	10
RSB-5A	29.0	Fat clay with sand	MC	17		7	7
S-12	12.2	Fat clay with sand	SPT	7			7
RSB-3D	9.1	Fat clay with sand and caliche nodules	MC	6		3	3
RSB-5I	10.7	Fat clay with sand and caliche nodules	MC	4		2	2
S-13	7.6	Gravelly fat clay	SPT	4			4
RSB-4D	9.1	Gravelly fat clay with caliche nodules	SPT	3			3
RSB-4D	15.2	Gravelly fat clay with caliche nodules	SPT	7			7
C-2	21.3	Lean clay	MC	69		30	30
C-22	9.1	Lean clay	MC	19		8	8
C-22	19.8	Lean clay	SPT	15			15
C-22	21.3	Lean clay	SPT	16			16
RSB-7A	25.9	Lean clay	MC	14		6	6
C-27	6.1	Lean clay	MC	5		2	2
C-14	6.1	Lean clay	SPT	6			6
C-22	8.2	Lean clay with sand	SPT	12			12
PSB-3	7.6	Lean clay with sand and caliche nodules	SPT	6			6
PSB-18	12.2	Poorly graded sand	MC	17		7	7
C-2	19.8	Poorly graded sand	SPT	33			33
C-6	9.8	Sandy elastic silt	SPT	8			8
C-15	7.6	Sandy fat clay	SPT	5			5
C-22	10.7	Sandy fat clay	SPT	8			8
C-22	12.2	Sandy fat clay	MC	24		11	11

Borehole name	Blow count depth (m)	Sediment description	Sampler type*	Field blow count	'Equivalent total' blow count for samples at refusal*	SPT-equivalent blow count	Final blow count (N)
C-22	14.3	Sandy fat clay	SPT	16			16
C-22	15.2	Sandy fat clay	MC	46		20	20
C-25	6.1	Sandy fat clay	SPT	6			6
RSB-4H	2.1	Sandy fat clay	MC	77		34	34
RSB-5A	5.3	Sandy fat clay	SPT	11			11
RSB-5A	6.1	Sandy fat clay	MC	16		7	7
RSB-5A	7.6	Sandy fat clay	MC	11		5	5
RSB-5A	9.1	Sandy fat clay	MC	11		5	5
RSB-5A	10.7	Sandy fat clay	SPT	12			12
RSB-5A	12.2	Sandy fat clay	MC	8		4	4
RSB-5A	15.2	Sandy fat clay	MC	41		18	18
RSB-5A	16.8	Sandy fat clay	SPT	19			19
RSB-7A	19.8	Sandy fat clay	MC	28		12	12
S-03	9.1	Sandy fat clay	MC	6		3	3
S-10	6.1	Sandy fat clay	SPT	5			5
C-2	0.8	Sandy fat clay	SPT	36			36
C-05	21.3	Sandy fat Clay	SPT	15			15
C-10	12.2	Sandy fat Clay	MC	7		3	3
C-10	13.7	Sandy fat Clay	SPT	4			4
C-22	13.7	Sandy fat Clay	SPT	16			16
C-5	21.8	Sandy fat Clay	SPT	15			15
R-4	19.8	Sandy fat Clay	MC	18		8	8
RSB -2C	9.8	Sandy fat Clay	SPT	4			4
RSB-2A	9.1	Sandy fat clay	SPT	6			6
RSB-4C	9.1	Sandy fat clay	SPT	12			12
RSB-5A	13.7	Sandy fat clay with caliche nodules	SPT	7			7
RSB-7F	13.7	Sandy gravel	MC	50/5"	120	53	53

Borehole name	Blow count depth (m)	Sediment description	Sampler type*	Field blow count	′Equivalent total′ blow count for samples at refusal*	SPT-equivalent blow count	Final blow count (N)
C-14	18.3	Sandy lean clay	SPT	12			12
C-21	1.5	Sandy lean clay	SPT	9			9
C-21	10.7	Sandy lean clay	MC	9		4	4
C-21	12.2	Sandy lean clay	SPT	4			4
C-22	3.0	Sandy lean clay	SPT	18			18
C-22	3.8	Sandy lean clay	MC	17		7	7
PSB-13	6.1	Sandy lean clay	MC	5		2	2
RSB-7A	4.6	Sandy lean clay	MC	41		18	18
RSB-7A	10.7	Sandy lean clay	MC	14		6	6
RSB-7A	12.2	Sandy lean clay	SPT	5			5
RSB-7A	15.2	Sandy lean clay	SPT	19			19
RSB-7A	18.3	Sandy lean clay	SPT	12			12
RSB-7F	4.6	Sandy lean clay	MC	30		13	13
RSB-7F	6.1	Sandy lean clay	SPT	5			5
RSB-7F	7.6	Sandy lean clay	MC	9		4	4
C-14	3.0	Sandy lean clay	SPT	53			53
C-14	3.8	Sandy lean clay	MC	76		33	33
C-14	10.7	Sandy lean clay	SPT	13			13
C-20	3.8	Sandy lean clay	MC	32		14	14
C-7	7.6	Sandy lean clay	MC	42		18	18
R-11	17.5	Sandy lean clay	MC	13		6	6
RSB - 1E	7.6	Sandy lean clay	MC	5		2	2
RSB-4A	6.1	Sandy lean clay	SPT	10			10
MSE-1	12.2	Sandy lean clay with caliche nodules	SPT	7			7
RSB-1H	15.2	Sandy lean clay with caliche nodules	MC	21		9	9
RSB-3E	7.6	Sandy lean clay with caliche nodules	SPT	7			7
RSB-4C	7.6	Sandy lean clay with caliche nodules	MC	14		6	6

Borehole name	Blow count depth (m)	Sediment description	Sampler type*	Field blow count	'Equivalent total' blow count for samples at refusal*	SPT-equivalent blow count	Final blow count (N)
RSB-4F	7.6	Sandy lean clay with caliche nodules	SPT	7			7
C-14	0.8	Sandy lean clay with some gravel	SPT	19			19
RSB-5A	18.3	Sandy silt	MC	13		6	6
RSB-5A	21.3	Sandy silt	MC	16		7	7
C-2	7.6	Sandy silty clay	SPT	34			34
C-2	9.1	Sandy silty clay	MC	38		17	17
C-14	16.8	Silty sand	SPT	4			4
C-22	18.3	Silty sand	MC	57		25	25
RSB-1H	7.6	Silty sand	SPT	18			18
RSB-1H	9.1	Silty sand	MC	53		23	23
RSB-7A	24.4	Silty sand	SPT	14			14
C-14	17.5	Silty sand	SPT	4			4
PSB-14	10.7	Silty sand	MC	10		4	4
RSB-7A	2.3	Silty sand with gravel	MC	17		7	7
RSB-7A	3.0	Silty sand with gravel	SPT	27			27

Table 2: Trop/I-15 - Borehole blow counts and their conversion

Borehole name	Blow count depth (m)	Sediment description	Sampler type	Field blow count	'Equivalent total' blow count for samples at refusal	SPT-equivalent blow count	Final blow count (N)
04B2-2	1.9	Cemented - Caliche	SPT	50/0"	6000		100
05-B11	1.3	Cemented - Caliche	SPT	50/0"	6000		100
04B2-2	3.7	Cemented - Caliche	SPT	50/0"	6000		100
04-B4	6.0	Cemented - Caliche	SPT	50/2"	300		100
04-B4	8.4	Cemented - Caliche	SPT	50/2"	300		100
05-B6	0.9	Cemented - Caliche	MC	50/1"	600	264	100
05-B6	5.6	Cemented - Caliche	MC	50/0"	6000	2640	100
04B2-1	2.8	Cemented - Clayey sand	SPT	50/5"	120		100
05-B14	2.7	Cemented - Clayey sand	SPT	50/2"	300		100
07B-2	2.8	Cemented - Clayey sand	SPT	50/2"	300		100
05B-12	5.0	Cemented - Clayey sand	SPT	50/2"	300		100
05B-12	1.8	Cemented - Clayey sand	SPT	50/3"	200		100
05-B1	1.0	Cemented - Sand and gravel	SPT	50/0"	6000		100
05-B1	1.5	Cemented - Sand and gravel	SPT	50/0"	6000		100
05-B1	2.0	Cemented - Sand and gravel	SPT	50/0"	6000		100
05-B11	2.2	Cemented - Sand and gravel	SPT	50/0"	6000		100
05-B14	1.8	Cemented - Sand and gravel	SPT	50/0"	6000		100
04B2-1	4.2	Cemented - Sand and gravel	SPT	50/5"	120		100
05B-12	5.5	Cemented - Sand and gravel	SPT	50/0"	6000		100
07B-3	3.3	Cemented - Sandy clay	SPT	50/5"	120		100
04-B4	6.5	Cemented - Sandy clay	SPT	50/3"	200		100
05B-12	1.3	Cemented - Sandy clay	SPT	50/0"	6000		100

Borehole name	Blow count depth (m)	Sediment description	Sampler type	Field blow count	'Equivalent total' blow count for samples at refusal	SPT-equivalent blow count	Final blow count (N)
07B-16	3.6	Cemented - Sandy clay	SPT	50/2"	300		100
04-B2	5.6	Cemented - Sandy clay	SPT	76/8"	114		100
05-B1	10.8	Cemented - Sandy clay	SPT	50/0"	6000		100
05B-12	5.9	Cemented - Silty clay /clayey sand	SPT	50/3"	200		100
04B2-2	3.3	Cemented -Sandy clay	SPT	50/2"	300		100
04-B2	0.9	Cemented - Silty clay	SPT	50/5"	120		100
04B2-1	8.4	Cemented- Silty clay w/ caliche	SPT	50/5"	120		100
05-B1	2.9	Gravelly clay	SPT	50/5"	120		100
05-B1	4.3	Gravelly clay	SPT	50/0"	6000		100
05-B1	9.4	Gravelly clay	SPT	50/3"	200		100
05-B1	3.3	Sandy clay	SPT	50/2"	300		100
05-B1	8.9	Silty clay	SPT	50/0"	6000		100
05-B11	3.2	Silty clay	SPT	50/1"	600		100
05-B14	0.3	Silty clay	SPT	50/0"	6000		100
04-B2	9.3	Silty sand	SPT	50/2"	300		100
04B2-1	4.6	Silty sand	SPT	50/5"	120		100
05-B1	8.5	Silty sand	SPT	50/3"	200		100
05-B6	3.7	Cemented - Clay w/ caliche, gravel	MC	17		7	7
04-B9	0.5	Cemented - Clayey gravel	SPT	82			82
04B2-2	1.4	Cemented - Clayey sand	SPT	15			15
05B-10	3.6	Cemented - Clayey sand	SPT	50/6"	100		100
07B-14	2.8	Cemented - Clayey sand	SPT	61/11"	67		67
07B-7	2.6	Cemented - Clayey sand	SPT	50			50
04B2-2	6.1	Cemented - Clayey sand	SPT	14			14
04-B2	7.9	Cemented - Clayey sand	SPT	50/6"	100		100

Borehole name	Blow count depth (m)	Sediment description	Sampler type	Field blow count	′Equivalent total′ blow count for samples at refusal	SPT-equivalent blow count	Final blow count (N)
05-B6	3.3	Cemented - Clayey sand	MC	28		12	12
05-B6	4.6	Cemented - Clayey sand	MC	40		18	18
05-B6	5.1	Cemented - Clayey sand	MC	70		31	31
05-B6	7.4	Cemented - Clayey sand	MC	50/6"	100	44	44
04B2-2	4.6	Cemented - Fat clay	SPT	10			10
05-B14	1.3	Cemented - Sand and gravel	SPT	40			40
04B-1	4.6	Cemented - Sandy clay	SPT	53			53
05-B6	8.8	Cemented - Sandy clay	MC	28		12	12
05-B6	9.3	Cemented - Sandy clay	MC	24		11	11
07B-20	5.5	Cemented - Sandy clay	SPT	59			59
07B-3	5.6	Cemented - Sandy clay	SPT	50/6"	100		100
04B2-2	2.8	Cemented - Sandy clay	SPT	9			9
04B2-1	9.3	Cemented - Sandy clay	SPT	66			66
05B-13	3.6	Cemented - Sandy clay	SPT	50/12"	50		50
05B-8	15.8	Cemented - Sandy clay	MC	45		20	20
07B-12	3.3	Cemented - Sandy clay	SPT	18			18
07B-2	5.1	Cemented - Sandy clay	SPT	29			29
04-B2	6.5	Cemented - Sandy clay	SPT	26			26
04-B4	3.3	Cemented - Sandy clay	SPT	40			40
05-B6	6.5	Cemented - Sandy clay	MC	41		18	18
04-B2	0.5	Cemented - Silty clay	SPT	22			22
04-B2	2.3	Cemented - Silty clay	SPT	34			34
04B2-1	2.3	Cemented - Silty clay	SPT	27			27
04-B4	2.8	Cemented - Silty clay	SPT	14			14
04B2-2	5.1	Cemented - Silty clay	SPT	53			53

Borehole name	Blow count depth (m)	Sediment description	Sampler type	Field blow count	′Equivalent total′ blow count for samples at refusal	SPT-equivalent blow count	Final blow count (N)
04B2-2	9.3	Cemented - Silty clay	SPT	50/6"	100		100
04-B4	0.5	Cemented - Silty clay	SPT	49			49
04-B2	1.9	Cemented - Silty clay	SPT	36			36
04-B2	2.8	Cemented - Silty clay	SPT	16			16
04-B2	4.6	Cemented - Silty clay	SPT	12			12
04-B2	5.1	Cemented - Silty clay	SPT	33			33
04-B2	6.0	Cemented - Silty clay	SPT	28			28
04-B2	8.4	Cemented - Silty clay	SPT	32			32
04-B4	1.4	Cemented - Silty clay	SPT	50/6"	100		100
05-B6	8.4	Cemented - Silty clay	MC	50		22	22
05-B6	7.9	Cemented - Silty gravel	MC	50/5"	120	53	53
04-B4	5.6	Cemented - Silty sand	SPT	28			28
05-B6	2.8	Clay	MC	16		7	7
07B-9	4.2	Clayey gravel	SPT	81			81
04B2-1	1.4	Clayey gravel	SPT	22			22
04B2-1	7.9	Clayey gravel	SPT	34			34
04B2-2	10.2	Clayey gravel	SPT	11			11
05-B1	7.1	Clayey gravel	SPT	25			25
05B-10	1.8	Clayey gravel	SPT	26			26
07B-8	11.8	Clayey gravel	SPT	6			6
04B2-1	0.5	Clayey sand	SPT	10			10
07B-4	2.2	Clayey sand	SPT	13			13
04-B2	7.4	Clayey sand	SPT	11			11
04B2-1	3.3	Clayey sand	SPT	35			35
04B2-1	6.0	Clayey sand	SPT	12			12

Borehole name	Blow count depth (m)	Sediment description	Sampler type	Field blow count	'Equivalent total' blow count for samples at refusal	SPT-equivalent blow count	Final blow count (N)
04B2-1	7.4	Clayey sand	SPT	18			18
04B2-1	10.2	Clayey sand	SPT	50/6"	100		100
04B2-1	11.0	Clayey sand	SPT	8			8
04B2-2	0.5	Clayey sand	SPT	4			4
04B2-2	0.8	Clayey sand	SPT	17			17
04B2-2	2.3	Clayey sand	SPT	11			11
04B2-2	5.6	Clayey sand	SPT	36			36
04B2-2	6.5	Clayey sand	SPT	7			7
04B2-2	7.0	Clayey sand	SPT	7			7
04B2-2	7.9	Clayey sand	SPT	13			13
04B2-2	11.0	Clayey sand	SPT	10			10
04-B4	1.9	Clayey sand	SPT	63			63
04-B4	2.3	Clayey sand	SPT	18			18
04-B4	7.4	Clayey sand	SPT	18			18
04-B4	9.3	Clayey sand	SPT	17			17
04-B4	10.0	Clayey sand	SPT	20			20
04-B9	1.4	Clayey sand	SPT	12			12
05-B1	2.4	Clayey sand	SPT	11			11
05-B1	9.8	Clayey sand	SPT	25			25
05-B1	13.6	Clayey sand	SPT	11			11
05-B11	1.8	Clayey sand	SPT	58			58
05-B11	3.6	Clayey sand	SPT	16			16
05B-12	0.4	Clayey sand	SPT	10			10
05B-12	3.2	Clayey sand	SPT	16			16
05B-12	3.6	Clayey sand	SPT	10			10

Borehole name	Blow count depth (m)	Sediment description	Sampler type	Field blow count	′Equivalent total′ blow count for samples at refusal	SPT-equivalent blow count	Final blow count (N)
05B-13	1.3	Clayey sand	SPT	27			27
05B-4	1.8	Clayey sand	SPT	3			3
05-B6	0.5	Clayey sand	MC	11		5	5
05-B6	1.4	Clayey sand	MC	22		10	10
05-B6	1.9	Clayey sand	MC	11		5	5
05-B6	2.3	Clayey sand	MC	17		7	7
05-B6	7.0	Clayey sand	MC	59		26	26
05B-7	3.2	Clayey sand	SPT	8			8
05B-7	5.5	Clayey sand	SPT	5			5
05B-8	6.5	Clayey sand	MC	36		16	16
07B-14	7.9	Clayey sand	SPT	14			14
07B-14	13.9	Clayey sand	SPT	28			28
07B-18	7.4	Clayey sand	SPT	52			52
07B-20	1.8	Clayey sand	SPT	33			33
07B-3	14.9	Clayey sand	SPT	26			26
07B-8	7.6	Clayey sand	SPT	22			22
07B-9	13.0	Clayey sand	SPT	74			74
04-B2	7.0	Fat clay	SPT	18			18
04-B4	4.6	Fat clay	SPT	22			22
05-B1	3.8	Gravelly clay	SPT	22			22
05-B1	6.1	Gravelly clay	SPT	54			54
05-B6	4.2	Gravelly clay	MC	14		6	6
04-B2	3.3	Lean clay	SPT	6			6
04-B2	1.4	Sandy clay	SPT	21			21
04B2-1	0.9	Sandy clay	SPT	20			20

Borehole name	Blow count depth (m)	Sediment description	Sampler type	Field blow count	'Equivalent total' blow count for samples at refusal	SPT-equivalent blow count	Final blow count (N)
04B2-1	5.6	Sandy clay	SPT	5			5
04B2-1	6.5	Sandy clay	SPT	28			28
04B2-2	7.4	Sandy clay	SPT	29			29
04-B4	3.7	Sandy clay	SPT	6			6
04-B4	7.9	Sandy clay	SPT	9			9
05-B1	4.7	Sandy clay	SPT	9			9
05-B1	5.2	Sandy clay	SPT	10			10
05-B1	6.6	Sandy clay	SPT	19			19
05-B1	11.2	Sandy clay	SPT	23			23
05B-12	0.8	Sandy clay	SPT	13			13
05B-5	1.8	Sandy clay	SPT	4			4
05B-5	2.0	Sandy clay	SPT	4			4
05B-8	8.4	Sandy clay	MC	47		21	21
05B-8	11.1	Sandy clay	MC	29		13	13
07B-10	2.7	Sandy clay	SPT	4			4
07B-12	8.8	Sandy clay	SPT	8			8
07B-19	13.9	Sandy clay	SPT	10			10
07B-5	4.3	Sandy clay	SPT	10			10
07B-9	8.8	Sandy clay	SPT	11			11
05-B1	10.3	Sandy clay w/ trace gravel	SPT	12			12
07B-19	4.6	Sandy fat clay	SPT	59			59
04B-1	10.2	Silty clay	SPT	38			38
04B2-2	8.4	Silty clay	SPT	11			11
04-B4	4.2	Silty clay	SPT	5			5
04-B4	7.0	Silty clay	SPT	24			24

Borehole name	Blow count depth (m)	Sediment description	Sampler type	Field blow count	'Equivalent total' blow count for samples at refusal	SPT-equivalent blow count	Final blow count (N)
05-B1	0.4	Silty clay	SPT	19			19
05-B1	5.7	Silty clay	SPT	65			65
05-B1	7.5	Silty clay	SPT	7			7
05-B1	8.0	Silty clay	SPT	38			38
05-B1	11.7	Silty clay	SPT	18			18
05-B1	12.2	Silty clay	SPT	24			24
05-B1	12.6	Silty clay	SPT	28			28
05-B1	13.1	Silty clay	SPT	20			20
05-B11	2.7	Silty clay	SPT	4			4
05-B11	0.4	Silty clay	SPT	9			9
05-B11	0.8	Silty clay	SPT	12			12
05B-12	2.2	Silty clay	SPT	12			12
05B-12	2.7	Silty clay	SPT	7			7
05-B14	2.2	Silty clay	SPT	13			13
05-B14	3.2	Silty clay	SPT	36			36
05B-4	4.1	Silty clay	SPT	7			7
07B-2	7.9	Silty clay	SPT	10			10
07B-6	7.4	Silty clay	SPT	3			3
04-B2	4.2	Silty gravel	SPT	64			64
04B2-1	3.7	Silty gravel	SPT	35			35
04-B9	0.9	Silty sand	SPT	13			13
04-B2	3.7	Silty sand	SPT	15			15
04-B2	8.8	Silty sand	SPT	38			38
04B2-1	1.9	Silty sand	SPT	15			15
04B2-1	8.8	Silty sand	SPT	18			18

Borehole name	Blow count depth (m)	Sediment description	Sampler type	Field blow count	′Equivalent total′ blow count for samples at refusal	SPT-equivalent blow count	Final blow count (N)
04B2-2	4.2	Silty sand	SPT	48			48
04-B4	5.1	Silty sand	SPT	36			36
05-B14	0.8	Silty sand	SPT	10			10
05-B14	3.6	Silty sand	SPT	31			31
07B-5	1.3	Silty sand	SPT	24			24
05B-12	4.6	Silty sand w/ gravel	SPT	25			25
05B-12	4.1	Silty, clayey sand	SPT	32			32
04B2-1	7.0	Silty, clayey sand	SPT	26			26
05-B6	6.0	Silty, clayey sand	MC	52		23	23
04-B4	0.9	Silty, clayey sand	SPT	9			9
04-B4	8.8	Silty, clayey sand	SPT	42			42

Table 3: 3rd & Gass- Borehole blow counts and their conversion

Borehole name	Blow count depth (m)	Sediment description	Sampler type	Field blow count	'Equivalent total' blow count for samples at refusal	SPT-equivalent blow count	Final blow count (N)
B-1	22.6	Cemented - Caliche	SPT	50/2"	300		100
B-1	10.4	Cemented - Caliche	SPT	50/3"	200		100
3	9.4	Cemented - Clayey sand	SPT	50/4"	150		100
B-1	5.8	Cemented - Sandy clay	SPT	50/2"	300		100
B-1	4.3	Cemented - Silty sand	SPT	50/3"	200		100
1	13.7	Cemented - Clayey sand	SPT	42			42
B-1	13.4	Cemented - Clayey sand	SPT	42			42
B-1	24.1	Cemented - Clayey sand	SPT	45			45
2	11.3	Cemented - Sandy clay	SPT	50/6"	100		100
B-1	2.7	Cemented - Sandy clay	SPT	9			9
B-1	25.6	Cemented - Sandy clay	SPT	35			35
B-1	30.2	Cemented - Sandy clay	SPT	19			19
B-1	1.2	Cemented - Silty clay	SPT	12			12
B-1	11.9	Cemented - Silty clay	SPT	25			25
B-1	33.2	Cemented - Silty clay	SPT	62			62
2	17.4	Cemented - Silty clay	SPT	49			49
1	33.5	Cemented - Silty clay	SPT	62			62
1	7.6	Clayey sand	SPT	4			4
3	20.1	Clayey sand	SPT	3			3
B-1	7.3	Clayey sand	SPT	4			4
B-1	14.9	Clayey sand	SPT	11			11
B-1	16.5	Clayey sand	SPT	20			20
1	25.9	Sandy clay	SPT	35			35

Borehole name	Blow count depth (m)	Sediment description	Sampler type	Field blow count	′Equivalent total′ blow count for samples at refusal	SPT-equivalent blow count	Final blow count (N)
B-1	8.8	Sandy clay	SPT	5			5
B-1	18.0	Sandy clay	SPT	19			19
B-1	19.5	Sandy clay	SPT	6			6
B-1	21.0	Sandy clay	SPT	13			13
B-1	27.1	Sandy clay	SPT	4			4
B-1	28.7	Sandy clay	SPT	5			5
3	15.5	Silty clay - High Plasticity	SPT	7			7
3	27.7	Silty clay - High Plasticity	SPT	6			6

Table 4: Neon - Borehole blow counts and their conversion

Borehole name	Blow count depth (m)	Sediment description	Sampler type	Field blow count	'Equivalent total' blow count for samples at refusal	SPT-equivalent blow count	Final blow count (N)
B-11-064	11.9	Cemented - Caliche	SPT	50/0"	6000		100
B-11-013	4.6	Cemented - Clayey sand with caliche	SPT	50/3"	200		100
B-11-077	31.5	Cemented - Fat clay with trace calcareous gravel	SPT	50/4"	150		100
B-11-077	32.0	Cemented - Fat clay with trace calcareous gravel	SPT	50/4"	150		100
B-11-012	3.0	Cemented - Clayey sand with caliche	MC	48		21	21
B-11-077	23.0	Cemented - Fat clay	SPT	68			68
B-11-077	25.5	Cemented - Fat clay	SPT	29			29
B-11-077	25.9	Cemented - Fat clay	SPT	29			29
B-11-077	6.7	Cemented - Sandy clayey gravel	SPT	24			24
B-11-077	34.4	Cemented - Sandy lean clay	SPT	66			66
B-11-064	11.4	Cemented - Sandy lean clay	SPT	20			20
B-11-064	33.1	Clayey sand	SPT	15			15
B-11-064	33.5	Clayey sand	SPT	15			15
B-11-015	6.1	Fat clay	MC	43		19	19
B-11-064	29.4	Fat clay	SPT	24			24
B-11-064	29.9	Fat clay	SPT	24			24
B-11-077	20.0	Fat clay	SPT	15			15
B-11-077	20.4	Fat clay	SPT	15			15
B-11-077	22.6	Fat clay	SPT	15			15
B-11-012	9.1	Fat clay with trace calcareous gravel	MC	25		11	11
B-11-015	30.5	Fat clay with trace calcareous gravel	MC	28		12	12
B-11-064	18.9	Gravelly clayey sand	SPT	32			32
B-11-064	19.4	Gravelly clayey sand	SPT	32			32

Borehole name	Blow count depth (m)	Sediment description	Sampler type	Field blow count	′Equivalent total′ blow count for samples at refusal	SPT-equivalent blow count	Final blow count (N)
B-11-015	39.6	Lean clay with sand	MC	50/5"	120	53	53
B-11-015	22.9	Sandy fat clay	MC	26		11	11
B-11-077	12.6	Sandy lean clay	SPT	19			19
B-11-077	13.1	Sandy lean clay	SPT	19			19
B-11-064	23.0	Silty sand	SPT	36			36

Table 5: City Center - Borehole blow counts and their conversion

Borehole name	Blow count depth (m)	Sediment description	Sampler type	Field blow count	'Equivalent total' blow count for samples at refusal	SPT-equivalent blow count	Final blow count (N)
B05-13	61.0	Cemented - Caliche	SPT	50/3"	200		100
B05-13	4.6	Cemented - Caliche	SPT	50/0"	6000		100
B05-13	6.1	Cemented - Caliche	SPT	50/0"	6000		100
B05-13	12.2	Cemented - Caliche	SPT	50/0"	6000		100
B05-05	29.3	Cemented - Gravelly clay / Clayey sand	SPT	50/3"	200		100
B05-05	29.3	Cemented - Gravelly clay / Clayey sand	SPT	50/3"	200		100
B05-13	7.6	Cemented - Sandy clay	SPT	50/4"	150		100
B05-13	36.6	Clayey sand	SPT	50/5"	120		100
B05-13	10.7	Clayey sand	SPT	50/0"	6000		100
B05-13	9.1	Clayey sand	SPT	50/3"	200		100
B05-13	16.8	Clayey sand w/gravel	SPT	50/3"	200		100
B05-11	45.4	Clayey, silty sand	SPT	100+			100
B05-11	45.4	Clayey, silty sand	SPT	100+			100
B05-09	3.5	Gravelly sand	SPT	100+			100
B05-13	19.8	Gravelly sand	SPT	50/3"	200		100
B05-09	3.5	Gravelly sand	SPT	100+			100
B05-13	57.9	Sand	SPT	50/3"	200		100
B05-13	18.3	Sandy clay	SPT	50/3"	200		100
B05-13	22.9	Sandy clay	SPT	50/3"	200		100
B05-09	11.1	Clayey sand / Sandy clay	SPT	100+			100
B05-09	11.1	Clayey sand / Sandy clay	SPT	100+			100
B05-05	49.2	Clayey sand / Sandy clay	SPT	17			17
B05-05	49.2	Clayey sand / Sandy clay	SPT	17			17

Borehole name	Blow count depth (m)	Sediment description	Sampler type	Field blow count	'Equivalent total' blow count for samples at refusal	SPT-equivalent blow count	Final blow count (N)
B05-05	40.1	Silty sand	SPT	20			20
B05-05	40.1	Silty sand w/ clay	SPT	20			20
B05-02	8.8	Clayey sand	SPT	9			9
B05-11	22.9	Clayey sand	SPT	21			21
B05-13	13.7	Clayey sand	SPT	20			20
B05-02	8.8	Clayey sand	SPT	9			9
B05-11	22.9	Clayey sand	SPT	21			21
B05-13	15.2	Clayey sand	SPT	45			45
B05-13	24.4	Clayey sand	SPT	72			72
B05-13	54.9	Clayey sand	SPT	44			44
B05-13	39.6	Clayey sand	SPT	19			19
B05-13	48.8	Clayey sand	SPT	16			16
B05-13	51.8	Clayey sand	SPT	33			33
B05-03	13.4	Sand	SPT	12			12
B05-03	13.4	Sand	SPT	12			12
B05-13	33.5	Sandy clay	SPT	15			15
B05-13	42.7	Sandy clay	SPT	16			16
B05-13	64.0	Sandy clay	SPT	21			21
B05-13	25.9	Sandy clay	SPT	16			16
B05-13	27.4	Sandy clay	SPT	20			20
B05-13	30.5	Sandy clay	SPT	46			46
B05-13	45.7	Sandy clay	SPT	25			25
B05-14	13.6	Sandy clay	SPT	36			36
B05-14	13.6	Sandy clay	SPT	36			36
B05-13	3.0	Silty gravel	SPT	66			66

Borehole name	Blow count depth (m)	Sediment description	Sampler type	Field blow count	′Equivalent total′ blow count for samples at refusal	SPT-equivalent blow count	Final blow count (N)
B05-09	24.8	Silty sand	SPT	85			85
B05-09	51.8	Silty sand	SPT	45			45
B05-09	51.8	Silty sand	SPT	45			45
B05-09	24.8	Silty sand	SPT	85			85
B05-05	15.5	Silty sand	SPT	45			45
B05-05	15.5	Silty sand	SPT	45			45
B05-13	21.3	Transitional - Clayey sand/sand	SPT	41			41
B05-05	6.4	Transitional - Sand w/ gravel/ Clay	SPT	19			19
B05-05	6.4	Transitional - Sand with gravel and clay	SPT	19			19
B05-05	79.6	Transitional - Silty sand / Sandy clay	SPT	34			34
B05-05	79.6	Transitional - Silty sand / Sandy clay	SPT	34			34

BIBLIOGRAPHY

AASHTO. (2012). *AASHTO LRFD bridge design specifications, customary U.S. units*. Washington, DC: American Association of State Highway and Transportation Officials.

ASTM D7400-08, (2008). *Standard test methods for downhole seismic testing*. West Conshohocken, PA: ASTM International.

ASTM D2488-09a, (2009). *Standard practice for description and identification of soils (visual-manual procedure).* West Conshohocken, PA: ASTM International.

ASTM D1586-11, (2011). *Standard test method for standard penetration test (SPT) and split-barrel sampling of soils*. West Conshohocken, PA: ASTM International.

ASTM D2487-11, (2011). *Standard practice for classification of soils for engineering purposes (Unified Soil Classification System).* West Conshohocken, PA: ASTM International.

ASTM D3080-11, (2011). *Standard test method for direct shear test of soils under consolidated drained conditions.* West Conshohocken, PA: ASTM International.

ASTM D6066-11, (2011). *Standard practice for determining the normalized penetration resistance of sands for evaluation of liquefaction potential*. West Conshohocken, PA: ASTM International.

ASTM D2166-13, (2013). *Standard test method for unconfined compressive strength of cohesive soil*. West Conshohocken, PA: ASTM International.

Bahar, R., Alimrina, N., & Belhassani, O. (2013) Interpretation of a pressuremeter test in cohesive soils. *Proceedings, 3rd International Conference on Geotechnical Engineering*, Hammamet, Tunisia, 1-9. Retrieved from http://www.ummto.dz/IMG/pdf/Article_Tunisie_Belhassani.pdf

Baxter, C. D. P., Page, M., Bradshaw, A. S., & Sherrill, M. (2005). *Guidelines for geotechnical site investigations in Rhode Island*. Providence, R.I: Rhode Island Dept. of Transportation. Retrieved from http://www.dot.ri.gov/documents/about/research/Geotechnical.pdf

Bellana, N. (2009). *Shear Wave Velocity as Function of SPT Penetration Resistance and Vertical Effective Stress at California Bridge Sites* (Master's Thesis). University of California, Los Angeles.

Blake, W. D., & Gilbert, R. B. (1997). Investigation of possible relationship between undrained shear strength and shear wave velocity for normally consolidated clays. *Offshore Technology Conference,* 411-420. doi:10.4043/8325-MS

Boore, D. M. (2007). *Some thoughts on relating density to velocity.* Retrieved from http://www.ce.memphis.edu/7137/PDFs/Boore/daves_notes_on_relating_density_to_velocity_v1.2.pdf

Bowles, J. E. (1996). *Foundation analysis and design*. New York: McGraw-Hill.

Brandenberg, S. J., Bellana, N., & Shantz, T. (2010). Shear wave velocity as function of standard penetration test resistance and vertical effective stress at California bridge sites. *Soil Dynamics and Earthquake Engineering, 30,* 10, 1026-1035.

Briaud, J. L. (1992). *The pressuremeter*. Rotterdam: A.A. Balkema.

Cha, M., & Cho, G. C. (2007). Shear strength estimation of sandy soils using shear wave velocity. *Geotechnical Testing Journal, 30,* 6, 484-495.

Clarke B. G., & Gambin M. P. (1998). Pressuremeter testing in onshore ground investigations, a report by the ISSMGE Committee TC16, *International Conference on Site Characterization,* Atlanta. Retrieved from http://www.apageo.com/upload/medias/documents/26_isc1---gambin-clarke_846.pdf

Clayton, C. R. I., Matthews, M. C., & Simons, N. E. (1995). *Site investigation*. Oxford, England: Blackwell Science.

Crice, D. (2011). Near-surface, downhole shear-wave surveys: A primer. *The Leading Edge, 30,* 2, 164-171.

Das, B. M. (2010). *Principles of geotechnical engineering (7th ed.)*. Stamford, Conn: Cengage Learning.

Djoenaidi, W. J. (1985). *A compendium of soil properties and correlations* (Master's Thesis). The University of Sydney.

Duncan, J. M., Wright, S. G., & Brandon, T. L. (2014). *Soil strength and slope stability (2nd ed.)*. Hoboken, NJ: Wiley.

Geotechdata.info. (2014). Soil Cohesion. Retrieved February 16, 2015, from http://www.geotechdata.info/parameter/cohesion.html

Hara, A., Ohta, T., Niwa, M., Tanaka, S., & Banno, T. (1974). Shear modulus and shear strength of cohesive soils. *Soils and Foundations, 14*, 3, 1-12.

Hasancebi, N., & Ulusay, R. (2007). Empirical correlations between shear wave velocity and penetration resistance for ground shaking assessments. *Bulletin of Engineering Geology and the Environment, 66,* 2, 203-213.

Hettiarachchi, H., & Brown, T. (2009). Use of SPT blow counts to estimate shear strength properties of soils: Energy balance approach. *Journal of Geotechnical and Geoenvironmental Engineering, 135*, 6, 830-834.

Holtz, R. D., Kovacs, W. D., & Sheahan, T. C. (2011). *An introduction to geotechnical engineering (2nd ed.)*. Upper Saddle River, NJ: Pearson.

In situ Engineering. (2012). Final report of *in situ* pressuremeter testing Project Neon Phase 1 Final Design Clark County, Nevada. In situ Engineering Project Number: 1033. Appendix D – In situ pressuremeter testing report, *Geotechnical*

Data Report Project NEON P3 Phase Las Vegas, Nevada. Retrieved from http://www.ndotprojectneon.com/existing_assests_condition_report/geotechnical/Appendix_D_PMT_Report.pdf

Kalantary, F., Ardalan, H., & Nariman-Zadeh, N. (2009). An investigation on the S_u-N_{SPT} correlation using GMDH type neural networks and genetic algorithms. *Engineering Geology, 104,* 144-155.

Kim, D. S., Bang, E. S., & Kim, W. C. (2004). Evaluation of various downhole data reduction methods for obtaining reliable Vs profiles. *Geotechnical Testing Journal, 27,* 6, 585.

Kleinfelder, Inc. (2011). *Draft Preliminary Geotechnical Data Report Phase 1 Preliminary Design CC-215/US95 System to System Interchange, Clark County, Nevada.* Kleinfelder Project No. 117419.7.

Kramer, S. L. (1996). *Geotechnical earthquake engineering*. Upper Saddle River, NJ: Prentice Hall.

Kulhawy, F. H., & Mayne, P. W. (1990). *Manual on estimating soil properties for foundation design.* Palo Alto, CA: Electric Power Research Institute.

Kulkarni, M. P., Singh, D. N., & Singh, D. N. (2010). Application of shear wave velocity for characterizing clays from coastal regions. *KSCE Journal of Civil Engineering, 14,* 3, 307-321.

Lin, Y. C., Joh, S. H., & Stokoe, K. H. (2014). Analyst J: Analysis of the UTexas 1 surface wave dataset using the SASW methodology. In *Geotechnical Special Publication.* (234 GSP ed.). ASCE (Reston, VA), 830-839. doi:10.1061/9780784413272.081

Louie, J. N., Pullammanappallil, S. K., Pancha, A., West, T., & Hellmer, W. K. (2011). Earthquake Hazard Class Mapping by Parcel in Las Vegas Valley. In *Structures Congress 2011.* ASCE (Reston, VA), 1794-1805.

Luke, B., Murvosh, H., Taylor, W., & Wagoner, J. (2009). Three-dimensional modeling of shallow shear-wave velocities for Las Vegas, Nevada, using sediment type. *Journal of Earth Science, 20,* 3, 555-562.

Lynn, R. L. (2008). Electronic Submittal of Geotechnical Information (ESGI) (Originally Published on September 18, 2007) [Memorandum]. Clark County (Nevada) Department of Development Services - Building Division. Retrieved from http://www.clarkcountynv.gov/Depts/development_services/Industry%20Notices/2008% 20Industry%20Notices/electronic_submittal_esgi.pdf

Maheswari, R. U., Boominathan, A., & Dodagoudar, G. R. (2010). Use of surface waves in statistical correlations of shear wave velocity and penetration resistance of Chennai soils. *Geotechnical and Geological Engineering, 28,* 2, 119-137.

Mair, R. J., & Wood, D. M. (1987). *Pressuremeter testing: Methods and interpretation*. London: Butterworth-Heinemann.

Menq, F. (2003). *Dynamic properties of sandy and gravelly soils* (Doctoral Dissertation). University of Texas at Austin, TX.

Mavko, G. (2005). Conceptual overview of rock and fluid factors that impact seismic velocity and impedance. *Stanford Rock Physics Laboratory.* Retrieved from https://pangea.stanford.edu/courses/gp262/Notes/8.SeismicVelocity.pdf

Murthy, V. N. S. (2003). *Geotechnical engineering: Principles and practices of soil mechanics and foundation engineering*. New York: Marcel Dekker.

Murvosh, H., Luke, B., & Calderón-Macías, C. (2013a). Shallow-to-deep shear wave velocity profiling by surface waves in complex ground for enhanced seismic microzonation of Las Vegas, Nevada. *Soil Dynamics and Earthquake Engineering, 44,* 168-182.

Murvosh, H., Luke, B., Taylor, W. J., & Wagoner, J. (2013b). Three-dimensional shallow shear-wave velocity model for the Las Vegas valley. *Environmental and Engineering Geoscience, 19,* 2, 115-134.

Nassaji, F., & Kalantari, B. (2011). SPT capability to estimate undrained shear strength of fine-grained soils of Tehran, Iran. *Electronic Journal of Geotechnical Engineering, 16,* 1229-1238.

Newcomb, D. E., & Birgisson, B. (1999). *Measuring in situ mechanical properties of pavement subgrade soils*. Washington, D.C: National Academy Press. Retrieved from http://onlinepubs.trb.org/onlinepubs/nchrp/nchrp_syn_278.pdf

Niehoff, J. W. (2010). The use of geophysical methods to detect abandoned mine workings. *Geotechnical Practice Publication, 6, ASCE,* 119-128. doi: 10.1061/41144(391)11

Park, C.B., Miller, R.D., & Xia, J. (1999). Multichannel analysis of surface waves. *Geophysics, 64,* 3, 800-808.

Rogers, J. D. (2006). Subsurface exploration using the Standard Penetration Test (SPT) and Cone Penetration Test (CPT). *Environmental & Engineering Geoscience, 12,* 2, 161-179.

Samuel, R., Badrzadeh, Y., Luke, B., Lawrence, A.J., Siddharthan, R., and Bafghi, A., (2015). Seismic site characterization in support of drilled shaft design in Southern Nevada. *Proceedings, IFCEE,* ed. M. Iskander, M. T. Suleiman, J. B. Anderson, D.F. Laefer. ASCE, doi: 10.1061/9780784479087, pp. 939-950.

Schmertmann, J. H., & Palacios, A. (1979). Energy Dynamics of the SPT. *Journal of the Geotechnical Engineering Division, 105,* 8, 909-926.

Sivrikaya, O., & Togrol, E. (2006). Determination of undrained strength of fine-grained soils by means of SPT and its application in Turkey. *Engineering Geology, 86*, 1, 52-69.

Spatz, C. (2011). *Basic statistics: Tales of distributions.* Belmont, CA: Wadsworth/Cengage Learning.

Stephenson, W. J., Louie, J. N., Pullammanappallil, S., Williams, R. A., & Odum, J. K. (2005). Blind shear-wave velocity comparison of ReMi and MASW results with boreholes to 200 m in Santa Clara Valley: Implications for earthquake ground-motion assessment. *Bulletin of the Seismological Society of America, 95*, 6, 2506-2516.

Stone, Richard C., Jr. (2009). Analysis of a caliche stiffened pile foundation. (Doctoral Dissertation). University of Nevada, Las Vegas, NV. http://digitalscholarship.unlv.edu/thesesdissertations/148

Subramanian, N. (2008). *Design of steel structures.* New Delhi: Oxford University Press.

Terzaghi, K., Peck, R. B., & Mesri, G. (1996). *Soil mechanics in engineering practice*. New York: Wiley.

Thompson, E.M. (2007). Surface-source downhole seismic analysis in R. *U.S. Geological Survey Open-File Report 2007-1124.*

Tsiambaos, G., & Sabatakakis, N. (2011). Empirical estimation of shear wave velocity from *in situ* tests on soil formations in Greece. *Bulletin of Engineering Geology and the Environment, 70,* 2, 291-297.

U.S. Department of the Interior (2001). *Engineering Geology Field Manual, Second Edition, Volume II.* Retrieved from http://www.usbr.gov/pmts/geology/geoman.html

Wair, B.R., DeJong, J.T., & Shantz .T. (2012). *Guidelines for estimation of shear wave velocity profiles.* Pacific Earthquake Engineering Research Center, Report 2012/08.

Werle, J. & Luke, B. (2007). Engineering with heavily cemented soils in Las Vegas, Nevada. *ASCE, 162,* 1-9.

Wyman, R., Karakouzian, M., Bax-Valentine, V., Slemmons, D. B., Peterson, L., & Palmer, S. (1993). Geology of Las Vegas, Nevada United States of America. *Bulletin of the Association of Engineering Geologists, 30*, 1, 33-78.

CURRICULUM VITA

Graduate College

University of Nevada, Las Vegas

Rinu Ann Samuel

Degrees:

Bachelor of Science, Geological Engineering, 2010

University of Alaska Fairbanks

Publications:

Samuel, R., Daanen, R., and Misra, D. (2007). Laboratory Scale Simulation of Water and Energy Fluxes in Non Sorted Circle Systems of Alaska, presented at the *Association of Engineering and Environmental Geologists (AEG) 50th Annual Meeting*, September 24-29, Los Angeles, CA.

Robinson, W.J., Obermiller, K., **Samuel, R**., and Misra, D. (2007). Development of a Geodatabase for Sediment Transport from Alaskan Watersheds, presented at the *Association of Engineering and Environmental Geologists (AEG) 50th Annual Meeting*, September 24-29, Los Angeles, CA.

Blackburn, A.J., Clilverd, H.M., **Samuel, R.,** Holland, K., and White, D.M. (2007). Chemistry of North Slope, Alaska, Lakes and Reservoirs: September 2005 to May 2007. *University of Alaska Fairbanks, Water and Environmental Research Center, Report INE/WERC 07.13*, Fairbanks, Alaska, 18 pp.

Samuel, R., Badrzadeh, Y., Luke, B., Lawrence, A.J., Siddharthan, R., and Bafghi, A. (2015). Seismic Site Characterization in Support of Drilled Shaft Design in Southern Nevada. *International Foundations Congress and Equipment Expo* – March 2015, San Antonio, TX.

Thesis Title: Geotechnical Surrogates for Sediment Shear Behavior in Southern Nevada

Thesis Examination Committee:

Chairperson, Barbara Luke, Ph. D.

Committee Member, William Savage, Ph. D.

Committee Member, Haroon Stephen, Ph.D.

Graduate Faculty Representative, Wanda Taylor, Ph. D.